# HARMONIC MINIMIZATION IN A VSI FED INDUCTION MOTOR DRIVE

## A DISSERTATION

***Submitted in partial fulfillment of the requirements for the award of the degree of***

**MASTER OF TECHNOLOGY**

**in**

**ELECTRICAL ENGINEERING**

**(With Specialization in Power Apparatus & Electric Drives)**

**By**

**ANIL KUMAR MATETI**



**DEPARTMENT OF ELECTRICAL ENGINEERING**
**INDIAN INSTITUTE OF TECHNOLOGY ROORKEE**
**ROORKEE - 247 667 (INDIA)**
**JUNE, 2008**

# CANDIDATE'S DECLARATION

I hereby declare that the work which is being presented in this dissertation entitled, "**Harmonic Minimization in a VSI Fed Induction Motor Drive**" submitted in the partial fulfillment of the requirements for the award of the degree "**Master of Technology**" with specialization in **Power Apparatus and Electric Drives**, to the **Department of Electrical Engineering, IIT Roorkee**, Roorkee is an authentic record of my own work carried out during the period from August 2007 to June 2008 under the supervision of **Dr. S. P. Gupta**, Professor and **Dr. G. K. Singh**, Professor, Department of Electrical Engineering, IIT Roorkee, Roorkee.

The matters embodied in this report have not been submitted by me for the award of any other degree or diploma.

Date: 29/06/08

Place: Roorkee

(ANIL KUMAR MATETI)

# CERTIFICATE

This is to certify that above statement made by candidates is correct to the best of our knowledge.

**Dr. G. K. Singh**
Professor
Department of Electrical Engineering,
Indian Institute of Technology Roorkee,
Roorkee – 247667

**Dr. S. P. Gupta**
Professor
Department of Electrical Engineering,
Indian Institute of Technology Roorkee,
Roorkee – 247667

# ACKNOWLEDGEMENT

I take this opportunity to express my sincere gratitude towards my guides, **Dr. S. P. Gupta**, Professor & Head, and **Dr. G. K. Singh**, Professor, Electrical Engineering Department, IIT Roorkee for the guidance, advice and encouraging support which were invaluable for the completion of this dissertation work. I feel it is my fortune to have opportunity of working under their valuable guidance.

I am indebted to all the faculty of Power Apparatus & Electric Drives group for their encouragement and suggestions which helped me in completing this work.

Finally, I wish to thank my friends and well wishers for their encouragement and support at various stages of this work.

# ABSTRACT

The programmed pulse width modulation (PPWM) technique was originally proposed by H. S. Patel and R. G. Hoft in 1973. PPWM inverter generates high quality output spectra by eliminating several lower order harmonics, which in turn results in minimum current ripples and reduced torque pulsations in an AC drive.

This technique necessitates solving a system of nonlinear transcendental equations and multiple solutions are possible. So, the main challenge of solving these equations is the convergence, and therefore, an initial guess which is considerably close to the exact solution is required. This report discusses a simple algorithm to generate the initial guess from the symmetry of exact switching angle trajectories at zero modulation index. Two objective functions for eliminating selected harmonics and minimizing total harmonic distortion, while controlling the fundamental, are formulated.

The main contribution in this work is development of a software program for minimizing the formulated objective functions using nonlinear constrained optimization functions in MATLAB and the optimal switching angles are obtained for a wide range of modulation index and number of switching angles. Usually minimization subroutines of NAG or IMSL library were employed in earlier work, which are not as easily available as MATLAB. Two sets of solutions have been identified, one in $0^0$-$60^0$ range and other in $0^0$-$90^0$ range. It is found that, the developed algorithm was able to find the optimal angles for all modulation indexes, even higher than unity, in a very less time.

Simulation model of the VSI fed induction motor drive is developed in MATLAB-SIMULINK environment. A firing pulse generator with digital logic is designed for converting the optimal angles into firing pulses to the inverter and the waveforms of the voltage and current at the input of the induction motor are obtained by simulating the system. The harmonic spectra of the obtained waveforms are analyzed at various operating conditions.

# CONTENTS


**CANDIDATE'S DECLARATION** ..... I

**CERTIFICATE** ..... I

**ACKNOWLEDGEMENT** ..... II

**ABSTRACT** ..... III

**LIST OF FIGURES** ..... VII

**CHAPTER 1 INTRODUCTION** ..... 1

1.1 INTRODUCTION ..... 1

1.2 LITERATURE REVIEW ..... 2

1.3 ORGANIZATION OF THE REPORT ..... 4

1.4 SCOPE OF THE WORK ..... 5

**CHAPTER 2 VOLTAGE SOURCE INVERTER** ..... 6

2.1 INTRODUCTION ..... 6

2.2 INVERTER REQUIREMENTS ..... 6

2.3 VOLTAGE SOURCE INVERTER ..... 7

2.4 PWM TECHNIQUES OF THREE-PHASE VSI ..... 8

2.4.1 Sinusoidal PWM (SPWM) ..... 9

2.4.2 Third-harmonic PWM ..... 10

2.4.1 Space vector modulation ..... 10

2.5 CONCLUSIONS ..... 11

**CHAPTER 3 PROGRAMMED PWM TECHNIQUE** ..... 12

3.1 INTRODUCTION ..... 12

3.2 BIPOLAR WAVEFORM AND ANALYSIS ..... 12

3.3 PROBLEM FORMULATION ..... 16

3.3.1 Selective Harmonic Elimination ..... 17

3.3.2 Harmonic Minimization ..... 18

3.4 CONCLUSIONS ..... 18

**CHAPTER 4 ALGORITHM FOR GENERATION OF SWITCHING ANGLES .....19**

4.1 INTRODUCTION ..... 19

4.2 FUNCTION (*FMINCON*) DETAILS ..... 20

4.3 DESIGN OF THE PROBLEM ..... 20

4.4 INITIAL GUESS TO THE PROBLEM ..... 23

4.4.1 Straight line approximation algorithm ..... 23

4.4.2 Solution at zero modulation index ..... 25

4.5 FLOWCHART ..... 29

4.6 SWITCHING ANGLE TRAJECTORIES ..... 33

4.6.1 Trajectories for odd values of N ..... 33

4.6.2 Observations ..... 38

4.6.3 Trajectories for even values of N ..... 39

4.6.4 Observations ..... 44

4.7 CONCLUSIONS ..... 44

**CHAPTER 5 SIMULINK IMPLEMENTATION OF PPWM VSI FED INDUCTION MOTOR DRIVE .....45**

5.1 INTRODUCTION ..... 45

5.2 MODELLING OF THREE PHASE INDUCTION MOTOR: ..... 47

5.2.1 Mathematical model of induction motor: ..... 47

5.2.2 SIMULINK implementation: ..... 49

5.3 PWM INVERTER ..... 51

5.4 FIRING PULSE GENERATOR ..... 52

**CHAPTER 6 RESULTS AND DISCUSSIONS .....55**

6.1 SIMULATION RESULTS ..... 55

6.2 CONCLUSIONS ..... 68

CHAPTER 7 CONCLUSIONS.....69
REFERENCES.....70
APPENDIX – A.....72
APPENDIX – B.....73

# List of Figures

Figure 2.1: Block Diagram of Variable Frequency Adjustable Speed Drive ..... 6

Figure 2.2: Voltage Source Inverter ..... 7

Figure 2.3: Line and Phase Voltages for $180^0$ Conduction ..... 8

Figure 2.4: Sinusoidal PWM Technique ..... 9

Figure 2.5: Reference waveform of third-harmonic PWM ..... 10

Figure 2.6: Representation of rotating vector in complex plane ..... 11

Figure 3.1: Two-level bipolar PWM Inverter voltage waveform ..... 13

Figure 4.1: Variation of average slopes $m_p$ and $m_n$ against $N$ ..... 24

Figure 4.2: Straight line approximation of exact switching pattern (N=11) ..... 25

Figure 4.3: Flowchart of main program ..... 30

Figure 4.4: Flowchart for ***objfun*** subroutine ..... 31

Figure 4.5: Flowchart for ***confun*** subroutine ..... 32

Figure 4.6 – 4.14: Switching angle trajectories for odd values of $N$ ..... 33 - 37

Figure 4.15 – 4.24: Switching angle trajectories for even values of $N$ ..... 39 - 43

Figure 5.1: Schematic model of VSI fed induction motor drive employing harmonic elimination/minimization ..... 45

Figure 5.2: SIMULINK model of VSI fed induction motor drive employing harmonic control ..... 46

Figure 5.3: The complete induction motor SIMULINK model ..... 49

Figure 5.4: Induction motor d-q model ..... 51

Figure 5.5: PWM Inverter ..... 51

Figure 5.6: Firing pulse generator ..... 52

Figure 5.7: Clock and zone-bit generator block ..... 53

Figure 5.8: Clock and zone-bit for three full cycles ..... 53

Figure 5.9: Logic switching circuit ..... 54

Figure 5.10: Subsystem for generating staircase wave ..... 54

Figure 6.1: Representation of line voltage and current ..... 55

Figure 6.2: Phase to Pole voltage ($N$=11) ..... 56

Figure 6.3: Phase Voltage waveform $V_{An}$ ($N$=11) ..... 56

Figure 6.4: Line current and voltage for $N$=2 (M=0.8) ..... 57

Figure 6.5: Line current and voltage for $N$=3 (M=0.8) ..... 58

Figure 6.6: Line current and voltage for $N$=4 (M=0.8) ..... 59

Figure 6.7: Line current and voltage for $N$=5 ($M$=0.8) ..... 60

Figure 6.8: Line current and voltage for $N$=6 ($M$=0.8) ..... 61

Figure 6.9: Line current and voltage for $N$=7 ($M$=0.8) ..... 62

Figure 6.10: Line current and voltage for $N$=8 ($M$=0.8) ..... 63

Figure 6.11: Line current and voltage for $N$=9 ($M$=0.8) ..... 64

Figure 6.12: Line current and voltage for $N$=10 ($M$=0.8) ..... 65

Figure 6.13: Line current and voltage for $N$=11 ($M$=0.8) ..... 66

Figure 6.14: Line current THD variation with Modulation Index ..... 67

Figure 6.15: Current THD variation with number of switchings ($N$) ..... 67

Figure 6.16: Induction motor free acceleration characteristics when fed from harmonic controlled VSI ..... 68

# Chapter 1
# Introduction

## 1.1 Introduction

Recent advancements in semiconductor and microprocessor technology have made the variable frequency adjustable speed AC drives a serious competitor for the conventional DC motor Drive. Some of the advantages of adjustable speed AC drive when compared to DC drive are:

- Ruggedness of the motors and superiority of their modified characteristics
- They are better suited for high speed operation with no size limit, since there are no brushes and commutation is not a problem.
- AC motors require virtually no maintenance
- AC motors are less expensive and more reliable

The Induction motor is an important class of AC motors which finds wide applicability in industry and several domestic drive applications. More than 85% of industrial motors in use today are in fact induction motors. Various methods can be used to control the speed of an induction motor. But the more efficient method involves variation of the stator supply frequency and stator voltage. A voltage source inverter used as a frequency converter is widely used in these variable frequency speed regulation systems. However, the benefits of variable frequency adjustable speed drives are not obtained without the introduction of some negative effects, particularly high harmonic content at the output of the inverter. Induction motors are sensitive to harmonic voltages; both their efficiency and performance can be considerably affected by the poor power quality of the supply. Therefore, research on improving the output spectra of the voltage source inverter (VSI) is given more importance in the electric drive system field. The development of pulse width modulation (PWM) technology made this task easier.

The PWM methods used in Voltage Source Inverters can be classified according to switching frequency. Method that works with high switching frequencies involves many switchings in one period of the fundamental output voltage. A very popular and well known method in most of the industrial applications is the carrier modulated sinusoidal pulse width modulation, which uses the phase shifting technique to improve the output spectra [1]. The other important PWM methods are regularly sampled PWM and Area Equalization PWM [2]. Although these methods produce high quality output with low Total Harmonic Distortion (THD), they provide no direct means of controlling the levels of harmonics present. Programmed PWM method is an optimal strategy that relies on eliminating selected harmonics from the PWM waveform. This method got more

importance in applications which are particularly sensitive to the presence of undesirable harmonics.

The Programmed PWM technique establishes a set of mathematical equations (detailed in chapter 3) of output waveform based on (a) the characteristic of the output waveform of man-made inverter, (b) the amplitude of the fundamental wave of output voltage and (c) the number of harmonics to be eliminated. These developed equations are solved for obtaining the exact switching angles. Thus, the aim of eliminating the desired lower order harmonics from the output of the inverter is achieved. The Selective Harmonic Elimination (SHE) technique is a PWM technique which has the advantages of lowering the switching frequency of the power device and eliminating the low order harmonics [3].

So far, the principle limitation with the application of Programmed PWM technique is solving the developed equations. These equations contain trigonometric terms, which are transcendental in nature and therefore exhibit multiple solutions. To obtain convergence with numerical techniques, the starting values (or the initial guess) must be selected properly. Therefore, the main drawback of Programmed PWM method is that it relies on heavily on off-line computing power since it involves solving nonlinear transcendental equations, which cannot be solved on-line by microprocessor based controller. Its implementation is thus based on look-up tables and interpolation between these tables, hence requires large storage memory. With advances in computing technology, these mentioned limitations become insignificant, making the Programmed PWM techniques more attractive and versatile means of power control.

## 1.2 Literature Review:

In 1973, at University of Missouri, H. S. Patel and R. G. Hoft for the first time introduced the selective harmonic elimination technique [4, 5]. Since then it has been the research topic in the power system field. The recent developments in microcomputer filed made this technique much more important in the industrial applications.

Due to the symmetry properties of the exact solution pattern, an algorithm based on two straight lines with positive and negative slopes that closely approximate the exact solution is proposed by Enjeti and Lindsay in 1987 [6]. With this algorithm, the starting values for obtaining exact solutions using numerical techniques can be found even for large numbers of harmonics to be eliminated. However, the algorithm is only applicable when (a) the number of switching angles per quarter cycle is chosen to be odd and (b) this number is greater than 3.

In 1990, Prasad N. Enjeti, Phoivos D. Ziogas, F. Lindsay discussed the various programmed PWM techniques to eliminate the harmonics [7]. They gave a general classification for various techniques depending on the inverter configuration that is three-phase and for single phase and also depending on whether it is line to neutral or line to

line PWM waveform. The techniques were also divided into those that seek solutions within $60^0$ and $90^0$. They used the International mathematical and statistical library (IMSL) for solving the non-linear equations.

In 1992, R.G. Hoft and J.A. Asumadu [8] described a method for the elimination of harmonics in PWM waveforms using the algebra of linear block digital codes which substitutes harmonic generator polynomials, with zero and unity coefficients, for the nonlinear equations requires in Fourier series harmonic elimination.

In 1995, Sidney R. Bowes and Paul R.Clarke [9] developed the modified regular-sampling techniques to generate the PWM strategies online in real time using a simple microprocessor algorithm without resorting to the offline mainframe computer harmonic elimination numerical techniques. Using this technique, they achieved the voltage/frequency range from PWM to Quasi-square wave operation.

In 1996, J. Sun, Stephen Beinke and H Grotstollen [10] implemented and described a new scheme based on real time solution of nonlinear harmonic elimination equations using a digital signal processor DSP56001.

In 1999, T. Kato proposed an approach that makes it possible to solve the HE problem based on a homotopy method which finds multiple solutions for a specific degree of freedom N from those existing for N-1 sequentially by the mathematical induction of varying a fundamental component value as the homotopy parameter [11]. However, the method is long and cumbersome, and the paper does not mention which set of solutions from the multiple available ones is optimum as measured against overall harmonic performance.

In 2002, D. Czarkowski, David V.C., Georgy V.C. and Ivan W.S. analyzed the basic algebraic properties of the optimal PWM problem [12]. They reformulated the nonlinear design equations given by standard mathematical formulation and found the solution by computing the roots of univariate polynomial. The reformulation is done based upon the Newton identities, Pade approximation theory and properties of symmetric functions.

In 2004, J. Chiasson, L. M. Tolbert and Z. Du converted the nonlinear transcendental equations into polynomials and applied theory of resultants to determine the switching angles to eliminate specific harmonics [13]. However, as the number of switching angles increases, the degree of the polynomial in these polynomials becomes large, which increases the computational difficulty. Moreover, the paper briefly treats the bipolar waveform and only reports the angles to eliminate $5^{th}$ and $7^{th}$ harmonics.

In 2005, Jason R. Wells, Xin Greg, Patrick L. Chapman and P.T. Krein, formulated the harmonic elimination problem without quarter wave symmetry constraint for the two classes of the m-level, n-harmonic control problem [14]. Here, they presented

the special cases of two and three level harmonic elimination in detail along with representative solutions for harmonic control problem.

In 2006, V.G. Agelidis, A. Baloutktsis, I. Balouktsis and Calum Cossor, discussed a minimization method as a way to obtain multiple set of switching angles [15]. A simple harmonic distortion factor that takes into account the first two most significant harmonics present in the generated waveform is considered in order to evaluate the performance of each set.

In 2007, Vladimir Blasko proposed a systematic design approach for applying signal processing methods (like modified adaptive selective harmonic elimination algorithms) as an addition to the conventional control [16]. Thus, both control objectives like fast transient response and efficient harmonic filtering are achieved.

Recently, Mohammed S.A. Dahidah, V.G. Agelidis and M.V. Rao proposed an efficient hybrid real coded algorithm for selective harmonic control [17]. Here, an objective function describing the measure of effectiveness of eliminating selected orders of harmonics while controlling the fundamental, namely weighted total harmonic distortion is derived.

## 1.3 Organization of the Report:

**Chapter – 1:** Introduction and Literature survey of Selective Harmonic Elimination is presented in this chapter including the scope of the present work.

**Chapter – 2:** In this chapter, the basic configuration of VSI fed Induction Motor drive is discussed explaining the operation of Voltage Source Inverter. Also, PWM techniques for voltage control are introduced.

**Chapter – 3:** This chapter discuses the Programmed PWM technique for controlling the desired harmonics in the inverter output. The formulation and analysis of the problem associated with the bipolar waveform is presented.

**Chapter – 4:** MATLAB Optimization algorithm implementation is presented in this chapter, along with the flowchart summarizing the algorithm. The switching angle trajectories are presented for various values of number of switchings.

**Chapter – 5:** This chapter gives the detailed implementation of the proposed PPWM fed Induction motor drive model in MATLAB-SIMULINK environment explaining every individual block operation.

**Chapter – 6:** This chapter illustrates the simulation results of line current and voltage waveforms along with the frequency spectrum of current at different operating points including discussion of the results.

**Chapter – 7:** Some conclusions and a summary of the proposed method are presented in this chapter pointing future research in this area.

## 1.4 Scope of the Work:

The main aim of this dissertation is to develop PWM voltage source inverter fed induction drive model with harmonic control, including the problem formulation, calculation of switching angles and SIMULINK implementation of the model.

For this purpose, a system of non-linear transcendental equations is formulated by means of Fourier analysis of the PWM Inverter output waveform. The objective functions are formulated for both harmonic elimination problem and harmonic minimization problem. The formulated objective functions are minimized with the help of Non linear constrained programming in MATLAB. As the developed equations produce multiple solution sets, the initial guess to the problem are generated with proper care. Here, the initial guess is generated from the straight-line approximation approach and from the study of the nature of exact solution trajectories. And also the performance of the algorithm is studied for both the cases. Two sets of solution vectors, one is in $0^0$ to $90^0$ range and other in $0^0$ to $60^0$ range, are obtained from the MATLAB program for both the harmonic elimination and minimization case. The results are presented for switching angles over wide range of modulation index and number of switching angles.

The obtained switching angles are stored in LOOKUP tables and a logic switching circuit is designed for generating the firing pulses to the inverter. The proposed method is simulated in MATLAB – SIMULINK environment. The drive performance is studied when fed from Programmed Pulse Width Modulated Inverter and the results are presented for various operating conditions.

# Chapter 2
# Voltage Source Inverter

In this chapter, the basic configuration of VSI fed Induction Motor drive is discussed explaining the operation of Voltage Source Inverter. Also, PWM techniques for voltage control are discussed briefly.

## 2.1 Introduction

The supply of an induction motor in variable frequency adjustable speed drive requires the use of an inverter which transforms the rectified DC-voltage into a three phase AC-system with variable frequency and voltage. The basic configuration of VSI fed adjustable speed drive is shown in Fig 2.1.There are two basic types of forced-commutated inverter: The *current source inverter* (CSI) and the *voltage source inverter* (VSI). In speed regulation applications, the latter inverter is used most widely.

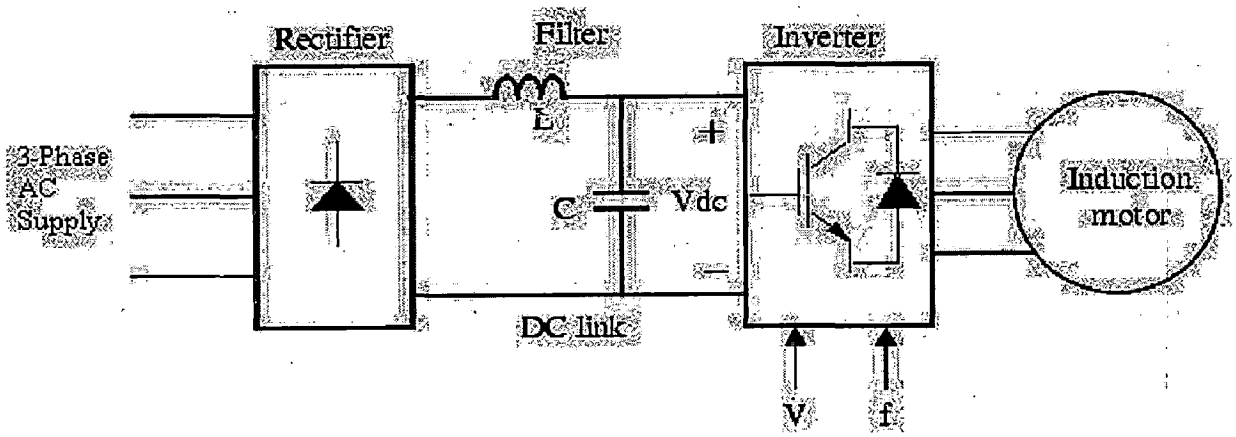


**Figure 2.1: Block Diagram of Variable Frequency Adjustable Speed Drive [21]**

## 2.2 Inverter Requirements:

The Voltage Source Inverter is expected to:

- generate smooth Variable-Frequency Variable-Voltage (VVVF) power
- produce nearly sinusoidal current waveforms throughout the operating range to avoid undesirable torque oscillations
- permit highly dynamic control both in motoring and braking operation
- provide as nearly as possible equivalent performance to the dual converter-fed dc drives with respect to cost, service reliability, and harmonic effect on the system

## 2.3 Voltage Source Inverter:

The inverter consists essentially of six power switches that can be metal-oxide semiconductor field-effect transistors (MOSFET), gate turn-off thyristors (GTO), or insulated gate bipolar transistors (IGBT), depending on the drive power capacity and the inverter switching frequency (Hz). The three phase Voltage Source Inverter is shown in Fig 2.2. The voltage source inverter (VSI) produces a relatively well-defined switched voltage waveform at the input terminals of the A.C. motor. A switching device conducts when the firing pulse is given to it and the switch is forward biased.

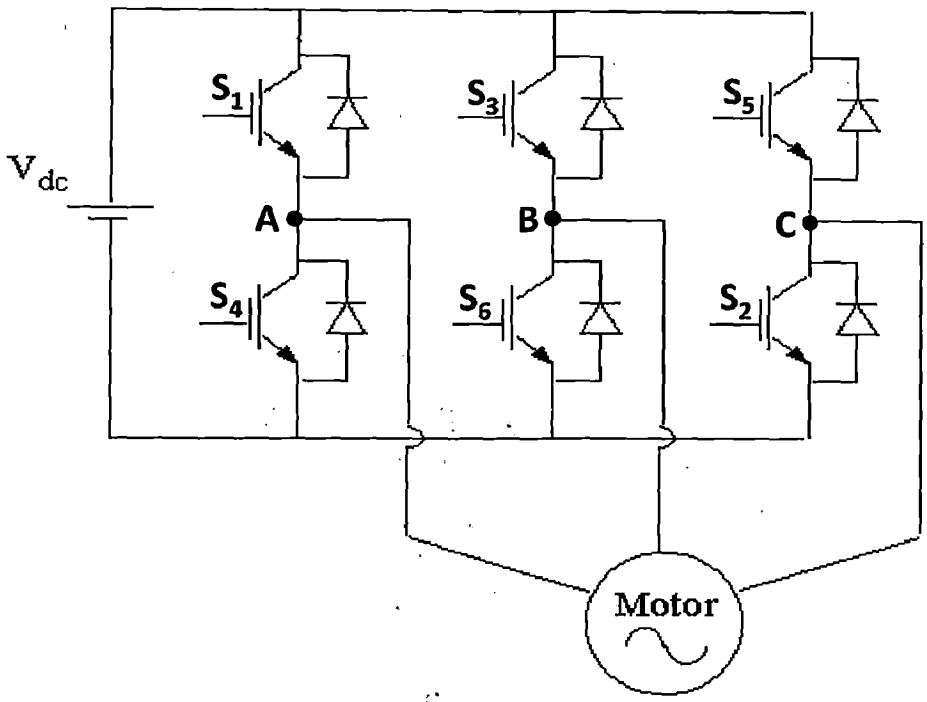


**Figure 2.2: Voltage Source Inverter [21]**

Three switches remain on at any instant of time. When S1 is turned on, terminal A is connected to the positive terminal of the D.C. supply source. When transistor S4 is switched on, the terminal A is connected to the negative side of the D. C. supply. The pole voltage waveform of phase A is obtained by switching the devices S1 and S4 in a complementary manner. The pole voltage waveforms of phase B and phase C are obtained by phase-shifting them with respect to phase A by $120^0$ and $240^0$ respectively, which results in a balanced three-phase supply (Fig 2.3).

If each switching device of the inverter is made to conduct for half cycle of the period, which is 180 degrees, then the pole voltage waveforms of all the three phases becomes quasi square wave consisting of one half-cycle with a magnitude of half the dc voltage and the second half cycle with a magnitude of half the dc voltage with negative sign. The line voltage $V_{ab}$, the pole voltages and the six-step phase voltage $V_{an}$ are shown in Fig 2.3.

The quasi square or square wave is characterized by dominant lower order harmonics. Fourier analysis reveals that a square wave, which is antisymmetrical about the 180 degree point, contains only odd harmonics, the 3rd, 5th, 7th etc. Induction Motors are sensitive to harmonic voltages; both their efficiency and performance can be considerably affected by the poor power quality of the supply. Therefore, research on improving the output spectra of the Voltage Source Inverter is given more importance in

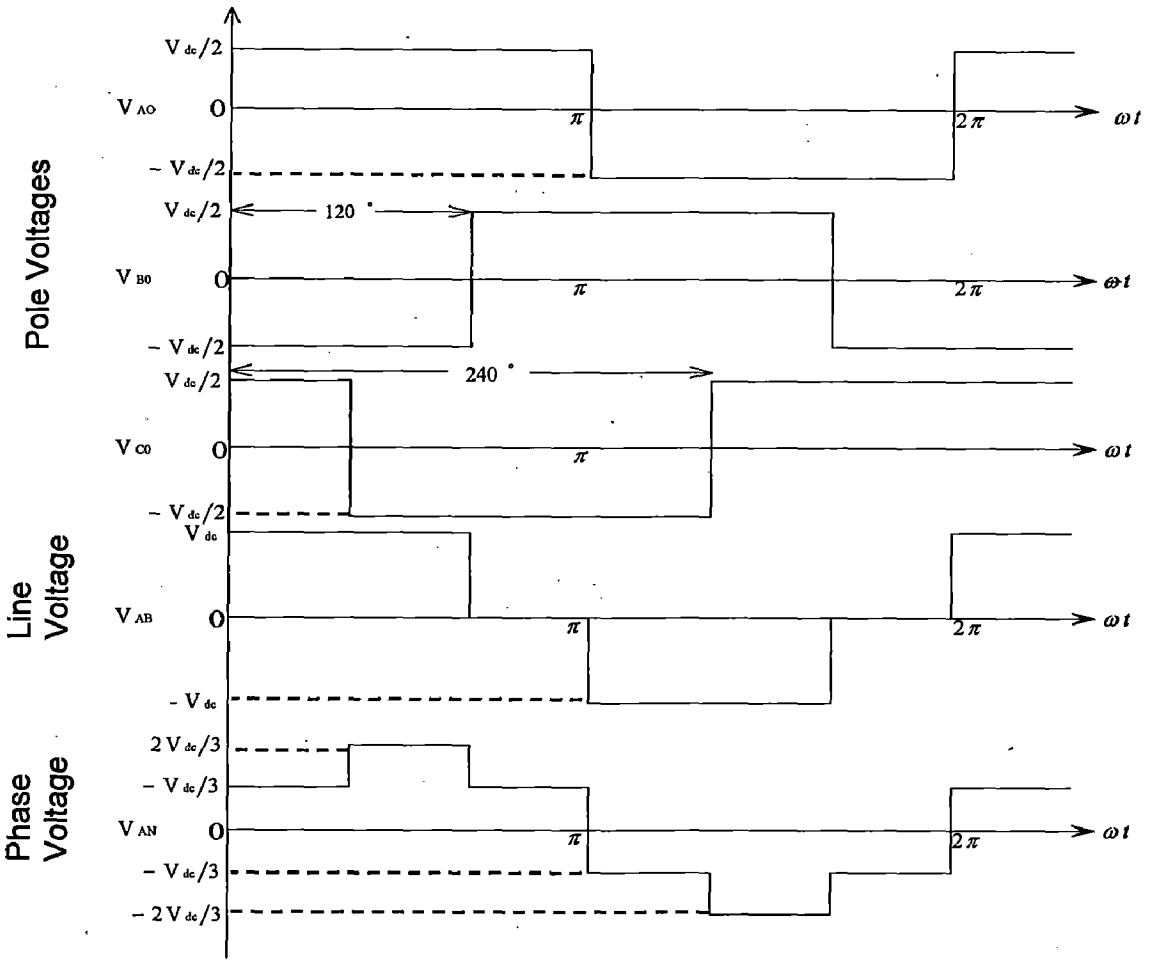


**Figure 2.3: Line and Phase Voltages for $180^0$ Conduction [21]**

the electric drive system field. The development of Pulse Width Modulation (PWM) technology made this task easier.

## 2.4 PWM Techniques of Three-Phase VSI

The common PWM techniques in use for controlling three-phase inverters are:

1. Sinusoidal PWM
2. Third-harmonic PWM
3. Space vector modulation

### 2.4.1 Sinusoidal PWM (SPWM)

The SPWM technique is very popular for industrial converters. The basic principle of the PWM technique involves the comparison of triangular carrier wave with the sinusoidal modulating wave. In this technique, there are three sinusoidal references waves (or modulating waves) each shifted by 120° as shown in fig 2.4 (a).

A carrier (triangular) wave of high frequency $f_{cr}$is compared with the reference signal corresponding to a phase to generate the gating signals for that phase. Comparing the carrier signal with the reference phases $V_A$, $V_B$, and $V_C$ produces $V_{AO}$, $V_{BO}$ and $V_{CO}$ respectively as shown in figure 2.4. Then the instantaneous line-to-line output voltage is $V_{AB}= V_{AO} - V_{BO}$.

The fundamental frequency component in the inverter output voltage can be controlled by amplitude modulation index,$M = \frac{\widehat{V_m}}{\widehat{V_{cr}}}$. Where $\widehat{V_m}$ and $\widehat{V_{cr}}$ are the peak values of the modulating and carrier waves respectively. The frequency ratio is defined by, $p = \frac{f_{cr}}{fm}$. Where $f_m$ and $f_{cr}$ are the frequencies of the modulating and carrier waves respectively.

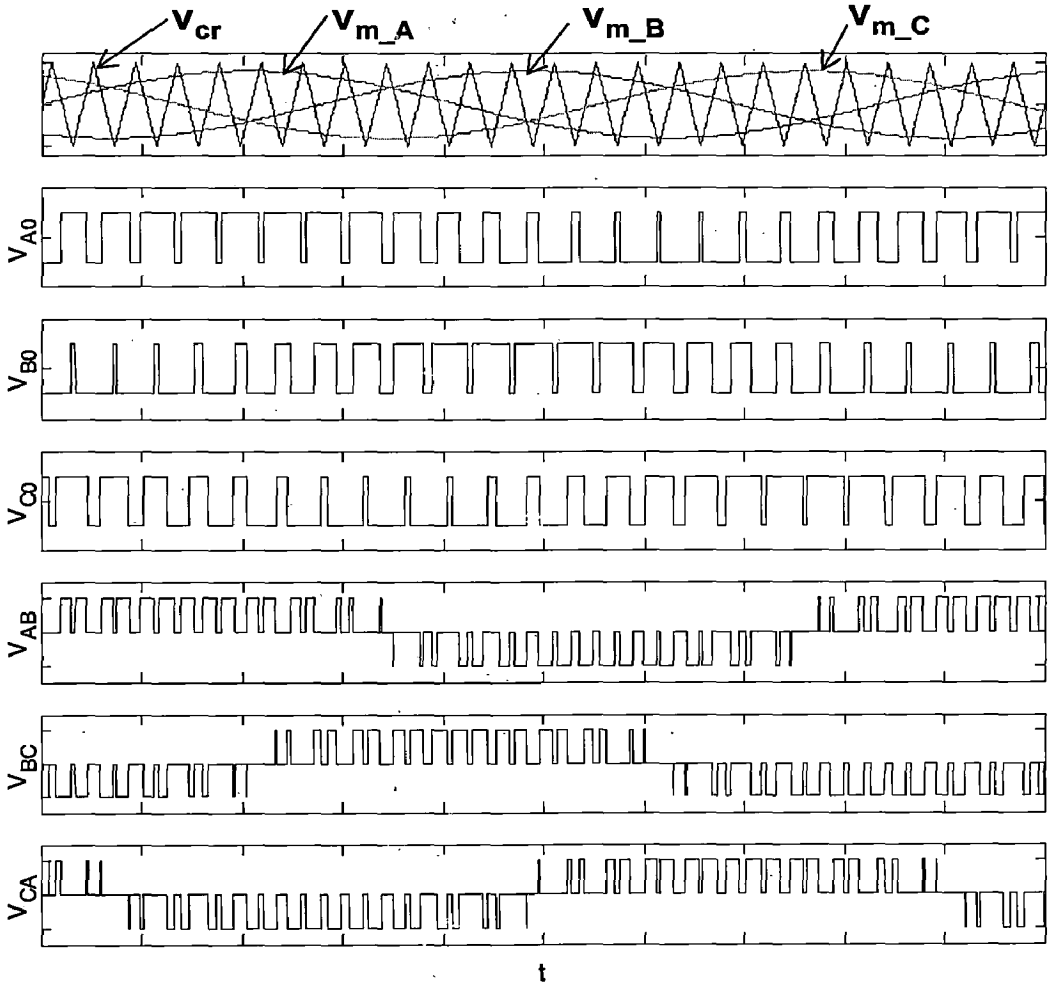


**Figure 2.4: Sinusoidal PWM Technique [21]**

Since the line voltage waveform is sine wave modulated, its harmonic spectrum approaches that of a sine wave. However, this applies to the values of M up to 1. For $M > 1$, over modulation takes place and benefits of SPWM is no longer available.

### 2.4.2 Third-harmonic PWM

This technique is implemented in the same manner as sinusoidal PWM. The difference is that the reference ac waveform is not sinusoidal but consists of both a fundamental component and a third-harmonic component as shown in fig 2.5. The advantage is, the harmonic spectrum of the resulting pole voltage is rich with third harmonic component. However, it cancels up in the line voltage in a three-phase system. Hence, line voltage harmonic spectrum is as good as in SPWM case. The available modulation depth is more in this case as compared to SPWM case, since the reference wave is 'flat topped'.

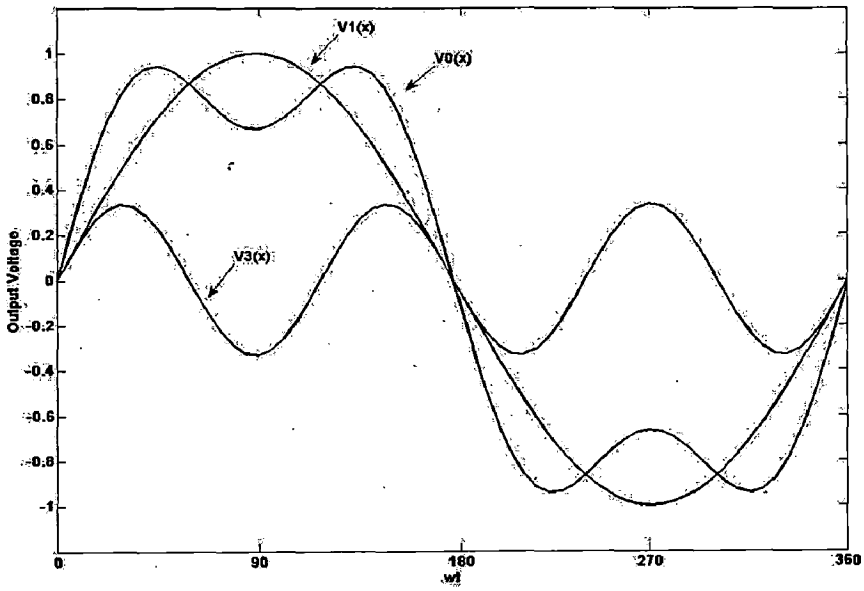


**Figure 2.5: Reference waveform of third-harmonic PWM [23]**

$V_0(x)$ is reference waveform with third-Harmonic injection
$V_1(x)$ is the fundamental component and
$V_3(x)$ is the third harmonic component

### 2.4.1 Space vector modulation

Space Vector Modulation(SVM) is a digital modulating technique where the objective is to generate PWM load line voltages that are in average equal to a given (or reference) load line voltages. SVM is quite different from the other PWM methods. With PWMs, the inverter can be thought of as three separate push-pull driver stages, which create each phase waveform independently. SVM, however, treats the inverter as a single unit; specifically, the inverter can be driven into eight unique states. Modulation is

accomplished by switching the state of the inverter. The control strategies are implemented in digital systems.

SVM was originally developed as a vector approach to PWM for three phase inverters. It is a more sophisticated technique for generating sine wave that provides a higher voltage to the motor with lower total harmonic distortion. It confines space vectors to be applied according to the region where the output voltage vector is located.

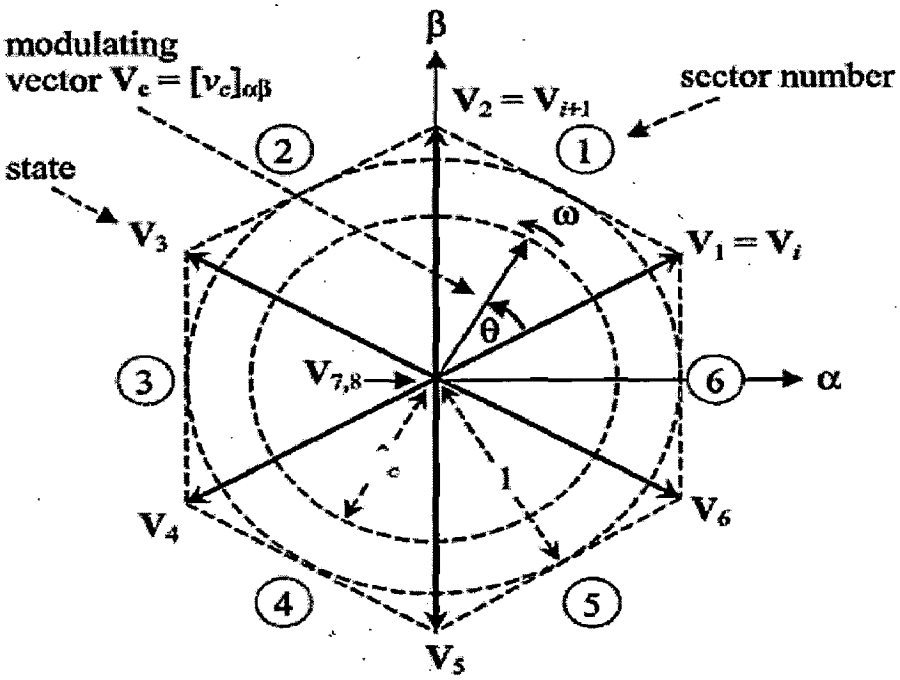


**Figure 2.6: Representation of rotating vector in complex plane [23]**

## 2.5 Conclusions:

The mentioned pulse-width and space vector modulation schemes result in converters with low-harmonic distortion waveform characteristics. Although these methods produce high quality output with low Total Harmonic Distortion (THD), they provide no direct means of controlling the levels of harmonics present. A generalized harmonic elimination technique to selectively eliminate and control the desired harmonics from the PWM waveforms was suggested in early 1970's. The main drawback of this technique is that it relies heavily on off-line computing since it involves solving non-linear transcendental equations, which cannot be solved online by a microprocessor based controller. Its implementation is thus based on look-up tables and the interpolation methods. Therefore, they require large storage memory for implementation. With advances in computing technology, these limitations become insignificant, making Programmed PWM techniques more attractive and versatile means of power control [2].

# Chapter 3
# Programmed PWM Technique

This chapter discuses the Programmed PWM technique for controlling the desired harmonics in the inverter output. The formulation and analysis of the problems associated with the bipolar waveform is presented.

## 3.1 Introduction

The objective of Programmed PWM techniques is to control amplitude levels of individual harmonics to the desired level for generating high quality output, thus satisfying several performance criteria. It was originally proposed by Patel and Hoft [4, 5] in 1973. Some advantages of the Programmed PWM over the conventional natural or regular-sampled PWM are:

i. About 50% reduction in the inverter switching frequency is achieved when compared with the conventional carrier-modulated sine PWM scheme [7].

ii. A much higher pole switching waveform fundamental amplitude is attainable before the minimum pulse-width limit of the inverter is reached.

iii. Due to the high quality of the output voltage and current, the ripple in the dc link current is also small. Thus, a reduction in the size of the dc link filter components is achieved.

iv. The reduction in the switching frequency contributes to the reduction in the switching losses of the inverter and permits the use of GTO switches for high-power converters.

v. Elimination of lower-order harmonics causes no harmonic interference such as resonance with external line filtering networks typically employed in inverter power supplies.

vi. The use of pre-calculated optimized programmed PWM switching patterns avoids online computations and provides straightforward implementation of a high-performance technique.

## 3.2 Bipolar Waveform and Analysis

In the development of SHE techniques, the two-state output waveform of the voltage source inverter, shown in fig. 2.3, has been investigated. The basic square wave output is chopped a number of times, and a fixed relationship between the number of chops and possible number of harmonics that can be eliminated is derived. The problem formulation and the Fourier analysis of the output waveform are illustrated in this section.

Fig 3.1 shows the two-level pole voltage waveform of a PWM Inverter with N chops per quarter cycle (i.e. 2N chops per half-cycle). The waveform has half-wave symmetry and unit amplitude.

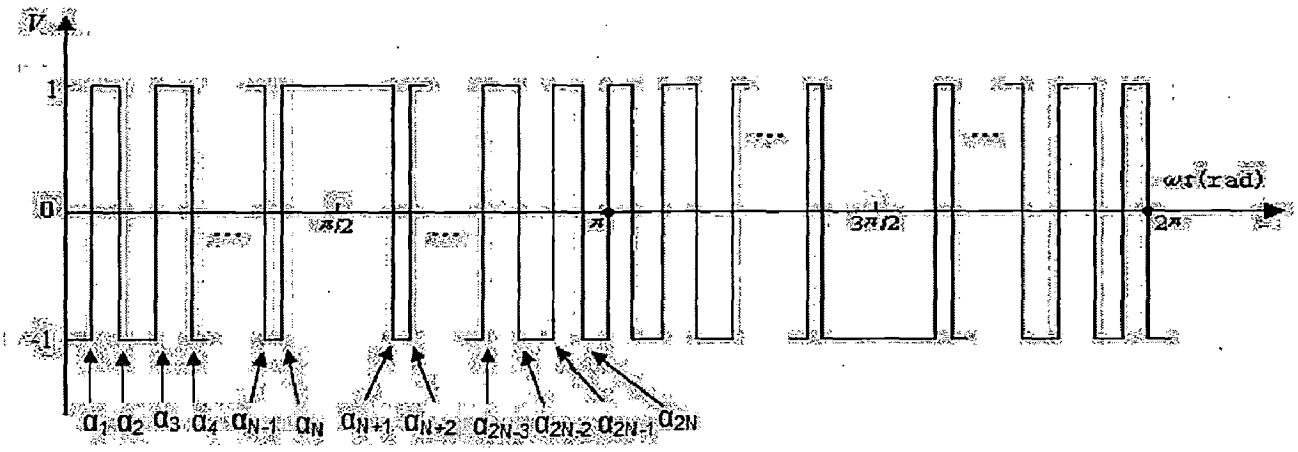


**Figure 3.1: Two-level bipolar PWM Inverter voltage waveform**

$\alpha_1, \alpha_2, \alpha_3 \ldots \alpha_{2N}$ represents the 2N chops in the half cycle. A Fourier series can represent the waveform shown above in general as

$$v(\omega t) = \sum_{n=1}^{\infty} [a_n \sin(n\omega t) + b_n \cos(n\omega t)] \quad \ldots\ldots\ldots\ldots\ldots\ldots\ldots (3.1)$$

Where, $a_n = \frac{1}{\pi}\int_0^{2\pi} v(\omega t) \sin(n\omega t)\, d(\omega t)$ $\ldots\ldots\ldots\ldots\ldots\ldots\ldots (3.2)$

and $b_n = \frac{1}{\pi}\int_0^{2\pi} v(\omega t) \cos(n\omega t)\, d(\omega t)$ $\ldots\ldots\ldots\ldots\ldots\ldots\ldots (3.3)$

Substituting Eq. (3.1) in Eq. (3.2) and using the half wave symmetry property

$$a_n = \frac{2}{\pi}\sum_{k=0}^{2N} (-1)^k \int_{\alpha_k}^{\alpha_{k+1}} \sin(n\omega t)\, d(\omega t) \quad \ldots\ldots\ldots\ldots\ldots\ldots\ldots (3.4)$$

Where, $\alpha_0 = 0, \alpha_{2N+1} = \pi$ and $\alpha_0 < \alpha_1 < \alpha_2 \ldots < \alpha_{2N+1}$

From Eq. (3.4), evaluating the integral

$$a_n = \frac{2}{n\pi}\sum_{k=0}^{2N} (-1)^k [\cos(n\alpha_k) - \cos(n\alpha_{k+1})]$$

$$= \frac{2}{n\pi}\left[\cos n\alpha_0 - \cos n\alpha_{2N+1} + 2\sum_{k=1}^{2N} (-1)^k \cos n\alpha_k\right] \ldots\ldots\ldots (3.5)$$

But, $\alpha_0 = 0$ *and* $\alpha_{2N+1} = \pi$. Hence

$$\cos n\alpha_0 = 0 \qquad \ldots\ldots\ldots\ldots\ldots\ldots (3.6)$$

$$\cos n\alpha_{2N+1} = (-1)^n \qquad \ldots\ldots\ldots\ldots\ldots\ldots (3.7)$$

Therefore, Eq. (3.5) reduces to

$$a_n = \frac{2}{n\pi}\left[1 - (-1)^n + 2\sum_{k=1}^{2N}(-1)^k \cos n\alpha_k\right] \qquad \ldots\ldots\ldots\ldots\ldots\ldots (3.8)$$

Similarly, we can write the second component of the Fourier expansion (Eq. 3.3) as,

$$b_n = -\frac{4}{n\pi}\left[\sum_{k=1}^{2N}(-1)^k \sin n\alpha_k\right] \qquad \ldots\ldots\ldots\ldots\ldots\ldots (3.9)$$

Utilizing the half-wave symmetry property of the waveform[$f(\omega t) = -f(\omega t + \pi)$], only the odd order harmonics exist. Therefore, for odd n

$$a_n = \frac{4}{n\pi}\left[1 + \sum_{k=1}^{2N}(-1)^k \cos n\alpha_k\right] \qquad \ldots\ldots\ldots\ldots\ldots\ldots (3.10)$$

$$b_n = \frac{4}{n\pi}\left[-\sum_{k=1}^{2N}(-1)^k \sin n\alpha_k\right] \qquad \ldots\ldots\ldots\ldots\ldots\ldots (3.11)$$

Equations 3.10 and 3.11 are functions of *2N* variables, $\alpha_1, \alpha_2, \alpha_3 \ldots \alpha_{2N}$. In order to obtain a unique solution for the *2N* variables, *2N* equations are required. By equating any *N* harmonics to zero, *2N* equations are derived from equations 3.10 and 3.11.

The *N* equations derived by equating $b_n$=*0* for *N* values of n, are solved by assuming quarter wave symmetry[$f(\omega t) = f(\pi - \omega t)$]. From the quarter wave symmetry property of the following relations are obvious, with regard to fig 3.1:

$$\alpha_1 = \pi - \alpha_{2N}$$
$$\alpha_2 = \pi - \alpha_{2N-1}$$
$$\alpha_3 = \pi - \alpha_{2N-2}$$
$$\ldots\ldots$$
$$\alpha_N = \pi - \alpha_{N+1}$$

In generalized form, we can say that

$$\alpha_k = \pi - \alpha_{2N-(k-1)}$$
$$\Rightarrow \quad \alpha_k = \pi - \alpha_{2N-k+1} \qquad for\ k = 1,2,\ldots,N \qquad \ldots (3.12)$$

Therefore, using Eq. 3.12

$$\sin n\alpha_k = \sin n(\pi - \alpha_{2N-k+1})$$
$$= [\sin n\pi \cos n\alpha_{2N-k+1} - \cos n\pi \sin n\alpha_{2N-k+1}], \quad for\ k = 1,2,\dots,N \quad ..(3.13)$$

For odd n,

$$\sin n\pi = 0 \quad and \quad \cos n\pi = -1 \qquad \dots\dots\dots\dots\dots\dots\dots (3.14)$$

On substituting Eq. 3.14 in Eq. 3.13

$$\sin n\alpha_k = \sin n\alpha_{2N-k+1} \qquad for\ k = 1,2,\dots,N \qquad \dots\dots\dots\dots\dots (3.15)$$

Now, on expanding equation 3.11

$$b_n = -\frac{4}{n\pi}\left[\sum_{k=1}^{N}(-1)^k \sin n\alpha_k + \sum_{k=N+1}^{2N}(-1)^k \sin n\alpha_k\right]$$

$$= -\frac{4}{n\pi}[-\sin n\alpha_1 + \sin n\alpha_2 - \sin n\alpha_3 + \cdots + (-1)^k \sin n\alpha_k + \cdots$$
$$+ (-1)^{2N-2} \sin n\alpha_{2N-2} + (-1)^{2N-1} \sin n\alpha_{2N-1} + (-1)^{2N} \sin n\alpha_{2N}]$$

$$= -\frac{4}{n\pi}[-\sin n\alpha_1 + \sin n\alpha_2 - \sin n\alpha_3 + \cdots + (-1)^k \sin n\alpha_k + \cdots + \sin n\alpha_{2N-2}$$
$$- \sin n\alpha_{2N-1} + \sin n\alpha_{2N}]$$

On rearranging the terms, $b_n$ becomes

$$b_n = -\frac{4}{n\pi}[-(\sin n\alpha_1 + \sin n\alpha_{2N}) + (\sin n\alpha_2 - \sin n\alpha_{2N-1}) + \cdots$$
$$+ (-1)^N(\sin n\alpha_N - \sin n\alpha_{N+1})]$$

$$= -\frac{4}{n\pi}\sum_{k=1}^{N}(-1)^k(\sin n\alpha_k - \sin n\alpha_{2N-k+1}) \qquad \dots\dots\dots\dots\dots\dots\dots\dots (3.16)$$

Substituting Eq. 3.15 in Eq. 3.16,

$$b_n = 0 \qquad \dots\dots\dots\dots\dots\dots\dots\dots (3.17)$$

Similarly, from Eq. 3.12

$$\cos n\alpha_k = \cos n(\pi - \alpha_{2N-k+1}), \qquad for\ k = 1,2,\dots,N \qquad (3.18)$$

For odd n, Eq. 3.18 becomes

$$\cos n\alpha_k = -\cos n\,\alpha_{2N-k+1}, \qquad for\ k = 1,2,\dots,N \qquad (3.19)$$

And by expanding Eq. 3.10 and rearranging the terms, $a_n$ becomes

$$a_n = \frac{4}{n\pi}\left[1 + \sum_{k=1}^{N}(-1)^k(\cos n\alpha_k - \cos n\alpha_{2N-k+1})\right] \qquad \dots\dots\dots\dots\dots\dots (3.20)$$

Substituting Eq. 3.19 in Eq. 3.20,

$$a_n = \frac{4}{n\pi}\left[1 + 2\sum_{k=1}^{N}(-1)^k \cos n\alpha_k\right] \qquad \dots\dots\dots\dots\dots\dots (3.21)$$

Equation 3.21 gives the amplitude of the $n^{th}$ harmonic when N switchings per quarter cycle are used. Hence, one can write the magnitude of the lower order non-triplen harmonic components, including the fundamental, as

$$V_1(\alpha_1, \alpha_2, \alpha_3 \dots \alpha_N) = (4/\pi)[1 + 2(-\cos\alpha_1 + \cos\alpha_2 - \cos\alpha_3 + \cdots + (-1)^N \cos\alpha_N)]$$
$$V_5(\alpha_1, \alpha_2, \alpha_3 \dots \alpha_N) = (4/5\pi)[1 + 2(-\cos 5\alpha_1 + \cos 5\alpha_2 - \cos 5\alpha_3 + \cdots + (-1)^N \cos 5\alpha_N)]$$
$$V_7(\alpha_1, \alpha_2, \alpha_3 \dots \alpha_N) = (4/7\pi)[1 + 2(-\cos 7\alpha_1 + \cos 7\alpha_2 - \cos 7\alpha_3 + \cdots + (-1)^N \cos 7\alpha_N)]$$
$$\dots\dots$$
$$V_n(\alpha_1, \alpha_2, \alpha_3 \dots \alpha_N) = (4/n\pi)[1 + 2(-\cos n\alpha_1 + \cos n\alpha_2 - \cos n\alpha_3 + \cdots + (-1)^N \cos n\alpha_N)]$$

$$\dots\dots\dots\dots\dots\dots\dots\dots (3.22)$$

Where,

$N$ is the number of switching angles per quarter cycle,
$n$ = 5, 7, … , 3$N$-2 when $N$ is even
= 5, 7, … , 3$N$-1 when $N$ is odd,
$\alpha_k$ is the $K^{th}$ switching angle.

## 3.3 Problem Formulation

Programmed PWM techniques optimize a particular objective function such as to obtain minimum losses, reduced torque pulsations, minimum total harmonic distortion, and selective elimination of harmonics [5]. Thus, these techniques are the most effective means of obtaining high-performance results.

In the scope of the present work, only harmonic elimination and harmonic minimization problems are discussed.

### 3.3.1 Selective Harmonic Elimination

The equation 3.21 has $N$ variables $(\alpha_1, \alpha_2, \alpha_3 \ldots \alpha_N)$ and set of solutions is obtainable by equating *(N-1)* number of harmonics to zero and assigning a specific value of the amplitude to the fundamental component $(V_1)$. These equations are non-linear and transcendental in nature and multiple solutions are possible. Two solutions have been identified. One is in $(0^0 - 60^0)$ range and other in $(0^0 - 90^0)$ range. So, solutions for the switching angles satisfying the criterion, as in equation 3.23, need to be obtained for each increment in the modulation index to provide voltage control with simultaneous elimination of harmonics.

$$\alpha_{min} < \alpha_1 < \alpha_2 < \alpha_3 < \cdots \alpha_N < \alpha_{max} \quad \ldots\ldots\ldots\ldots\ldots\ldots\ldots (3.23)$$

Where, $\alpha_{min} = 0$ and $\alpha_{max} = \begin{cases} 60 \ for\ 0^0 - 60^0\ solution\ set \\ 90 \ for\ 0^0 - 90^0\ solution\ set \end{cases}$

Therefore, the nonlinear equations for selective elimination of $N$-1 number of lower order non-triplen harmonics can be written as

$$\begin{aligned} V_1 &= M \\ V_5 &= 0 \\ V_7 &= 0 \\ &\ldots\ldots \\ V_n &= 0 \end{aligned} \quad \ldots\ldots\ldots\ldots\ldots\ldots\ldots (3.24)$$

where, $n = \begin{cases} 3N - 2 & for\ even\ N \\ 3N - 1 & for\ odd\ N \end{cases}$

On solving, the equation set 3.24 provides switching angles of the PWM waveform which is free of $5^{th}$, $7^{th}$, …, $n^{th}$ harmonics and with a fundamental component magnitude equal to $M$. These $N$ equations can be solved offline using numerical techniques. Standard nonlinear constrained optimization functions are available in MATLAB for solving these equations. For this an objective function describing a measure of effectiveness of eliminating selected order of harmonics is specified as

$$F(\alpha_1, \alpha_2, \alpha_3 \ldots \alpha_N) = V_5^2 + V_7^2 + V_{11}^2 + \cdots + V_n^2 \quad \ldots\ldots\ldots\ldots\ldots\ldots\ldots (3.25)$$

Subjected to constraints

$$\left.\begin{aligned} V_1 &= M \\ \alpha_{min} < \alpha_1 < \alpha_2 < \alpha_3 < \cdots \alpha_N < \alpha_{max} \end{aligned}\right\} \quad \ldots\ldots\ldots\ldots\ldots\ldots\ldots (3.26)$$

*and*

Minimizing $F$, subjected to constraints of 3.26, will result the optimal switching angles for the elimination of selected harmonics. The switching angles are generated for different modulation index and stored in lookup tables for controlling the inverter at certain operating point. The function minimization using MATLAB programming is clearly discussed in chapter – 4.

The selective harmonic elimination technique eliminates ($N$-1) harmonics from the output PWM waveform when $N$ switchings per half cycle are provided. In three phase applications, when certain non-triplen harmonics are eliminated the magnitude of next non-triplen harmonic component becomes very high. For example, if 5 switchings per half cycle are provided, the harmonics eliminated are $5^{th}$, $7^{th}$, $11^{th}$ and $13^{th}$. The next non-triplen harmonic i.e. $17^{th}$ harmonic is found to be more than 50%. Under low frequency operation of the drive, this harmonic may cause undesirable effects on the drive performance. However, if $N$ is high, this harmonic amplitude is quite low to cause any problems. Another limitation in Selective Harmonic Elimination technique is the accuracy of implementation. A small error in the calculated switching angles may reintroduce the eliminated harmonics with appreciable magnitude.

There is an alternative approach to selective harmonic elimination which aims at harmonic minimization rather than harmonic elimination.

### 3.3.2 Harmonic Minimization

In this method, a performance index is defined which is the measure of total harmonic distortion in the output waveform. In general, the THD is expressed as per unit of the fundamental component of the voltage as follows:

$$THD = \frac{\sqrt{\sum_{k=5,7,11,\ldots}^{\infty} \left(\frac{V_k}{k}\right)^2}}{V_1} \qquad \ldots\ldots\ldots\ldots\ldots\ldots (3.27)$$

Where, $V_1$ and $V_k$ are the amplitudes of the fundamental and $k^{th}$ harmonic components as given in Eq. 3.22. Minimizing *THD*, subjected to constraints of 3.26, will result the optimal switching angles which produces a PWM waveform with low total harmonic distortion. The MATLAB nonlinear constrained minimization functions are used for minimizing the objective function. The order of highest harmonic to be included is kept reasonably high. It should be noted that the highest harmonic to be eliminated in SHE technique is $3N$-$2$ for odd $N$ or $3N$-$1$ for even $N$. The calculation of switching angles in harmonic minimization technique is discussed in chapter – 4.

## 3.4 Conclusions

The basic principle of PPWM technique is illustrated in this chapter. The Fourier series of the two-level bipolar PWM Inverter voltage waveform is derived to formulate the objective functions for harmonic elimination and minimization problems, which can be solved to obtain the optimal switching angles. The obtained objective functions involve transcendental equations which may possess multiple solutions. The algorithm for obtaining the optimal angles for harmonic control is discussed in the next chapter.

# Chapter 4
# Algorithm for Generation of Switching Angles

The problem formulation and design for obtaining the optimal angles with the help of MATLAB® nonlinear constrained minimization functions is presented in this chapter, along with the flowchart summarizing the algorithm. Also, the switching angle trajectories are presented for various values of number of switchings.

## 4.1 Introduction

Determination of switching angles, with which the harmonic elimination objective is achieved, necessitated solving a system of nonlinear transcendental equations as discussed in the previous chapter. Due to their high complexity, real-time solution of harmonic elimination equations has been considered impractical. Consequently, all implementation systems reported so far are based on off-line solution of these equations. As a result, many people have utilized numerical iterative techniques in order to solve these equations such as Newton-Raphson method, gauss-seidel method etc. Newton-Raphson method is a derivative dependent and may end in local optima. Further, a judicious choice of the initial values alone will guarantee convergence [17]. Another approach uses Walsh functions [18] where solving linear equations, instead of solving non-linear transcendental equations, optimizes switching angles. Chiasson proposed theory of resultants where these transcendental equations are converted into polynomials [13]. Recently evolutionary techniques such as Genetic Algorithms are gaining importance in finding the solution without using initial guess to the problem.

In the current work, the objective functions provided in equations 3.25 and 3.27, for harmonic elimination and minimization respectively, are minimized with help of Optimization Toolbox available with MATLAB Software Package. The Toolbox includes routines for many types of optimization including

- Unconstrained nonlinear minimization
- Constrained nonlinear minimization, including goal attainment problems, minimax problems, and semi-infinite minimization problems
- Quadratic and linear programming
- Nonlinear least-squares and curve fitting
- Nonlinear system of equation solving
- Constrained linear least squares
- Sparse and structured large-scale problems.

The proposed harmonic elimination/minimization problem in the previous chapter can be solved constrained nonlinear minimization programming. The available function for non linear constrained minimization in MATLAB is *fmincon* which finds the minimum of constrained nonlinear multivariable function.

## 4.2 Function (*fmincon*) details

*fmincon* finds the minimum of a problem specified by

$$\min_x f(x)$$

Subjected to,

$$c(x) \leq 0$$
$$ceq(x) = 0$$
$$A.x \leq b$$
$$Aeq.x = beq$$
$$lb \leq x \leq ub$$

where *x, b, beq, lb,* and *ub* are vectors, *A* and *Aeq* are matrices, *c(x)* and *ceq(x)* are functions that return vectors, and *f(x)* is a function that returns a scalar. *f(x), c(x),* and *ceq(x)* can be nonlinear functions [19].

***Syntax:***

$$[x, fval, exitflag, output, lambda, grad, hessian] = fmincon(fun, x0, A, b, Aeq, beq, lb, ub, nonlcon, options)$$

Where,

- $fun$ is the function to be optimized,
- $x0$ is the initial guess to the problem,
- $lb$ *and* $ub$ are the lower and upper bounds on the variable $x$,
- $nonlcon$ defines nonlinear inequalities $c(x)$ and equalities $ceq(x)$,
- $options$ is a structure which specifies the optimization options,
- $fval$ is the value of the objective function $fun$ at solution $x$,
- $exitflag$ describes the exit condition of $fmincon$,
- $output$ is structure which contains the information about the optimization,
- $lambda$ is also a structure whose fields contain the Lagrange multipliers,
- $grad$ and $hessian$ are the values of gradient and hessian at the solution $x$ respectively.

## 4.3 Design of the problem

This section describes the formulation and design of the problem for both harmonic elimination and minimization problems with the help of $fmincon$.

Firstly, the magnitude of the fundamental, number of switching angles, highest harmonic to be optimized and the range of the optimal switching angles ($60^0$ or $90^0$) are read from the user. With the help of the input given by the user, the objective function of both the harmonic minimization and elimination cases are formulated as described in section 3.2. The objective functions thus formulated are passed as the input arguments to the optimization function $fmincon$.

Following are the key points in designing the optimization problem, for both harmonic minimization and elimination methods, with $fmincon$.

i. ***Objective function fun***

$fun$ is the objective function to be minimized. It a accepts a vector $x$ and returns a scalar $f$ which is the objective function evaluated at $x$. This function can be specified as a function handle for an M-file function. The format of the function $fmincon$ become,

$$x = fmincon(@objfun, x0, A, b \ldots)$$

Where, the $objfun$ is a MATLAB function which defines the objective function for harmonic elimination/minimization problem

ii. ***Specifying linear inequality constraints***

The linear inequality constraint of the problem is

$$\alpha_{min} < \alpha_1 < \alpha_2 < \alpha_3 < \cdots \alpha_N < \alpha_{max}$$

Where, $\alpha_{max}$ can be 60 or 90 and $\alpha_{min}$ is always zero. If the variables are designated as $x(1), x(2), \ldots, x(N)$ for $N$ switching angles per quarter cycle. Then the linear inequality constraints can be written as

$$\begin{aligned} &x(1) - x(2) < 0 \\ &x(2) - x(3) < 0 \\ &x(3) - x(4) < 0 \\ &\ldots\ldots \\ &x(N-1) - x(N) < 0 \end{aligned}$$

These constraints are imposed by specifying the elements of matrices A and b. The size of matrix A is $(N-1) \times N$ with $0, -1\ or\ +1$ as its elements and matrix b is a null matrix with size $N \times 1$. For example, if 5 switching instants per quarter cycle are required, then the linear inequality constraints are

$$\begin{aligned} &x(1) - x(2) < 0 \\ &x(2) - x(3) < 0 \\ &x(3) - x(4) < 0 \end{aligned}$$

$$x(4) - x(5) < 0$$

And the matrices A and b becomes,

$$A = \begin{bmatrix} 1 & -1 & 0 & 0 & 0 \\ 0 & 1 & -1 & 0 & 0 \\ 0 & 0 & 1 & -1 & 0 \\ 0 & 0 & 0 & 1 & -1 \end{bmatrix} \; and \; b = \begin{bmatrix} 0 \\ 0 \\ 0 \\ 0 \end{bmatrix} \; such \; that \; A * x < b$$

Therefore, we can say that $A(i,i) = 1 \; and \; A(i,i+1) = -1$, where $i = 1,2 \ldots N-1$ and all the other elements of $A$ are zero.

iii. ***Specifying linear equality constraints***

As there are no linear equality constraints for harmonic elimination/minimization problem, the equality matrices $Aeq \; and \; beq$ are set to NULL matrices.

$$Aeq = [\;\;] \; and \; beq = [\;\;]$$

iv. ***Specifying lower and upper limits of the variables***

The lower and upper bounds on the solution set are imposed by specifying the values of $lb$ and $ub$.

$$lb = 0$$

$$ub = \begin{cases} 60^0 & for \; [0 - 60^0] solution \; set \\ 90^0 & for \; [0 - 90^0] solution \; set \end{cases}$$

v. ***Specifying the nonlinear constraints (nonlcon)***

$nonlcon$ is a function that computes the nonlinear inequality constraints $c(x) \leq 0$ and $ceq(x) = 0$. It accepts a vector x and returns two vectors $c$ and $ceq$. The vector $c$ contains the nonlinear inequalities and $ceq$ contains the nonlinear equalities. The function $nonlcon$ can be specifies as function handle similar to objective function i.e.,

$$x = fmincon(@objfun, x0, A, b, Aeq, beq, lb, ub, @confun)$$

Where, $confun$ is a MATLAB function which defines the nonlinear equality and inequality constraints of the problem.

There is only one non linear equality constraint,$V_1 = M$, which can be written in the equality form as,

$$V_1 - M = 0$$

Where, $V_1$ is the amplitude of the fundamental voltage and $M$ is the Modulation Index.

Therefore, the linear equality constraint $ceq$ becomes,

$$ceq = V_1 - M$$

As there are no inequality constraints, vector $c$ can be set to null values.

$$c = [\ ]$$

## 4.4 Initial guess to the problem

The problem formulated so far can be solved with the help of nonlinear constrained optimization program ($fmincon$) to get the switching angles. But, the key issue is the selection of the initial guess, because it is related with the convergence of the solution. It should be sufficiently close to the exact solution to guarantee the convergence. In the present work, the initial guess is obtained by two ways based on the symmetry properties of the exact switching patterns. They are,

1. straight line approximation algorithm
2. solution at zero modulation index

### 4.4.1 Straight line approximation algorithm

The straight line approximation algorithm is proposed by P.Enjeti and J. F. Lindsay in 1987 based on the study of exact switching trajectories [6]. For odd values of *N*, it is noted that with the exception of $\alpha_1$, the odd switching trajectories $(\alpha_3, \alpha_5, \alpha_7, \ldots)$ exhibit negative slopes and even switching trajectories $(\alpha_2, \alpha_4, \alpha_6, \ldots)$ exhibit positive slopes. These trajectories of exact switching angles exhibit near-straight line behavior and at zero modulation index these angles are separated by $120/(N+1)$ degrees. This symmetry is valid for all values of odd *N* greater than 3.

The approximation algorithm generates two sets of straight lines with positive and negative slopes that closely approximate the exact solution pattern of the nonlinear equations. The general algorithm is valid for all odd values of *N* greater than 3. Fig 4.1 shows the exponential behavior of the average positive slope $m_p$ of the odd switching instants against number of switching angles per quarter cycle *N*. A similar characteristic behavior of the negative-slope $m_n$ trajectories is also noted.

A least squares exponential fit algorithms is employed to characterize $m_p$ and $m_n$. The slopes $m_p$ and $m_n$ can be expressed as functions of *N* by,

$$m_p = 5.0391\, e^{-0.07125*N} \quad \ldots\ldots\ldots\ldots\ldots (4.1)$$

$$m_n = -6.4384\, e^{-0.05672*N} \quad \ldots\ldots\ldots\ldots\ldots (4.2)$$

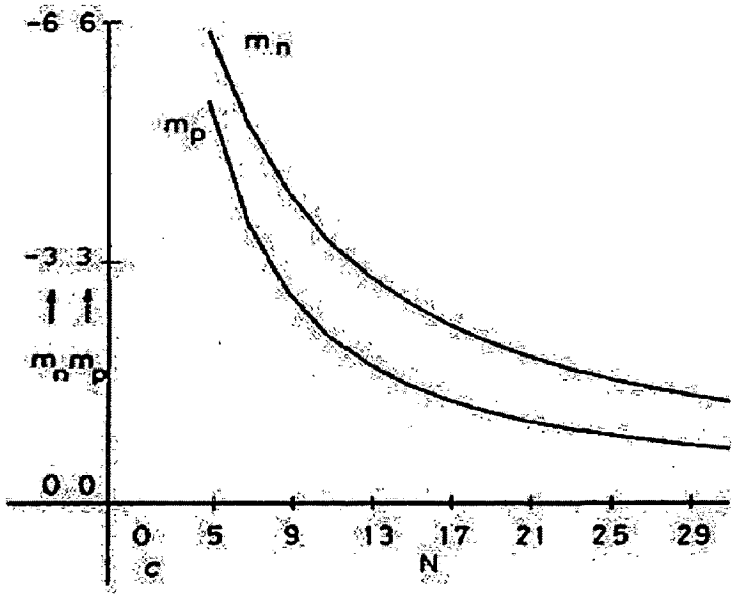


**Figure 4.1: Variation of average slopes $m_p$ and $m_n$ against $N$ [6]**

For the generalized straight-line approximation of the switching angles, as $\alpha_k = m.M + C_k$, the constant term $C_k$ has to be determined. At zero modulation index, the constant $C_k$ can be expressed as follows:

$$C_1 = 0$$
$$C_2 = \frac{120}{(N+1)}$$
$$C_k = C_{k+1} = \frac{(K+1)60}{N+1} \quad for\ 3 \leq k \leq N-1, odd\ k$$
$$C_{N-2} = \frac{(N-1)60}{N+1}$$
$$C_{N-1} = 60$$
$$C_N = 0$$

The generalized positive slope lines can be expressed as,

$$\alpha_k = m_p.M + C_k \quad for\ k = 1,2,4 \ldots \qquad \ldots\ldots\ldots\ldots\ldots (4.3)$$

and the negative-slope lines are given by,

$$\alpha_k = m_n.M + C_k \quad for\ k = 3,5,7 \ldots \qquad \ldots\ldots\ldots\ldots\ldots (4.4)$$

Where, $M$ is the modulation index. The fig 4.2 illustrates the proposed algorithm where the dotted lines are the straight-line approximations of the exact switching patterns.

This algorithm ensures convergence by closely approximating the exact switching angles and thus reduces the computational time to great extent. But, it fails to approximate the switching angles when the number of switchings per quarter cycle is even and cannot guarantee convergence for harmonic minimization problem.

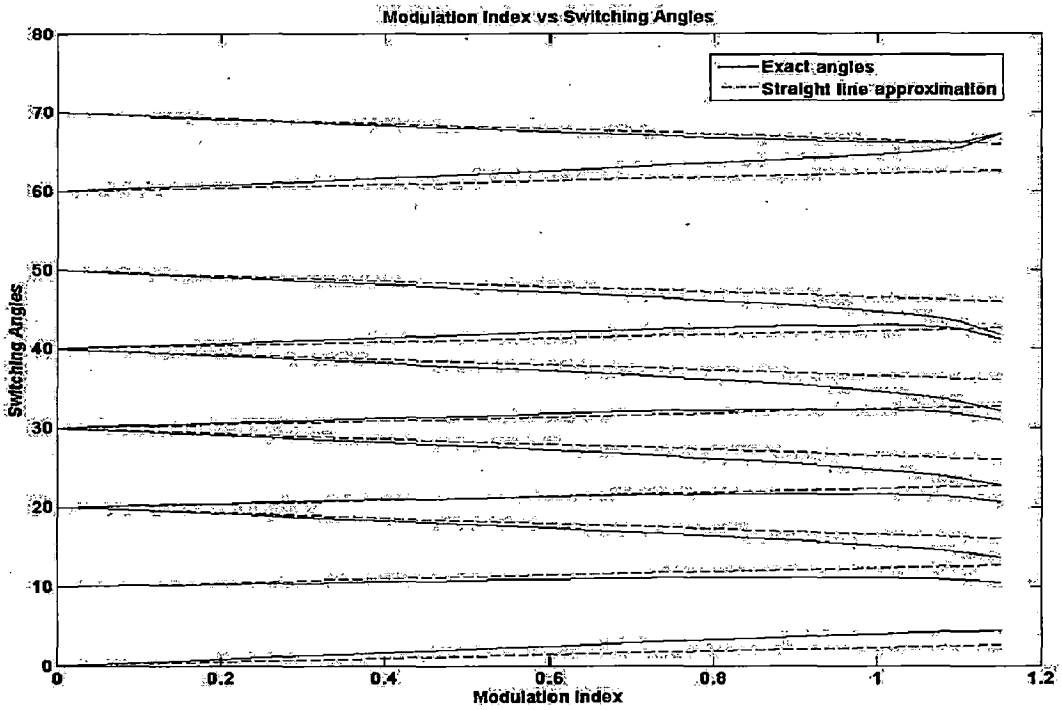


**Figure 4.2: Straight line approximation of exact switching pattern (N=11)**

### 4.4.2 Solution at zero modulation index

At zero modulation index, the equation set 3.24 can take up the following form

$$[1 + 2(-\cos\alpha_1 + \cos\alpha_2 - \cos\alpha_3 + \cdots + (-1)^N \cos\alpha_N)] = 0$$
$$[1 + 2(-\cos 5\alpha_1 + \cos 5\alpha_2 - \cos 5\alpha_3 + \cdots + (-1)^N \cos 5\alpha_N)] = 0$$
$$[1 + 2(-\cos 7\alpha_1 + \cos 7\alpha_2 - \cos 7\alpha_3 + \cdots + (-1)^N \cos 7\alpha_N)] = 0 \qquad \ldots\ldots (4.5)$$
$$\vdots$$
$$[1 + 2(-\cos n\alpha_1 + \cos n\alpha_2 - \cos n\alpha_3 + \cdots + (-1)^N \cos n\alpha_N)] = 0$$

From the above equations, we can say that, the variable terms in all equations are equal to 0.5. This can be written as,

$$\cos(6i \pm 1)\alpha_1 - \cos(6i \pm 1)\alpha_2 + \cos(6i \pm 1)\alpha_3 - \cdots + (-1)^{N+1} \cos(6i \pm 1)\alpha_N = 0.5 \qquad \ldots\ldots (4.6)$$

Where, $i = \begin{cases} 0,1,2,3,\ldots N/2 & for\ even\ n \\ 0,1,2,3,\ldots (N-1)/2 & for\ odd\ n \end{cases}$

The angles satisfying equation 4.6 are the optimal switching angles for the harmonic elimination problem at zero modulation index. These switching angles can closely approximate the optimal switching angles for a modulation index greater than and near to zero. Therefore, these angles can be given as the initial guess to the problem when the modulation index is close to zero. This process of computing the optimal switching

angles is repeated for higher values of modulation indexes in small incremental steps and the optimal switching angles of the previous step is taken as the initial guess to the next step. The switching angles are calculated for a given range of modulation index and step size. The step increment in the modulation index should be sufficiently small for ensuring convergence.

The solution to the equation 4.6 is considered separately for odd and even values of $N$ and the following relations are used in obtaining the solution

$$\cos(6i \pm 1)\alpha = \begin{cases} 0.5 & for\ \alpha = \pi/3 \\ 1 & for\ \alpha = 0 \end{cases} \quad \ldots\ldots\ldots\ldots\ldots\ldots (4.7)$$

and

$$\cos(6i \pm 1)(\pi/3 - \alpha) - \cos(6i \pm 1)(\pi/3 + \alpha) = \cos(6i \pm 1)\alpha \quad \ldots\ldots\ldots (4.8)$$

***Odd N:***

For odd $N$, the equation 4.6 is always satisfied if the angles $\alpha_1, \alpha_2, \alpha_3, \ldots \alpha_N$ occupy values between $0^0$ and $90^0$ and such that these values are integral multiples of an angular unit $\theta$, given by

$$\theta = \frac{120}{(N+1)} \ degrees$$

Two sets of solutions have been identified; one is in $0^0$ & $60^0$ range and other in $0^0$ & $90^0$ range.

i. $0^0$-$60^0$ solution:

For $0^0$-$60^0$ range, the equation 4.6 is satisfied if the angles $\alpha_1, \alpha_2, \alpha_3, \ldots \alpha_N$ satisfy the following constraints

$$\alpha_1 = \alpha_2, \alpha_3 = \alpha_4, \alpha_5 = \alpha_6, \ldots, \alpha_{N-2} = \alpha_{N-1}$$
$$and\ \alpha_N = 60^0$$

With these angles,

a. The last term of the equation 4.6 will be equal to the required value 0.5
b. All the remaining terms cancels in pairs

As the switching angles are multiples of the angular unit $\theta$, we can write the values of the angles as

$$\alpha_1 = \alpha_2 = \theta,$$
$$\alpha_3 = \alpha_4 = 2\theta,$$
$$\alpha_5 = \alpha_6 = 3\theta,$$

...

$$\alpha_{N-2} = \alpha_{N-1} = \frac{(N-1)}{2}\theta$$
$$and\ \alpha_N = 60^0$$

For example, if 9 switchings per quarter cycle ($N = 9$) are considered, then the angles at zero modulation index can have the following values

$$\alpha_1 = \alpha_2 = 12^0, \alpha_3 = \alpha_4 = 24^0, \alpha_5 = \alpha_6 = 36^0, \alpha_7 = \alpha_8 = 48^0$$
$$and\ \alpha_9 = 60^0$$

ii. $0^0$-$90^0$ solution:

For $0^0$-$90^0$ range, the solution to the equation 4.6 at zero modulation index is given by

$$\alpha_1 = 0,$$
$$\alpha_2 = \theta,$$
$$\alpha_3 = \alpha_4 = 2\theta,$$
$$\alpha_5 = \alpha_6 = 3\theta,$$
...
$$\alpha_{N-4} = \alpha_{N-3} = \frac{(N-3)}{2}\theta$$
$$\alpha_{N-2} = 60 - \theta,$$
$$\alpha_{N-1} = 60,$$
$$and\ \alpha_N = 60 + \theta$$

With these angles,

a. The cosine terms of angles $\alpha_1$ and $\alpha_{N-1}$ in equation 4.6 sum up to 0.5
b. Sum of second and (N-2)$^{th}$ terms cancels the N$^{th}$ term
c. Remaining all terms cancels in pairs

It should be noted that, solution does not exist at zero modulation index when $N$ is less than 5.

For example, if 9 switchings per quarter cycle ($N = 9$) are considered, then the angles at zero modulation index can have the following values

$$\alpha_1 = 0^0,$$
$$\alpha_2 = 12^0,$$
$$\alpha_3 = \alpha_4 = 24^0, \alpha_5 = \alpha_6 = 36^0,$$
$$\alpha_7 = 48^0,$$
$$\alpha_8 = 60^0$$
$$and\ \alpha_9 = 72^0$$

***Even N:***

We can say that, for even values of *N*, the equation 4.6 will have even number of cosine terms with the last term becoming negative. Here also two sets of solutions have been identified ($0^0$-$60^0$ range and $0^0$-$90^0$ range). For even values of *N*, the angular unit $\theta$ found to have different values for different ranges ($0^0$-$60^0$ range and $0^0$-$90^0$ range) of the solution.

i. $0^0$-$60^0$ solution:

For $0^0$-$60^0$ range, solution to the equation 4.6 for even number of switching angles per quarter cycle are given by,

$$\alpha_1 = 0,$$
$$\alpha_2 = \alpha_3 = \theta,$$
$$\alpha_4 = \alpha_5 = 2\theta,$$
$$\ldots$$
$$\alpha_{N-2} = \alpha_{N-1} = \frac{(N-2)}{2}\theta$$
$$and\ \alpha_N = 60^0$$

where, $\theta = \frac{120}{N}$

With these switching angles,

a. The difference of the cosine terms of angles $\alpha_1$ and $\alpha_N$ in equation 4.6 gives 0.5
b. Remaining all terms cancels in pairs

For example, if 8 switching angles per quarter cycle are considered, then the angles at zero modulation index can have the following values

$$\alpha_1 = 0^0,$$
$$\alpha_2 = \alpha_3 = 15^0,$$
$$\alpha_4 = \alpha_5 = 30^0, \alpha_6 = \alpha_7 = 45^0,$$
$$and\ \alpha_8 = 60^0$$

ii. $0^0$-$90^0$ solution:

The solution to the equation is given by

$$\alpha_1 = \theta,$$
$$\alpha_2 = \alpha_3 = 2\theta,$$
$$\alpha_4 = \alpha_5 = 3\theta,$$
$$\ldots$$

$$\alpha_{N-4} = \alpha_{N-3} = \frac{(N-2)}{2}\theta$$
$$\alpha_{N-2} = 60 - \theta$$
$$\alpha_{N-1} = 60$$
$$and\ \alpha_N = 60 + \theta$$

where, $\theta = \frac{120}{N+2}$

With there switching angles,

a. The (N-1)$^{th}$ term in equation 4.6 will be equal to 0.5
b. Sum of N$^{th}$ and (N-2)$^{th}$ terms cancels the first term
c. Remaining all terms cancels in pairs

For example, if 8 switching angles per quarter cycle are considered, then the angles at zero modulation index can have the following values

$$\alpha_1 = 12^0,$$
$$\alpha_2 = \alpha_3 = 24^0,$$
$$\alpha_4 = \alpha_5 = 36^0,$$
$$\alpha_6 = 48^0,$$
$$\alpha_7 = 60^0,$$
$$and\ \alpha_8 = 72^0$$

It should be noted that, for $0^0$-$90^0$ range, solution does not exist at zero modulation index for number of switchings less than 4.

The switching angles derived above will eliminate all the non-triplen harmonics at $M = 0$. Since, the equations 4.7 and 4.8 are true for all values of $i$. These switching angles also coincide with the harmonic minimization solution at $M = 0$, because the THD due to all non-triplen harmonics is also minimum (zero) in this case.

The resulted angles from the above discussion can be used as the initial guess($x0$) to the problem when the modulation index ($M$) is very close to zero ($say\ M = 0.01$). The obtained switching angles after minimization process, started at $x0$, can be used as the initial guess to obtain the optimal angles for next modulation index incremented by step size $\Delta M$. This process is repeated for a given range of modulation index 0.01 to $Mmax$.

## 4.5 Flowchart

The flowcharts given in figures 4.3 to 4.5 illustrate the entire minimization algorithm including the subroutines for objective function and constraint function.

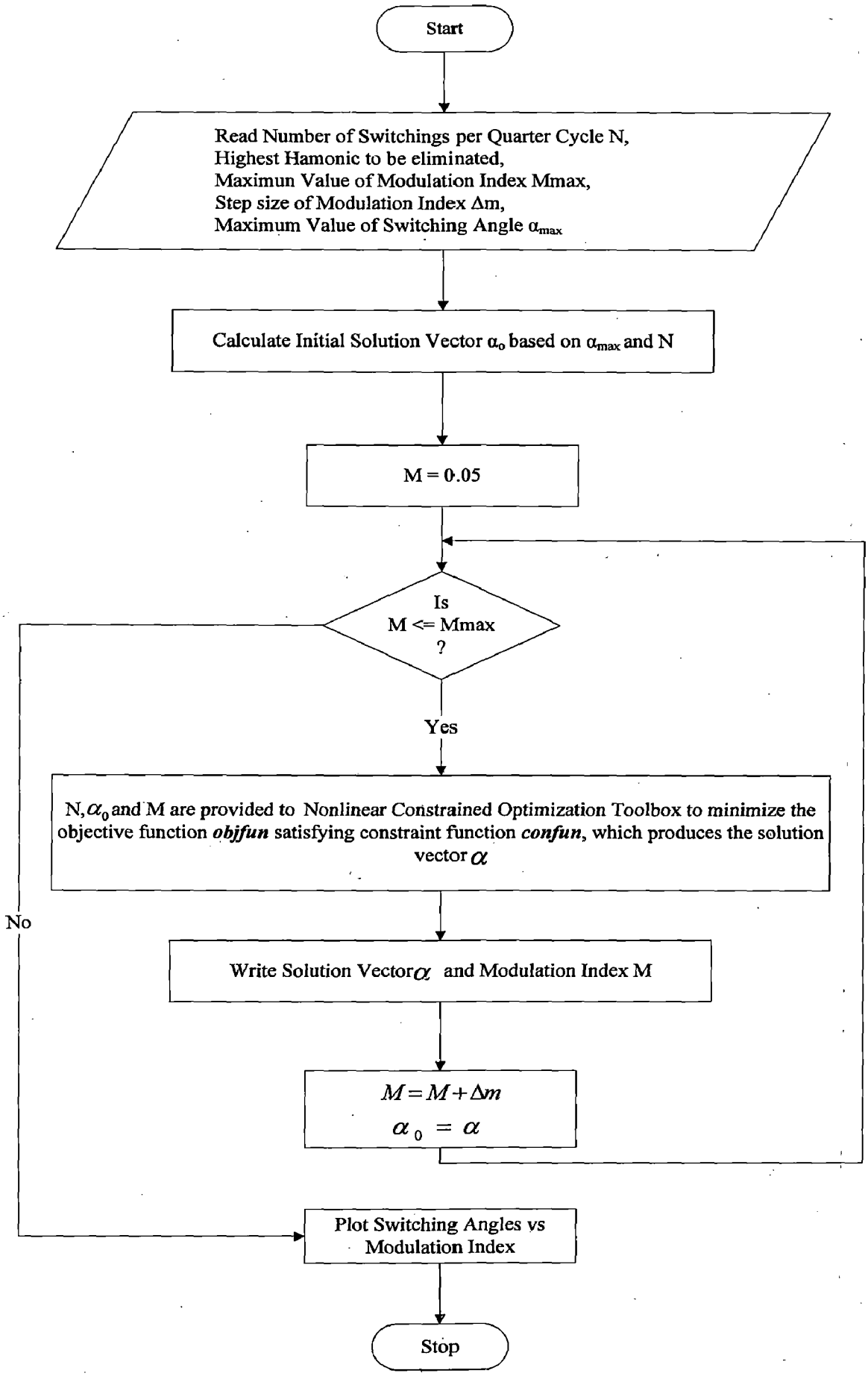


**Figure 4.3: Flowchart of main program**

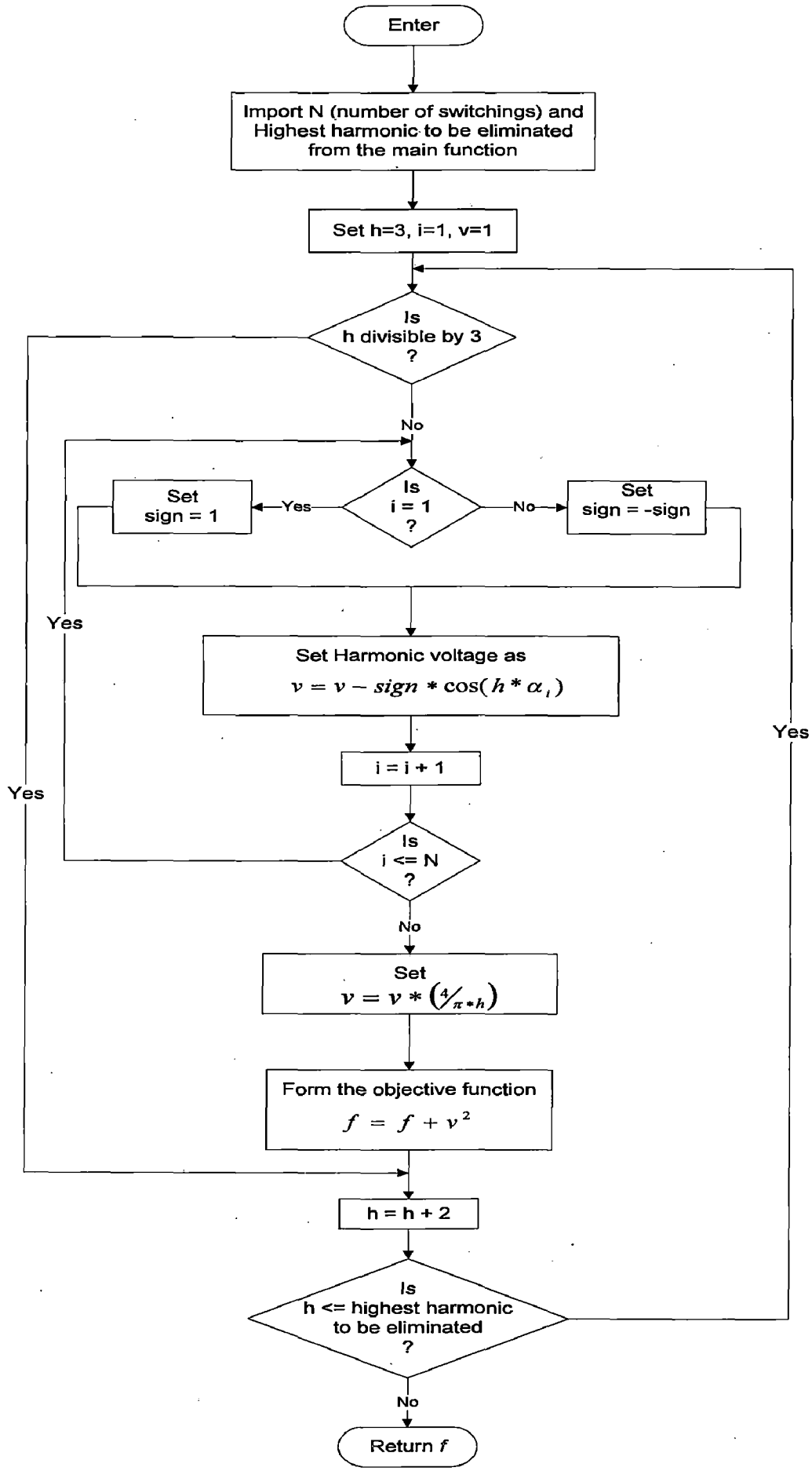


**Figure 4.4: Flowchart for *objfun* subroutine**

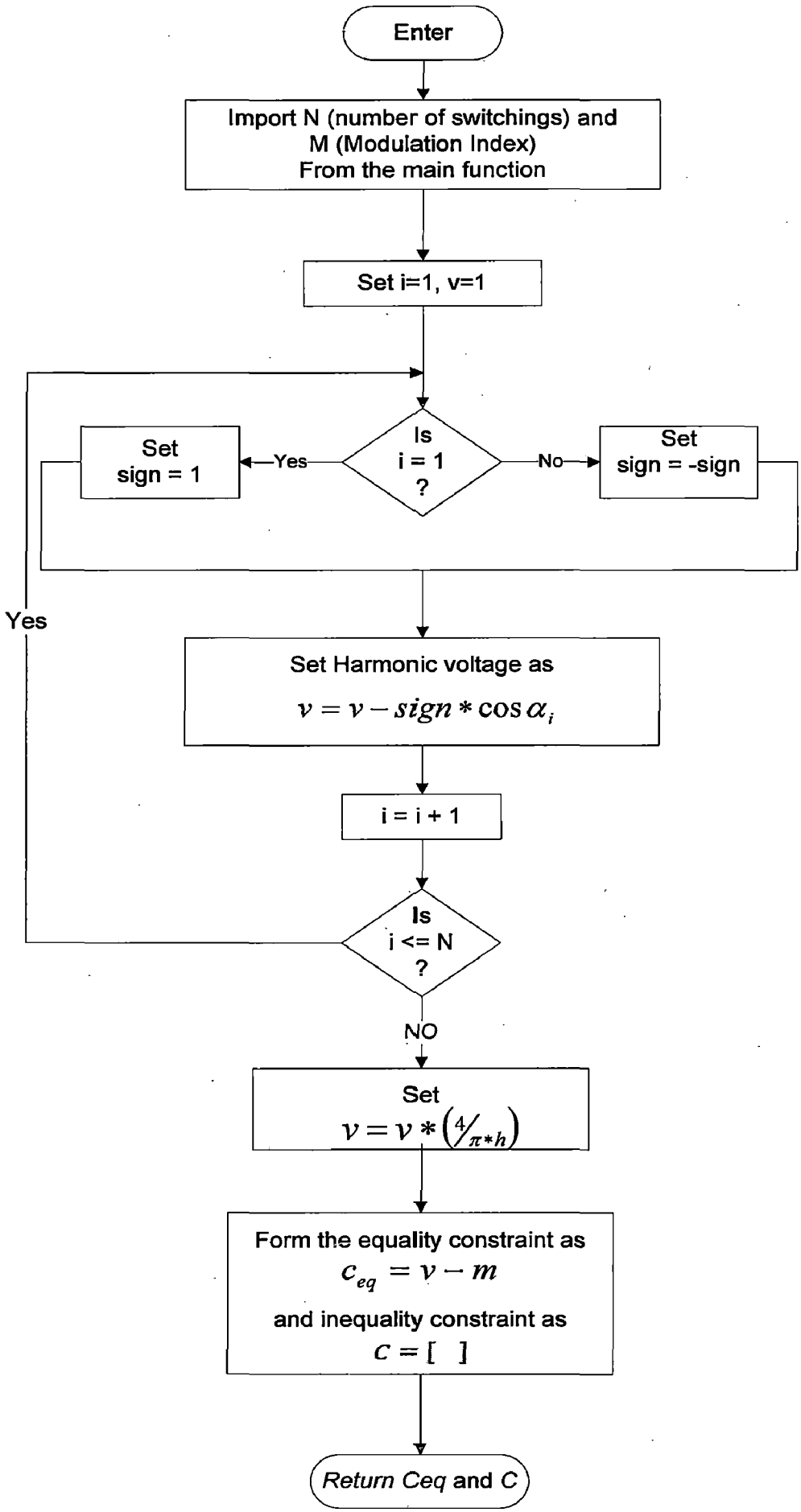


**Figure 4.5: Flowchart for *confun* subroutine**

These flow charts are valid for both harmonic elimination and minimization problems except that, the number of harmonics to be eliminated is kept reasonably high for harmonic minimization problem. Where as, the number of harmonics to be eliminated for harmonic elimination problem is $(3N-1)$ for even values of $N$ or $(3N-2)$ for odd values of $N$.

## 4.6 Switching angle trajectories

The optimal angles for both the harmonic elimination and minimization cases have been obtained by the algorithm described above. The MATLAB program for calculation of these angles is given in appendix A. This section gives the plots of the obtained angles with respect to modulation index for both the harmonic elimination and minimization problems. The plots have been given separately for odd and even values of $N$.

### 4.6.1 Trajectories for odd values of N

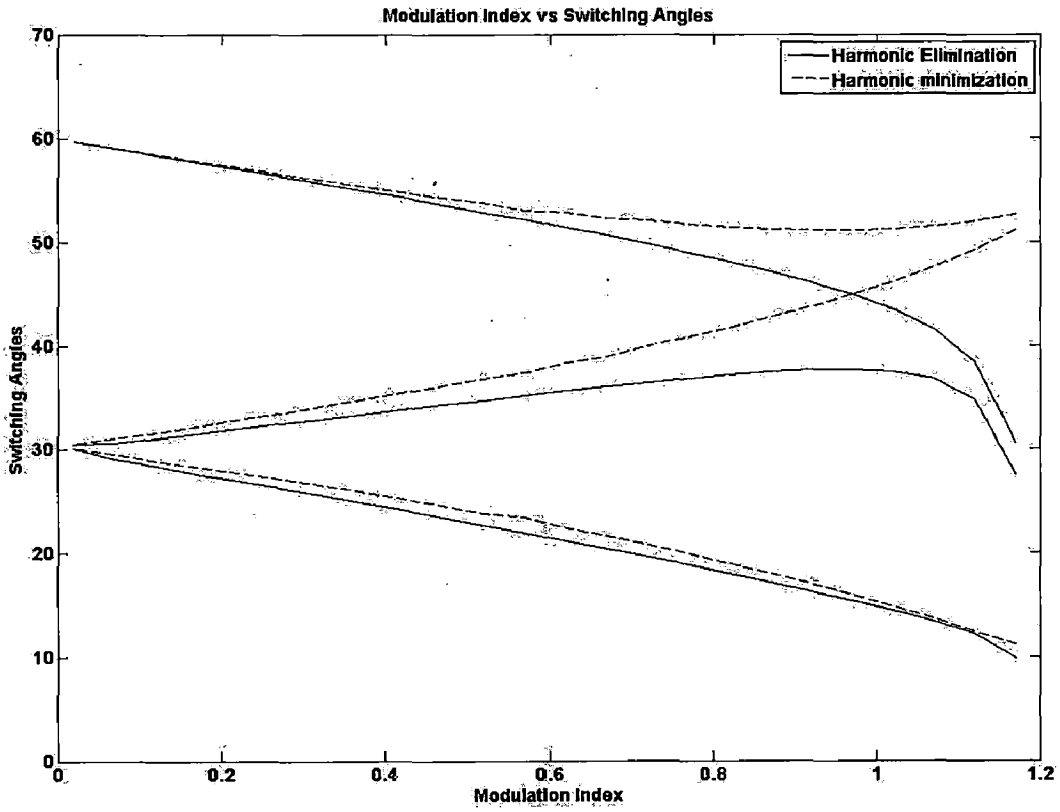


**Figure 4.6: Switching angle trajectories for $N$=3 ($0^0$-$60^0$)**

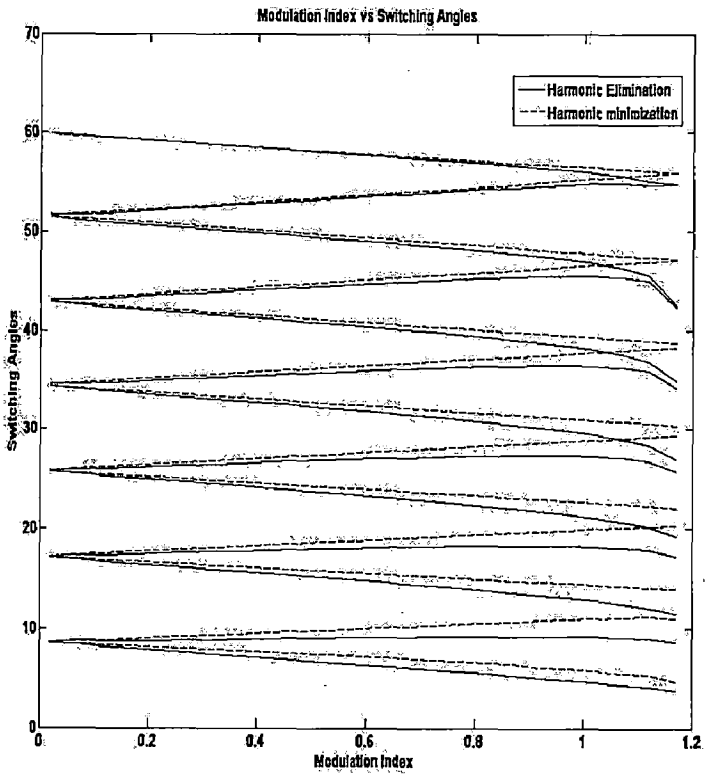


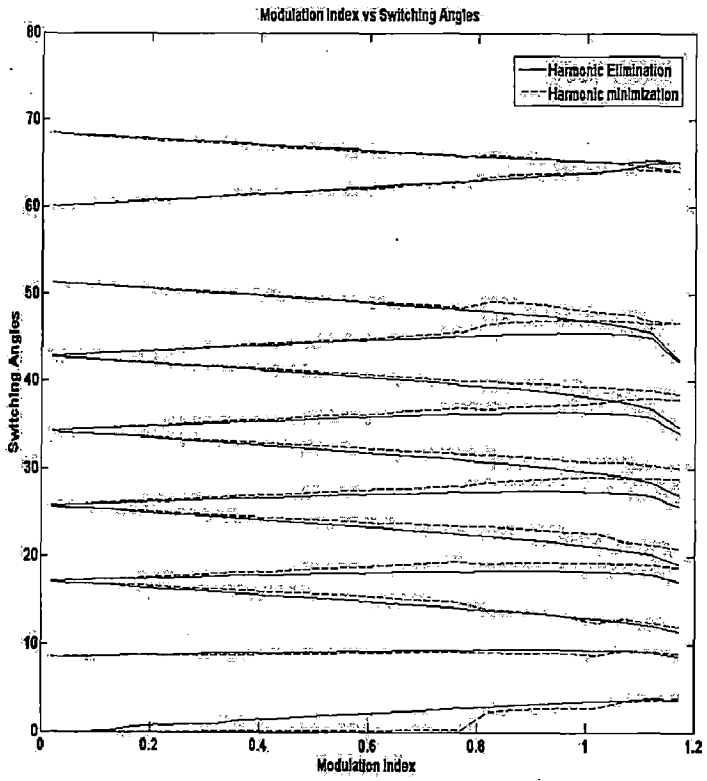


**($0^0$-$60^0$)** **($0^0$-$90^0$)**

**Figure 4.11: Switching angle trajectories for *N*=13**

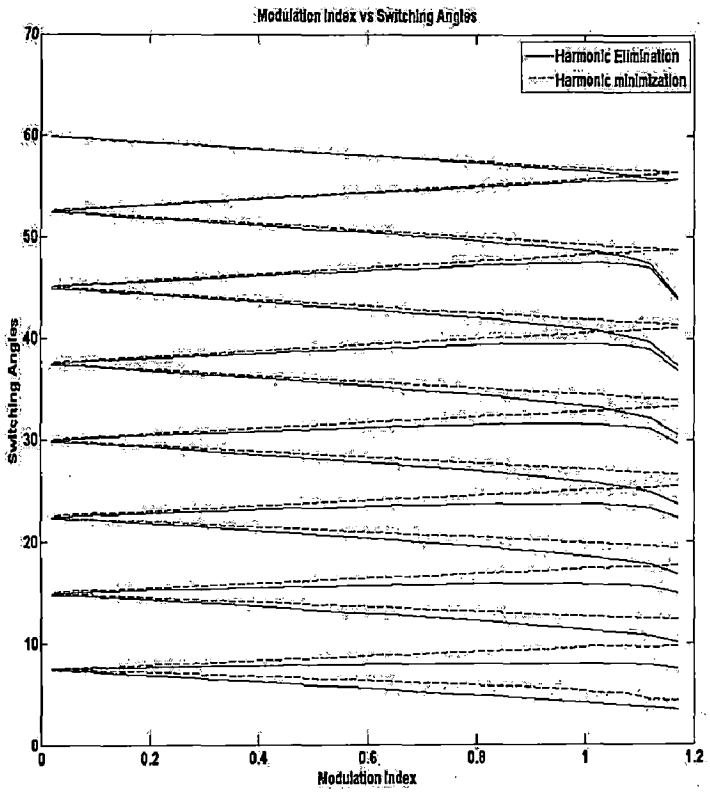


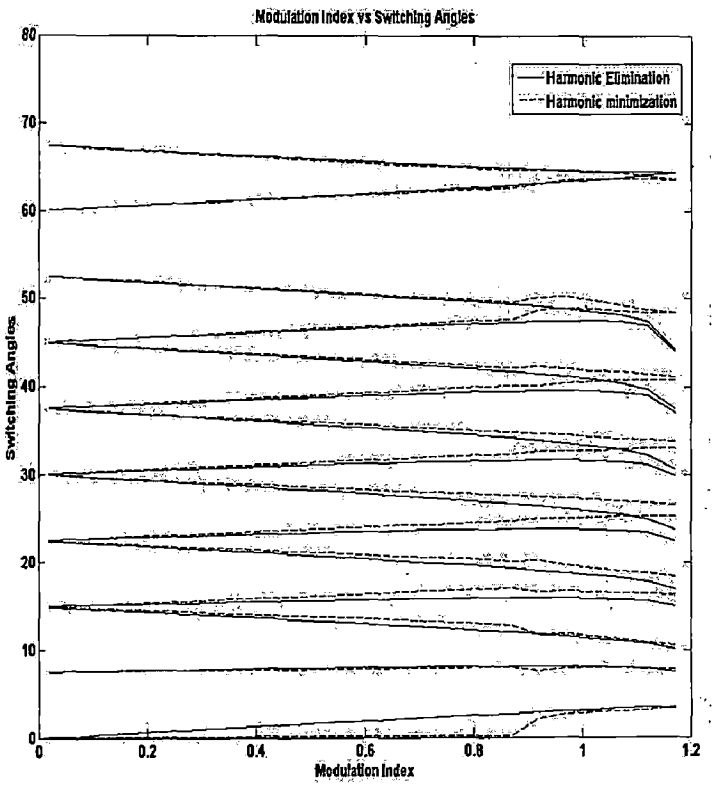


**($0^0$-$60^0$)** **($0^0$-$90^0$)**

**Figure 4.12: Switching angle trajectories for *N*=15**

### 4.6.2 Observations

*Harmonic Elimination*

1. As discussed, at zero modulation index, the equal angle pairs are separated by an angle $120/(N+1)$.
2. For ($0^0$-$60^0$) range, all the odd switching angles $(\alpha_1, \alpha_3, \alpha_5, \alpha_7, \dots)$ have negative slopes and all the even switching angles $(\alpha_2, \alpha_4, \alpha_6, \dots)$ have positive slopes.
3. For ($0^0$-$90^0$) range, the first angle $(\alpha_1)$ and all even switching angles $(\alpha_2, \alpha_4, \alpha_6, \dots)$ have positive slopes and all the remaining odd switching angles $(\alpha_3, \alpha_5, \alpha_7, \dots)$ have negative slopes.
4. The trajectories are linear in the range of modulation index between 0 and 0.8.
5. Above modulation index of 0.8, the trajectories are nonlinear

*Harmonic minimization*

1. The switching angle trajectories in case harmonic minimization follow the similar pattern as that of harmonic elimination. But, they are found to be less linear when compared with harmonic elimination switching trajectories.
2. The nonlinearity in all the angles increases at modulation index greater than 0.8.
3. In case of ($0^0$-$90^0$) range, the first angle $\alpha_1$ varies in a nonlinear manner with respect to modulation index.

### 4.6.3 Trajectories for even values of N

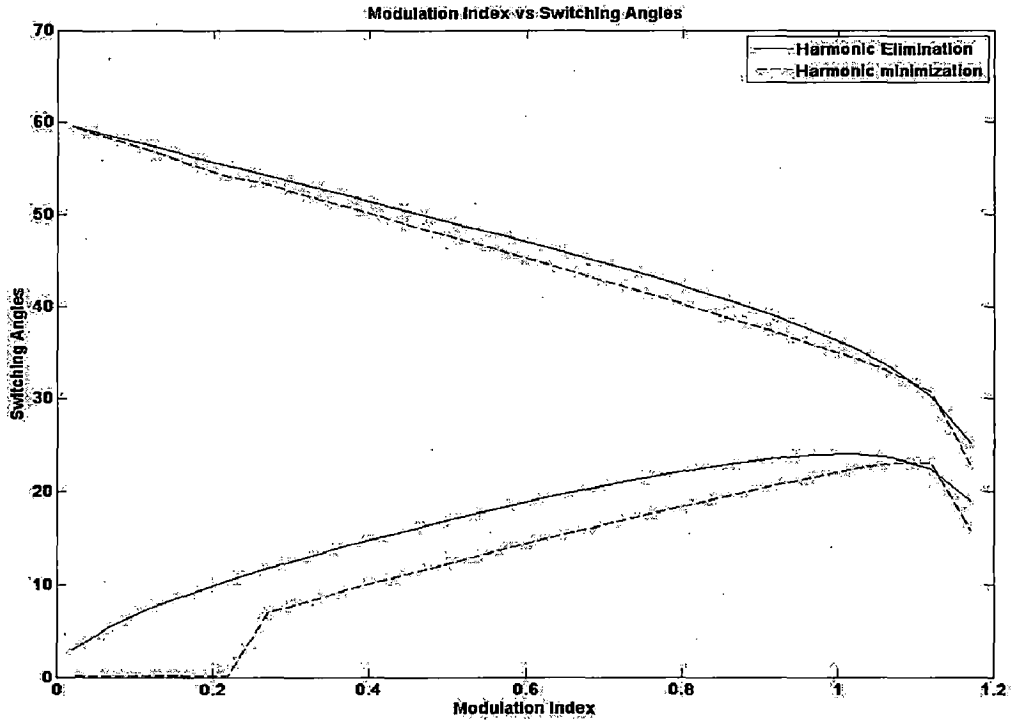


**Figure 4.15: Switching angle trajectories for $N$=2 ($0^0$-$60^0$)**

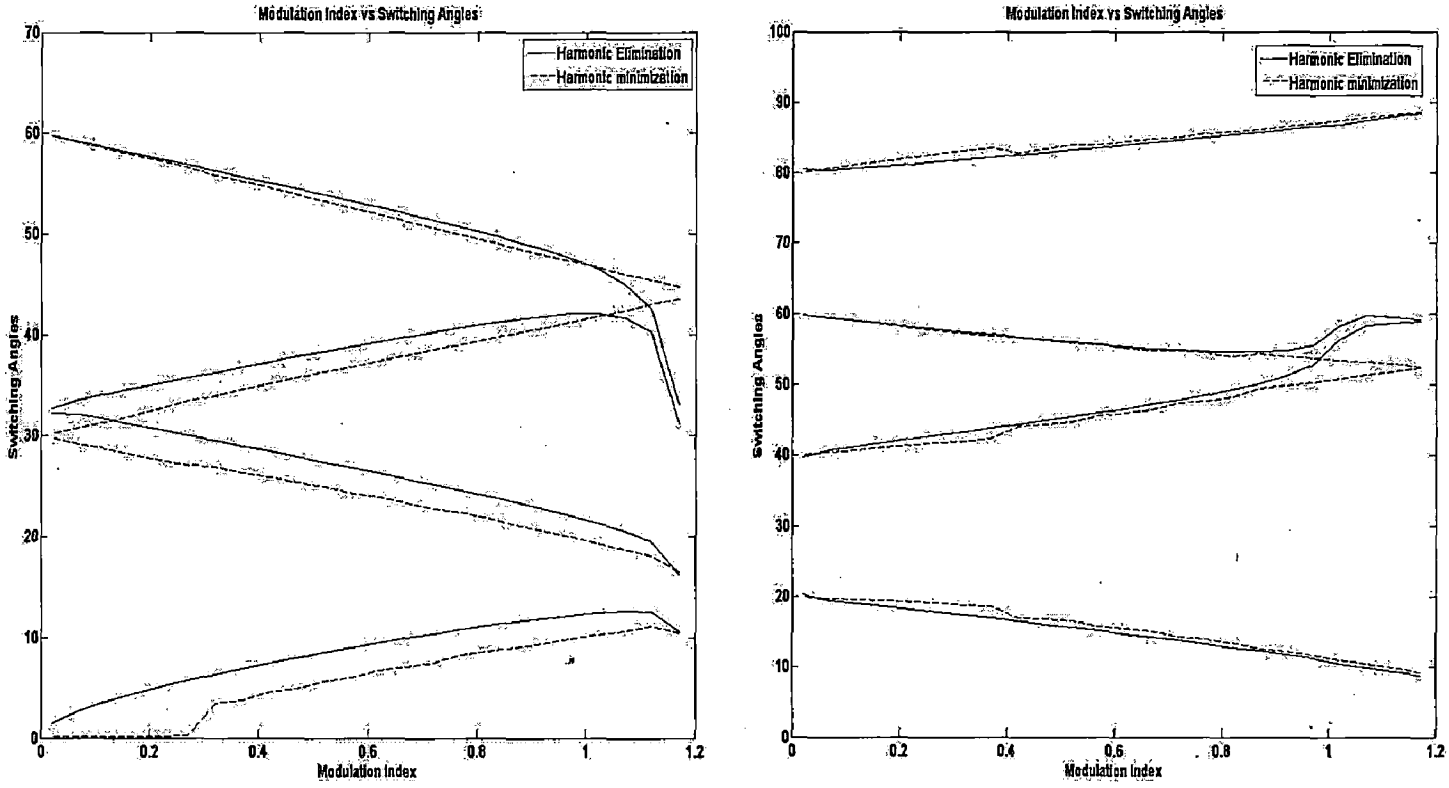


**($0^0$-$60^0$)** **($0^0$-$90^0$)**

**Figure 4.16: Switching angle trajectories for $N$=4**

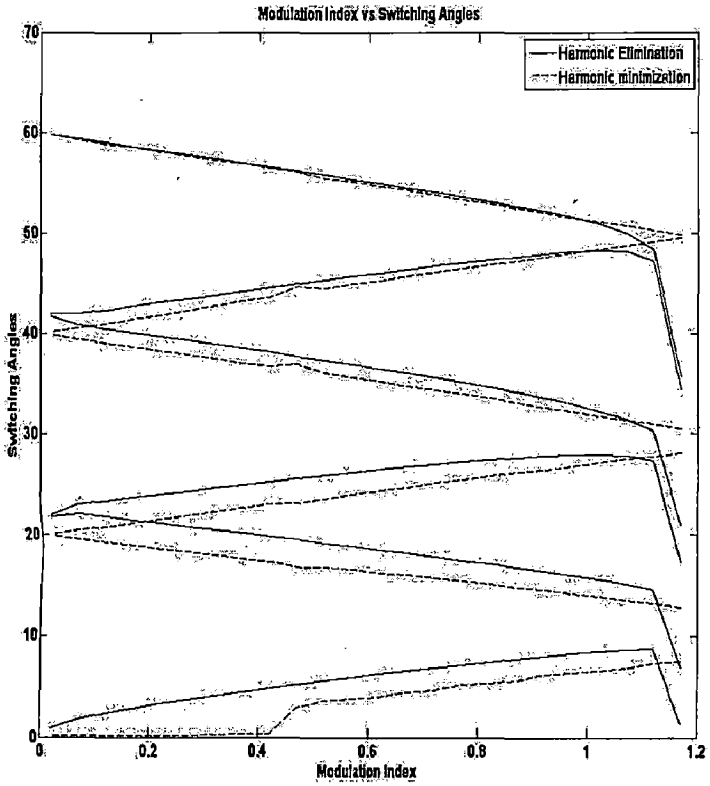


$(0^0\text{-}60^0)$

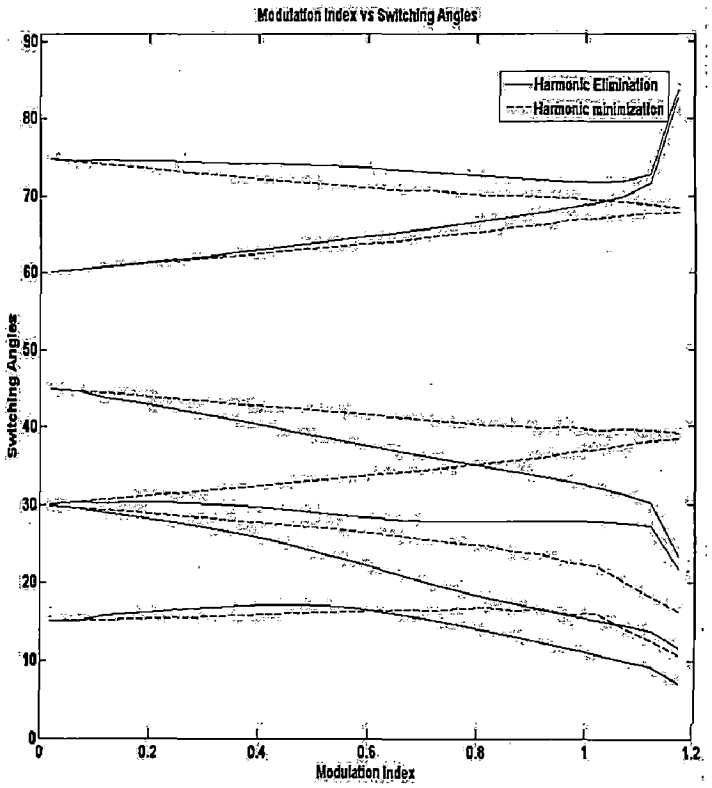


$(0^0\text{-}90^0)$

**Figure 4.17: Switching angle trajectories for *N*=6**

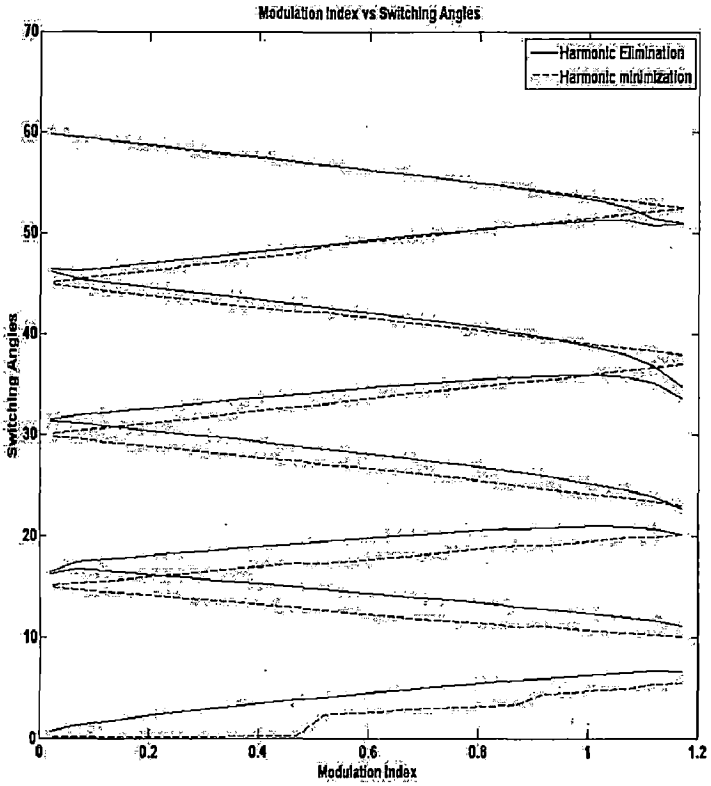


$(0^0\text{-}60^0)$

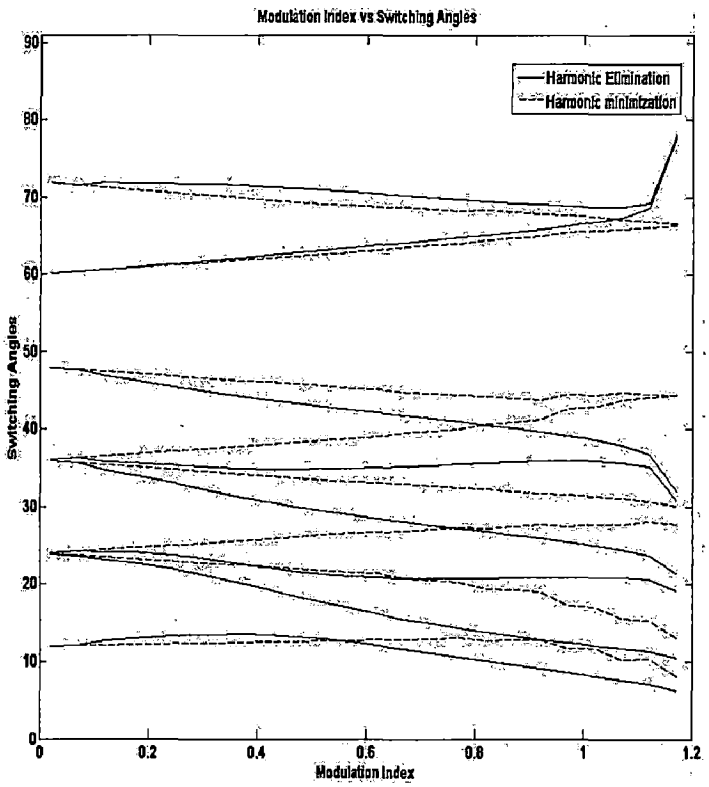


$(0^0\text{-}90^0)$

**Figure 4.18: Switching angle trajectories for *N*=8**

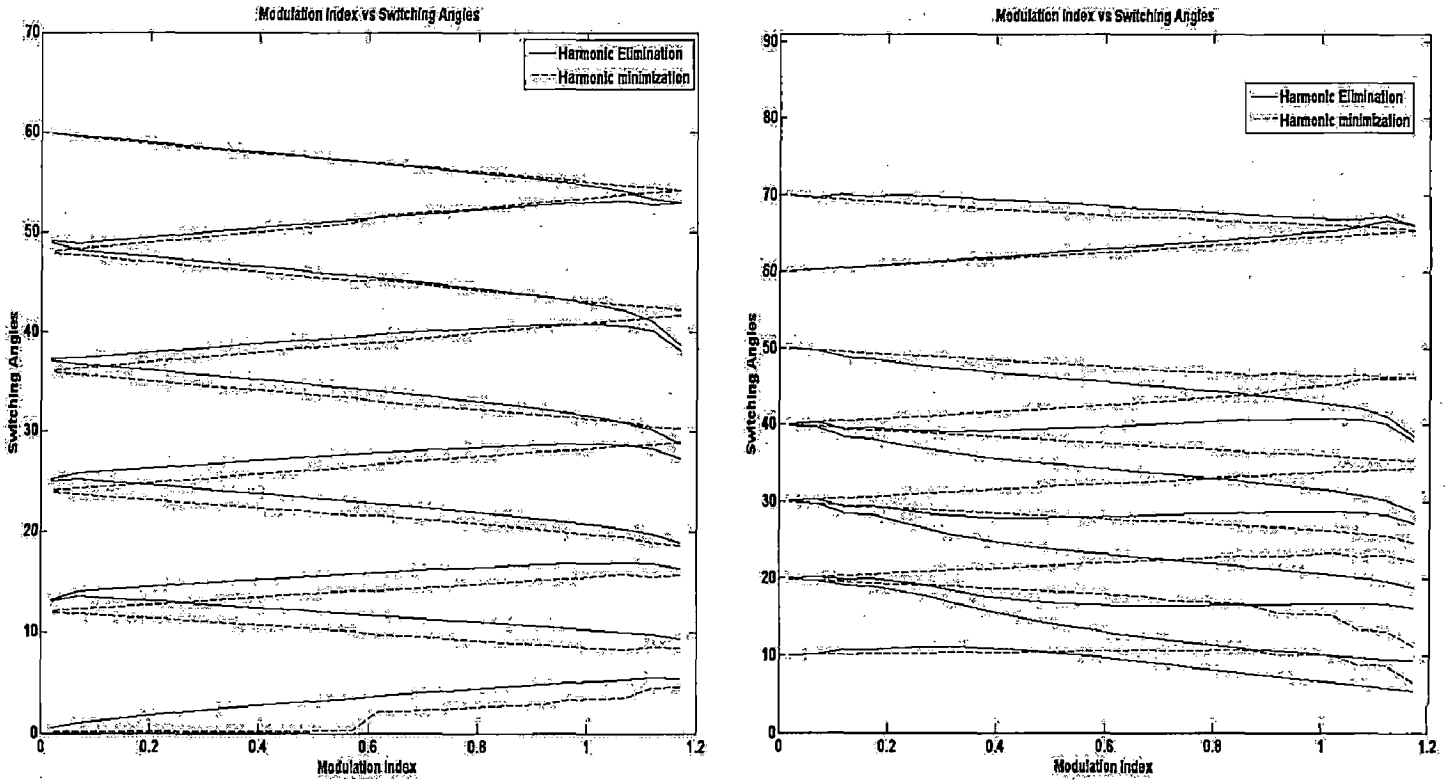


$(0^0\text{-}60^0)$ $(0^0\text{-}90^0)$

**Figure 4.19: Switching angle trajectories for $N$=10**

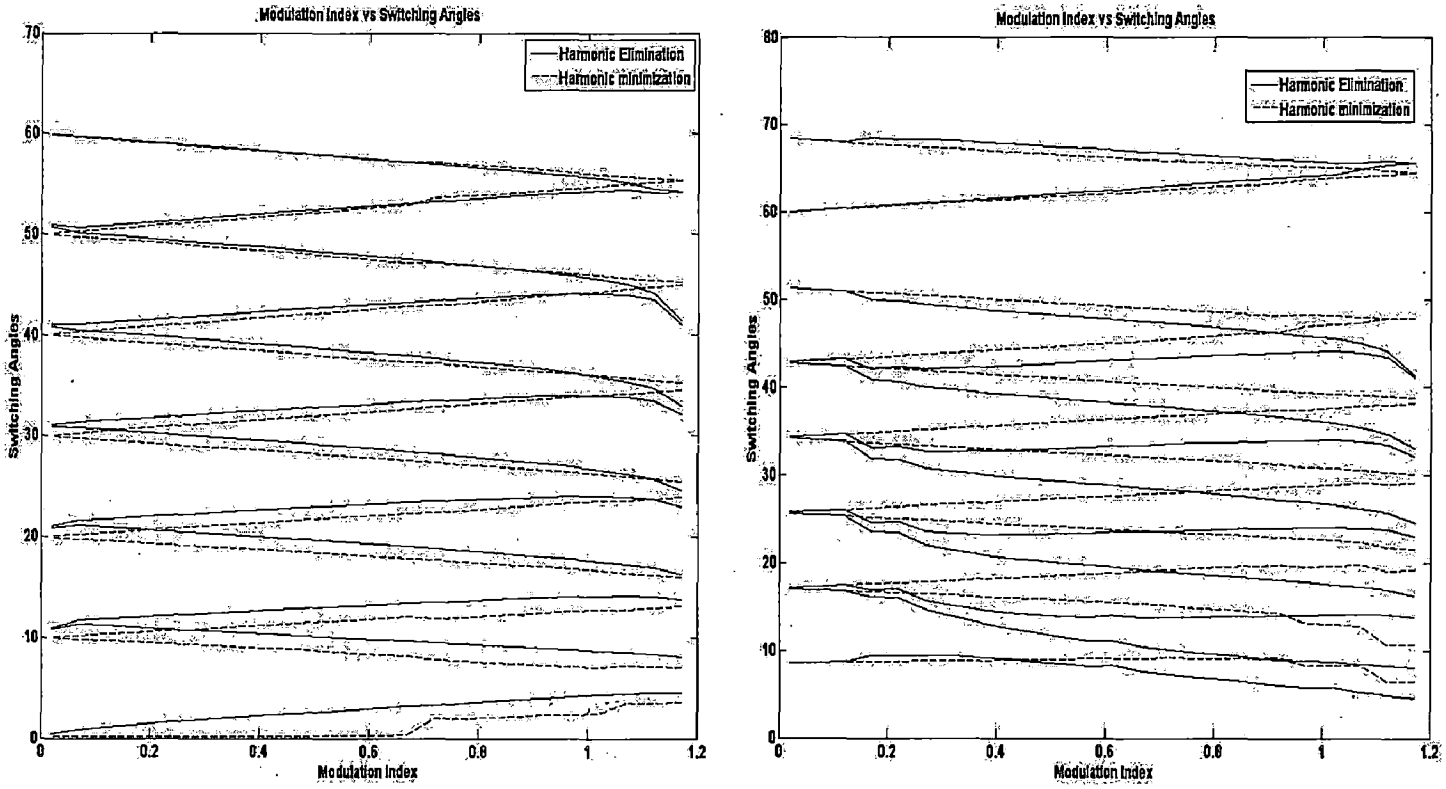


$(0^0\text{-}60^0)$ $(0^0\text{-}90^0)$

**Figure 4.20: Switching angle trajectories for $N$=12**

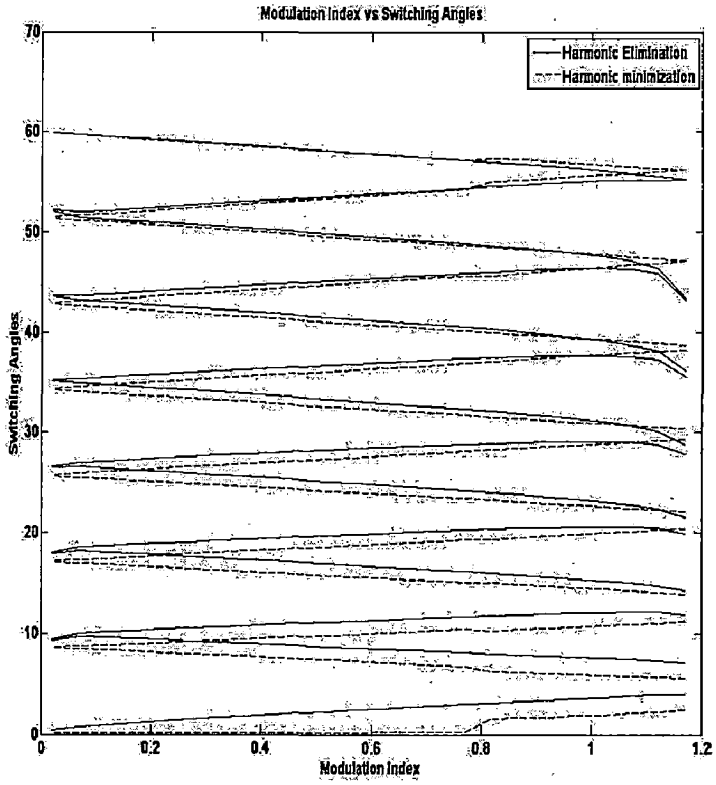


$(0^0\text{-}60^0)$

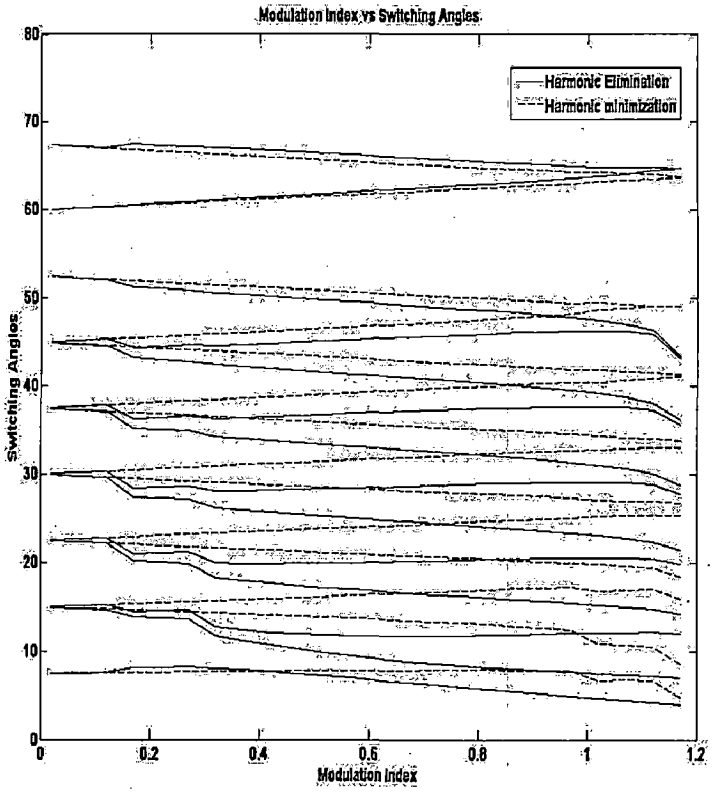


$(0^0\text{-}90^0)$

**Figure 4.21: Switching angle trajectories for *N*=14**

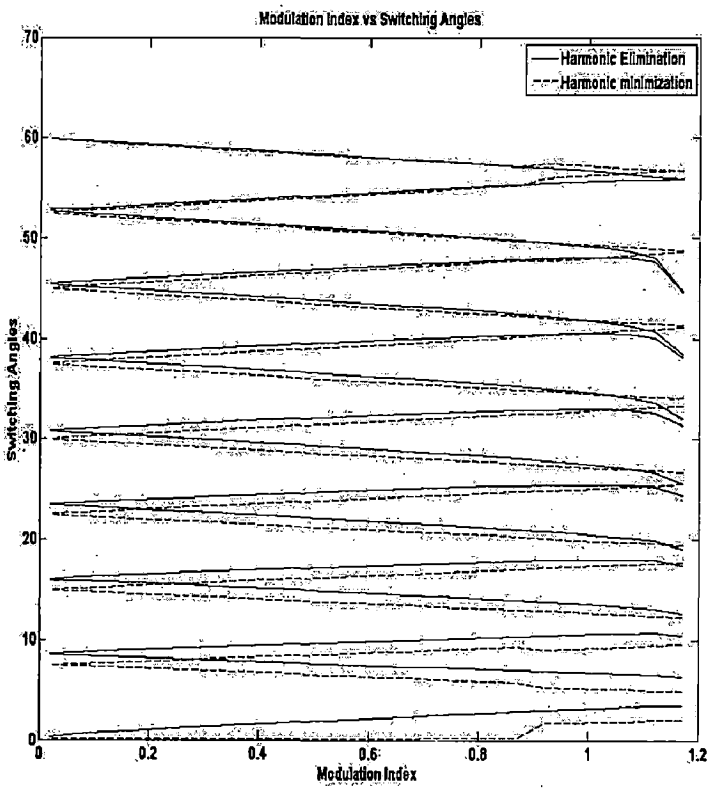


$(0^0\text{-}60^0)$

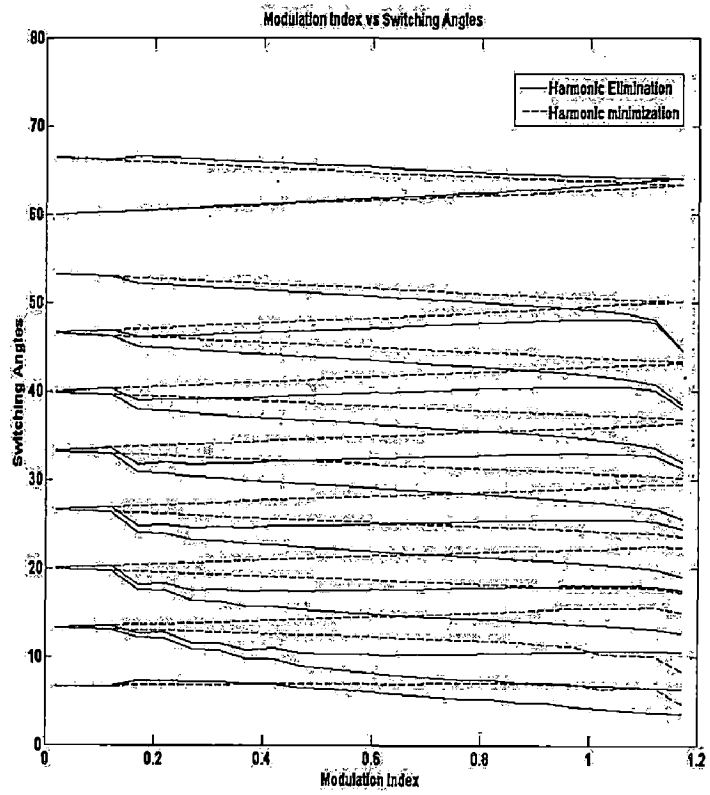


$(0^0\text{-}90^0)$

**Figure 4.22: Switching angle trajectories for *N*=16**

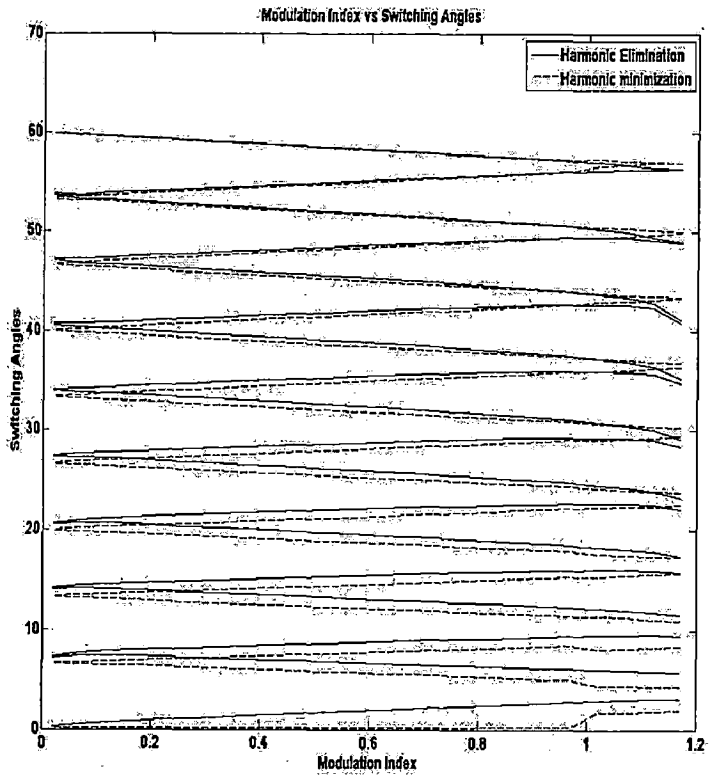


$(0^0\text{-}60^0)$

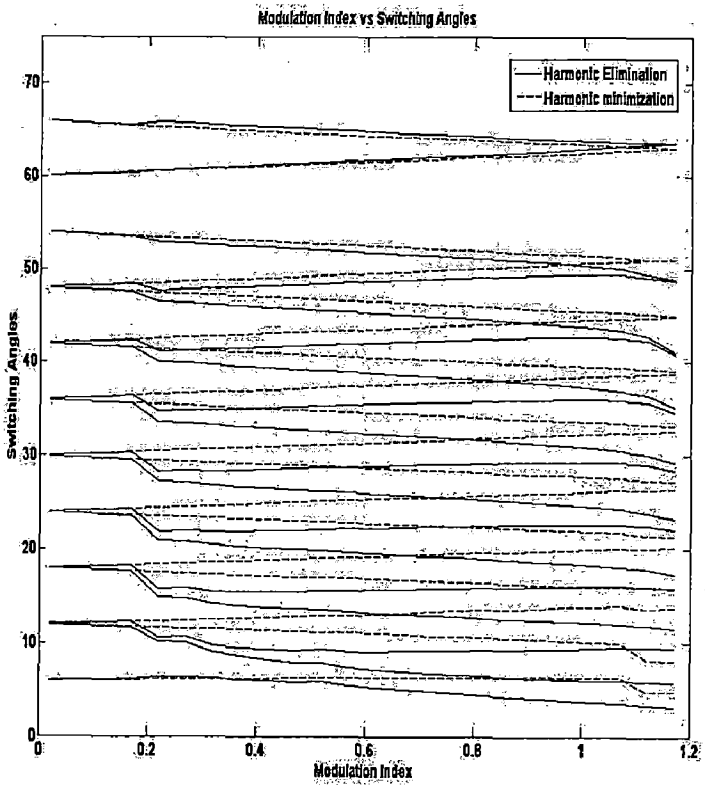


$(0^0\text{-}90^0)$

**Figure 4.23: Switching angle trajectories for $N$=18**

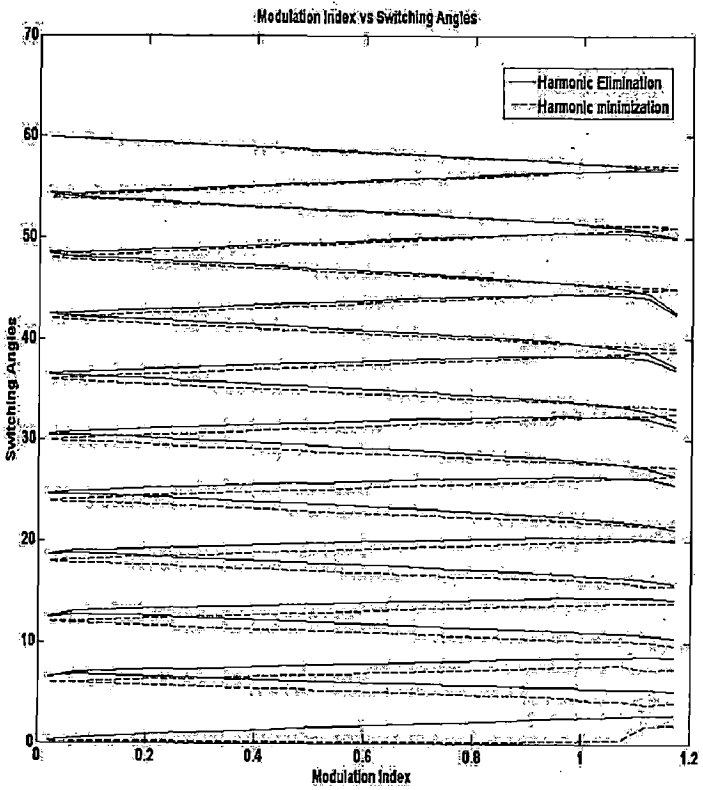


$(0^0\text{-}60^0)$

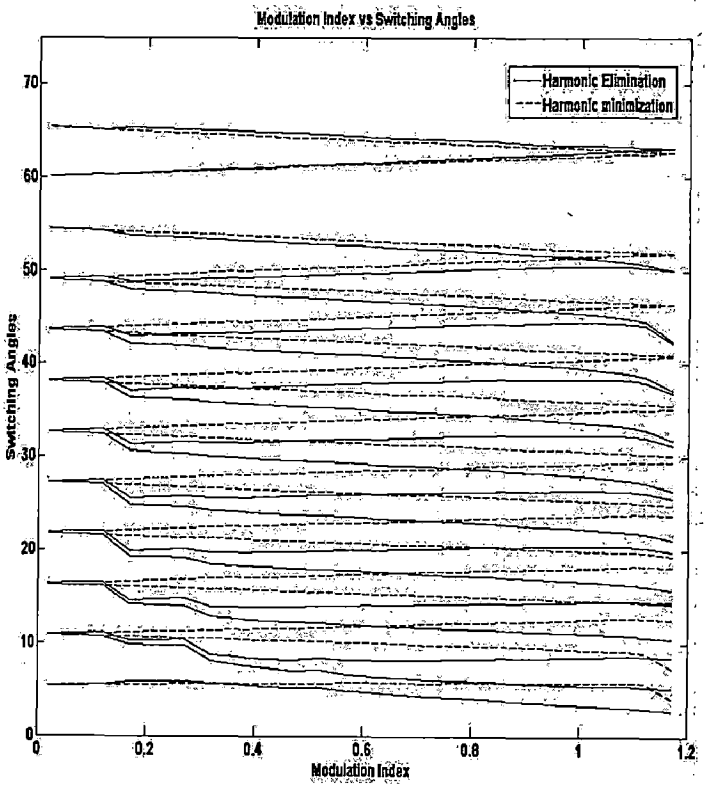


$(0^0\text{-}90^0)$

**Figure 4.24: Switching angle trajectories for $N$=20**

### 4.6.4 Observations

*Harmonic Elimination*

1. Unlike the case of odd value of *N*, the angular spacing between equal angle pairs is not equal. If the angular interval between two equal angle pairs is denoted by $\theta_{ab}$, where $a$ and $b$ points the angles involved, then

$$\theta_{12} > \theta_{34} > \theta_{56} > \cdots > \theta_{(N-1)N}$$

2. For ($0^0$-$60^0$) range, all the odd switching angles $(\alpha_1, \alpha_3, \alpha_5, \alpha_7, \ldots)$ have positive slopes and all the even switching angles $(\alpha_2, \alpha_4, \alpha_6, \ldots)$ have negative slopes.

3. For ($0^0$-$90^0$) range, the switching angle trajectories are found to be nonlinear over the entire range of modulation index which cannot be defined.

*Harmonic minimization*

1. For ($0^0$-$60^0$) range, the first angle $\alpha_1$ is found to nonlinear with respect to modulation index.

2. All the remaining switching trajectories are linear for a modulation index of 0 to 0.9.

3. The switching trajectories are highly nonlinear for a modulation index of above 0.9.

## 4.7 Conclusions

The problem formulation and design for solving the harmonic control problem is discussed in this chapter. As the objective functions formulated involve nonlinear transcendental equations, the convergence of the solution is difficult and multiple solutions may exist. The convergence can be ensured by proper selection of the initial guess to the problem. A simple algorithm for generation of optimal angles is proposed in this chapter and the plots of obtained optimal angles against modulation index are presented for various values of number of switching angles. This algorithm is found to be simple in implementation and fast in convergence. It is also proved to be an appropriate technique when over modulation operation is demanded, since it can find the solution for modulation indexes which are higher than unity.

# Chapter 5
# SIMULINK Implementation of PPWM VSI fed Induction Motor Drive

This chapter gives the detailed implementation of the proposed PPWM fed Induction motor drive model in MATLAB-SIMULINK environment explaining every individual block operation.

## 5.1 Introduction

A SIMULINK model VSI fed induction motor drive is developed for analyzing the performance of the harmonic elimination/minimization method proposed in the previous chapter. For this purpose, mathematical models of three phase induction motor and inverter are developed in MATLAB-SIMULINK environment. The calculated angles are given as the firing pulses to the inverter to generate harmonic controlled waveform. The induction motor developed is fed from the inverter employing selective harmonic elimination/minimization.

The schematic model of the programmed pulse width modulated VSI fed Induction motor drive system is shown in figure 5.1 and the SIMULINK model is shown in figure 5.2. Here, the switching angles obtained from the nonlinear constrained programming are stored in the lookup table for varying modulation index. For a given modulation index, the lookup table produces the switching angles by interpolation-extrapolation method. The switching angles from the lookup table are converted into the firing pulses to the inverter by a firing pulse generator for a given frequency. The inverter thus produces a PWM waveform which is free from selected harmonics with desired fundamental component.

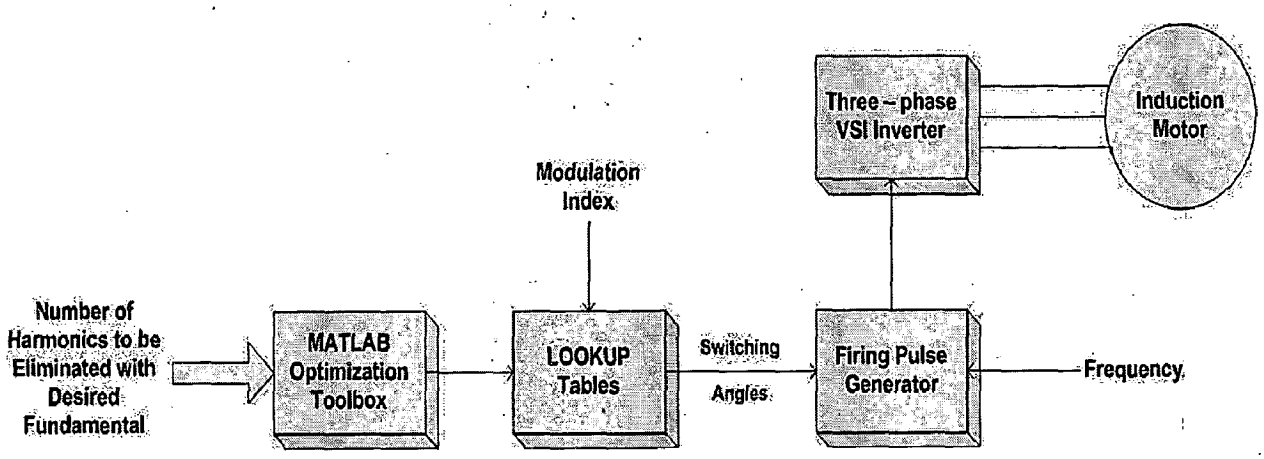


**Figure 5.1: Schematic model of VSI fed induction motor drive employing harmonic elimination/minimization**

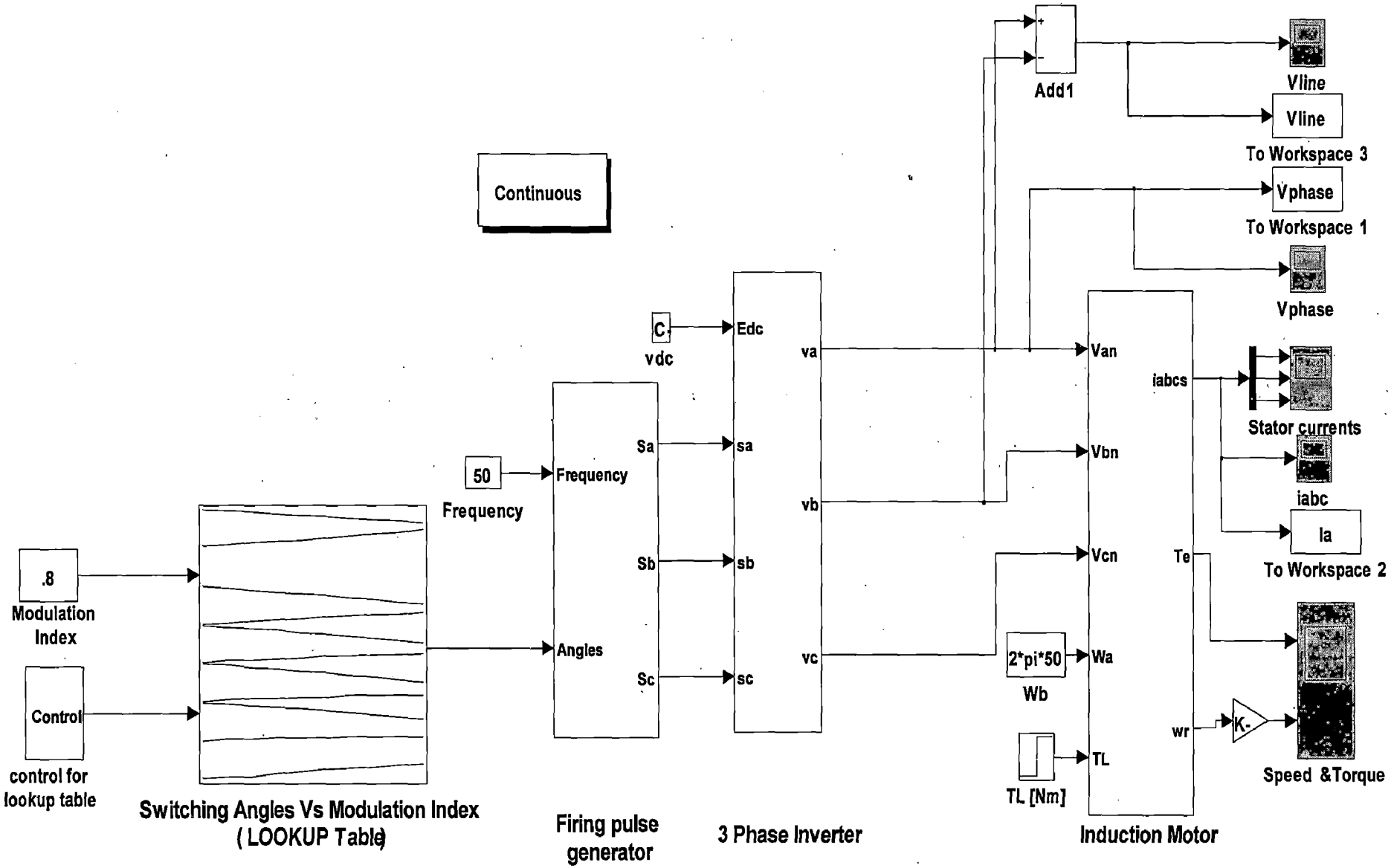


**Figure 5.2: SIMULINK model of VSI fed induction motor drive employing harmonic control**

## 5.2 Modelling of three phase induction motor:

### 5.2.1 Mathematical model of induction motor:

One of the most popular induction motor models is Krause's model detailed in[22]. According to his model, the modeling equations in flux linkage form are as follows:

$$\frac{dF_{qs}}{dt} = \omega_b \left[ v_{qs} - \frac{\omega_e}{\omega_b} F_{ds} + \frac{R_s}{x_{ls}} (F_{mq} + F_{qs}) \right] \quad \ldots\ldots\ldots (5.1)$$

$$\frac{dF_{ds}}{dt} = \omega_b \left[ v_{ds} + \frac{\omega_e}{\omega_b} F_{qs} + \frac{R_s}{x_{ls}} (F_{md} + F_{ds}) \right] \quad \ldots\ldots\ldots (5.2)$$

$$\frac{dF_{qr}}{dt} = \omega_b \left[ v_{qr} - \frac{(\omega_e - \omega_r)}{\omega_b} F_{dr} + \frac{R_r}{x_{lr}} (F_{mq} - F_{qr}) \right] \quad \ldots\ldots\ldots (5.3)$$

$$\frac{dF_{dr}}{dt} = \omega_b \left[ v_{dr} + \frac{(\omega_e - \omega_r)}{\omega_b} F_{qr} + \frac{R_r}{x_{lr}} (F_{md} - F_{dr}) \right] \quad \ldots\ldots\ldots (5.4)$$

$$F_{mq} = x_{ml} \left[ \frac{F_{qs}}{x_{ls}} + \frac{F_{qr}}{x_{lr}} \right] \quad \ldots\ldots\ldots\ldots\ldots (5.5)$$

$$F_{md} = x_{ml} \left[ \frac{F_{ds}}{x_{ls}} + \frac{F_{dr}}{x_{lr}} \right] \quad \ldots\ldots\ldots\ldots\ldots (5.6)$$

$$i_{qs} = \frac{1}{x_{ls}} (F_{qs} - F_{mq}) \quad \ldots\ldots\ldots\ldots\ldots (5.7)$$

$$i_{ds} = \frac{1}{x_{ls}} (F_{ds} - F_{md}) \quad \ldots\ldots\ldots\ldots\ldots (5.8)$$

$$i_{qr} = \frac{1}{x_{lr}} (F_{qr} - F_{mq}) \quad \ldots\ldots\ldots\ldots\ldots (5.9)$$

$$i_{dr} = \frac{1}{x_{lr}} (F_{dr} - F_{md}) \quad \ldots\ldots\ldots\ldots\ldots (5.10)$$

$$T_e = \frac{3}{2} \left( \frac{p}{2} \right) \frac{1}{\omega_b} (F_{ds} i_{qs} - F_{qs} i_{ds}) \quad \ldots\ldots\ldots\ldots\ldots (5.11)$$

$$T_e - T_L = J \left( \frac{2}{p} \right) \frac{d\omega_r}{dt} \quad \ldots\ldots\ldots\ldots\ldots (5.12)$$

Where,

Subscripts: d – direct axis, q – quadrature axis, s – stator variable and r – rotor variable,

$F_{ij}$ is the flux linkages (i=q or d, j=s or r),

$v_{qs}$ *and* $v_{ds}$ are the q and d – axis stator voltages,

$v_{qr}$ *and* $v_{dr}$ are the q and d – axis rotor voltages,

$F_{mq}$ *and* $F_{md}$ are the q and d – axis magnetizing flux linkages,

$R_r$ *and* $R_s$ are the rotor and stator resistances,

$x_{lr}$ *and* $x_{ls}$ are the rotor and stator leakage reactances,

$x_{ml} = \frac{1}{\left(\frac{1}{x_m} + \frac{1}{x_{ls}} + \frac{1}{x_{lr}}\right)}$,

$i_{qs}$ *and* $i_{ds}$ are the q and d – axis stator currents,

$i_{qr}$ *and* $i_{dr}$ are the q and d – axis rotor currents,

$p$ is the number of poles,

$J$ is the moment of inertia,

$T_e$ is the electrical output torque,

$T_l$ is the load torque,

$\omega_e$ is the stator angular electrical frequency,

$\omega_b$ is the motor angular electrical base frequency,

$\omega_r$ is the rotor angular electrical speed,

For squirrel cage induction machine, as in the case of current work, $v_{qr}$ *and* $v_{dr}$ in equations 5.3 and 5.4 are set to zero.

To solve the above mentioned differential equations, they have to be rearranged in the state space form $\dot{x} = Ax + b$. Where, $x = [F_{qs} \quad F_{ds} \quad F_{qr} \quad F_{dr} \quad \omega_r]^T$ is the state vector.

In this case, state-space form can be achieved by substituting equations 5.5 and 5.6 in equations 5.1 to 5.4 and collecting the similar terms together so that each state derivative is a function of only other state variables and model inputs. Then the modeling equations 5.1 to 5.4 and 5.12 for a squirrel cage induction motor in state space form become [20]

$$\frac{dF_{qs}}{dt} = \omega_b \left[ v_{qs} - \frac{\omega_e}{\omega_b} F_{ds} + \frac{R_s}{x_{ls}} \left( \frac{x_{ml}}{x_{lr}} F_{qr} + \left( \frac{x_{ml}}{x_{ls}} - 1 \right) F_{qs} \right) \right] \quad \ldots\ldots\ldots (5.13)$$

$$\frac{dF_{ds}}{dt} = \omega_b \left[ v_{ds} + \frac{\omega_e}{\omega_b} F_{qs} + \frac{R_s}{x_{ls}} \left( \frac{x_{ml}}{x_{lr}} F_{dr} + \left( \frac{x_{ml}}{x_{ls}} - 1 \right) F_{ds} \right) \right] \quad \ldots\ldots\ldots (5.14)$$

$$\frac{dF_{qr}}{dt} = \omega_b \left[ -\frac{(\omega_e - \omega_r)}{\omega_b} F_{dr} + \frac{R_r}{x_{lr}} \left( \frac{x_{ml}}{x_{lr}} F_{qs} + \left( \frac{x_{ml}}{x_{lr}} - 1 \right) F_{qr} \right) \right] \quad \ldots\ldots\ldots (5.15)$$

*abc-dq conversion block:*

To convert three phase voltages to voltages in the two-phase synchronously rotating frame, they are first converted to two-phase stationary frame and then from the stationary frame to the synchronously rotating frame.

$$\begin{bmatrix} v_{qs}^{s} \\ v_{ds}^{s} \end{bmatrix} = \begin{bmatrix} 1 & 0 & 0 \\ 0 & -\frac{1}{\sqrt{3}} & \frac{1}{\sqrt{3}} \end{bmatrix} \begin{bmatrix} v_{an} \\ v_{bn} \\ v_{cn} \end{bmatrix} \quad \ldots\ldots\ldots\ldots\ldots (5.18)$$

$$v_{qs} = v_{qs}^{s} \cos\theta_e - v_{ds}^{s} \sin\theta_e \quad \ldots\ldots\ldots\ldots\ldots (5.19)$$

$$v_{qs} = v_{qs}^{s} \sin\theta_e + v_{ds}^{s} \cos\theta_e \quad \ldots\ldots\ldots\ldots\ldots (5.20)$$

where the superscript "s" refers to stationary frame.

*dq-abc conversion block:*

The three phase current variables can be obtained from the stationary frame by

$$i_{qs}^{s} = v_{qs} \cos\theta_e + v_{ds} \sin\theta_e \quad \ldots\ldots\ldots\ldots\ldots (5.21)$$

$$i_{ds}^{s} = -v_{qs} \sin\theta_e + v_{ds} \cos\theta_e \quad \ldots\ldots\ldots\ldots\ldots (5.22)$$

$$\begin{bmatrix} i_a \\ i_b \\ i_c \end{bmatrix} = \begin{bmatrix} 1 & 0 \\ -\frac{1}{2} & -\frac{\sqrt{3}}{2} \\ -\frac{1}{2} & \frac{\sqrt{3}}{2} \end{bmatrix} \begin{bmatrix} i_{qs}^{s} \\ i_{ds}^{s} \end{bmatrix} \quad \ldots\ldots\ldots\ldots\ldots (5.23)$$

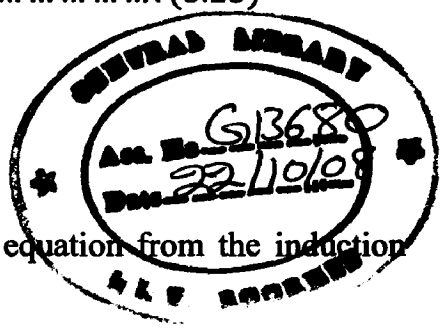


*Induction motor d-q model block:*

Fig 5.4 shows the inside of this block where each equation from the induction motor model is implemented in a different block.

First consider the flux linkage equations because flux linkages are required to calculate all the other variables. These equations are implemented using discrete blocks so as to have access to each point of the model. Once the flux linkages are calculated, the rest of the equations can be implemented without any difficulty. With the help of the obtained flux linkages the equations 5.5 and 5.6 can be implemented for magnetizing flux linkages. The equations 5.7 to 5.10 use the flux linkages to solve for the stator and rotor d-q currents. The electrical torque and rotor speed can be calculated using the equations 5.11 and 5.12 respectively. The rotor speed information obtained is required for the calculation of the rotor flux linkages of equations 5.15 and 5.16.

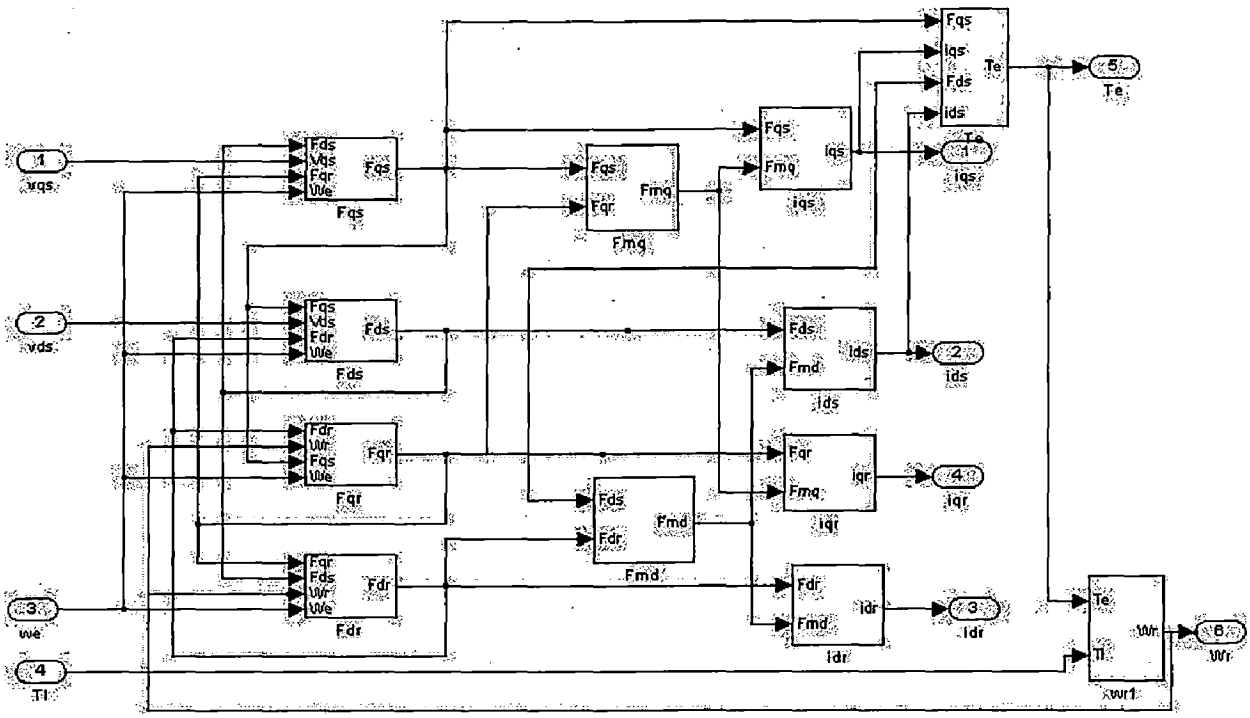


**Figure 5.4: Induction motor d-q model**

## 5.3 PWM Inverter

The SIMULINK block for a three phase, two level PWM inverter is shown in fig 5.5. Each leg of the inverter is represented by a 'switch' which has a three input terminals and one output terminal. The output of a switch ($v_{ao}, v_{bo}\ ov_{co}$) is connected to the upper input terminal (+0.5 $V_d$) if the PWM control signal (middle input) is positive. Otherwise, the output is connected to the lower input terminal (-0.5 $V_d$). The output, or ($v_{ao}$), voltage thus oscillates between +0.5 $V_d$ and -0.5 $V_d$, which is characteristic of a pole of an inverter [21].

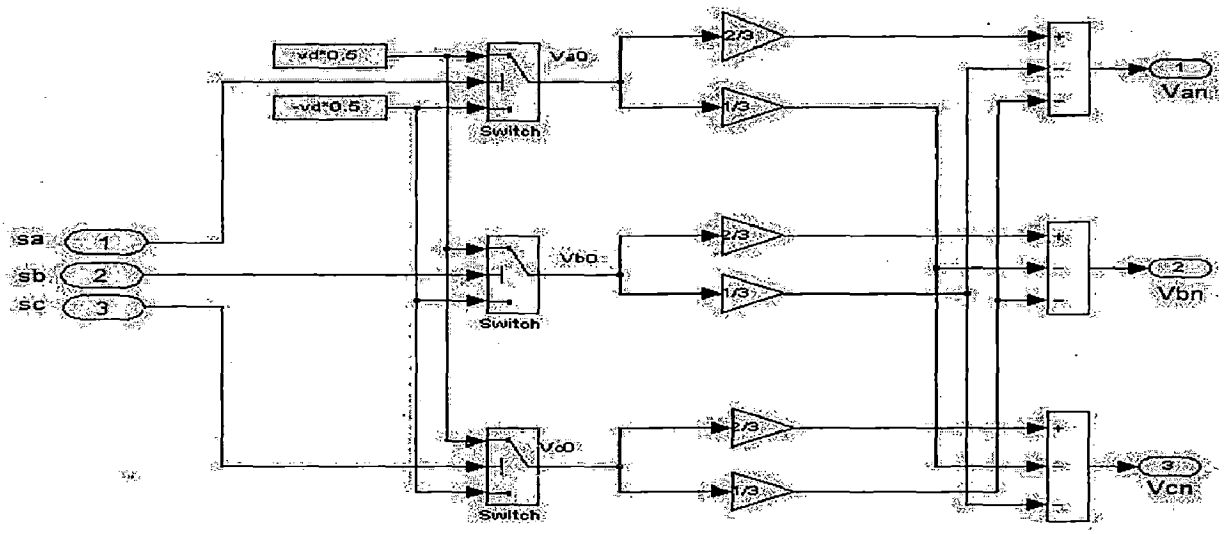


**Figure 5.5: PWM Inverter**

The output phase voltages are constructed by the following equations:

$$v_{an} = \frac{2}{3}v_{ao} - \frac{1}{3}v_{bo} - \frac{1}{3}v_{co} \quad \ldots\ldots\ldots\ldots\ldots (5.24)$$

$$v_{bn} = \frac{2}{3}v_{bo} - \frac{1}{3}v_{ao} - \frac{1}{3}v_{co} \quad \ldots\ldots\ldots\ldots\ldots (5.25)$$

$$v_{cn} = \frac{2}{3}v_{co} - \frac{1}{3}v_{ao} - \frac{1}{3}v_{bo} \quad \ldots\ldots\ldots\ldots\ldots (5.26)$$

## 5.4 Firing pulse generator

The firing pulse generator converts the switching angles obtained from the lookup tables into the firing pulses to the inverter. Fig 5.6 shows the SIMULINK implementation of firing pulse generator. It mainly consists of clock and zone bit generator, logic switching circuit and firing pulse selector blocks. The following subsections will explain each block.

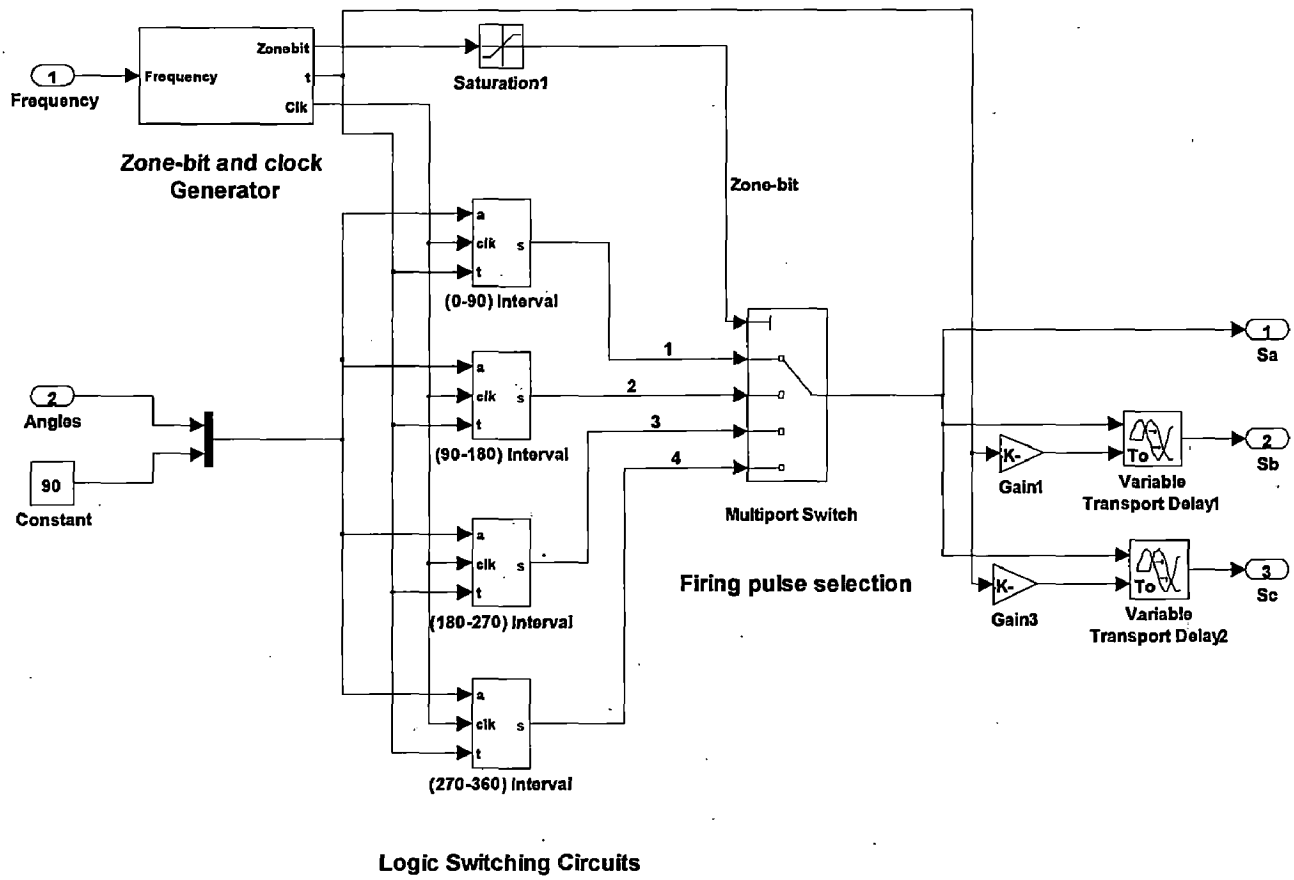


**Figure 5.6: Firing pulse generator**

*Clock and Zone bit generator block:*

For the quarter wave symmetry of the desired output waveform, the complete one cycle of the wave can be divided into four symmetrical intervals: ($0^0$-$90^0$), ($90^0$-$180^0$),

($180^0$-$270^0$) and ($270^0$-$360^0$). At an instant, the simulation time can lie in one of the mentioned intervals.

The clock and zone bit generator block generates the zone-bit (1, 2, 3 or 4) based on the interval in which current simulation time is lying and the clock required by the comparators in the logic switching circuits. It accepts simulation time and frequency of operation as inputs to generate the zone bit and clock. Fig 5.7 shows the SMULINK implementation of clock and zone bit generator block.

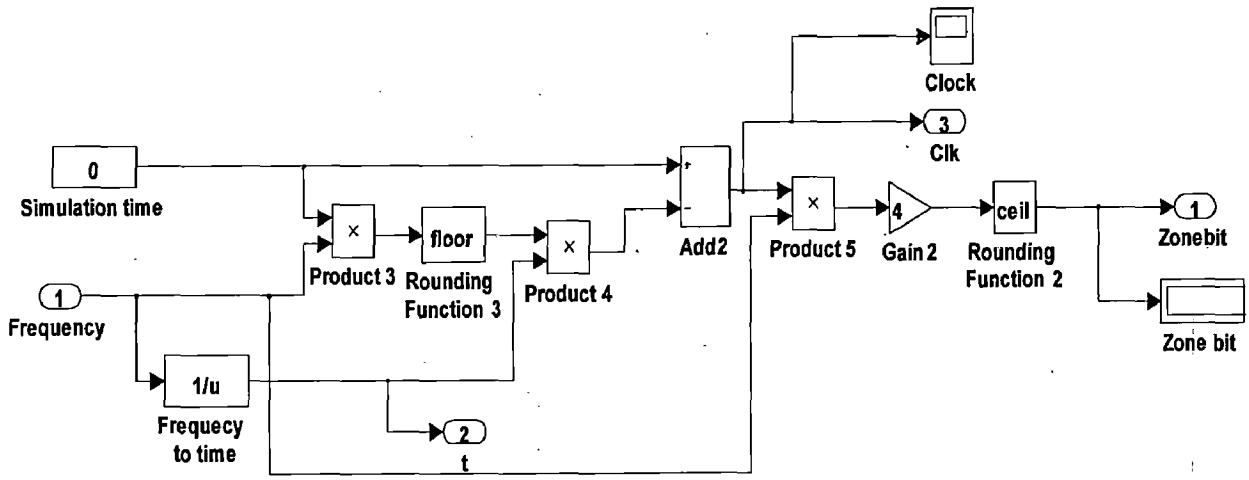


**Figure 5.7:** Clock and zone-bit generator block

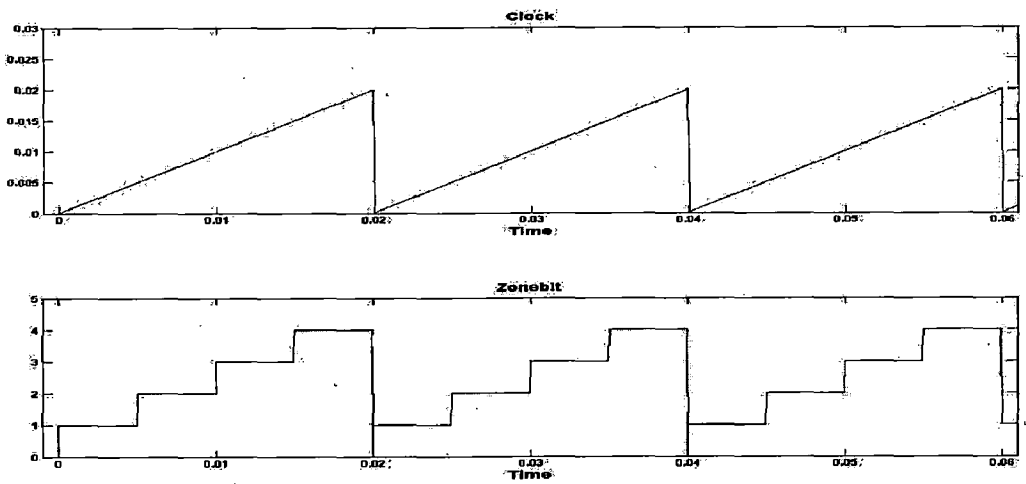


**Figure 5.8: Clock and zone-bit for three full cycles**

*Logic switching circuit:*

The firing pulses to the inverter are generated individually for all the four intervals. Proper switching angles are selected based on the zone-bit obtained from the above discussion through a multiport switch (firing pulse selection block). Fig 5.9 shows the generation of firing pulses for $0^0$-$90^0$ interval. It mainly consists two blocks: staircase wave generator block and a multiport switch.

The staircase wave generator block generates a staircase wave with each raising edge corresponding to the appropriate switching angle. For this purpose, the switching angles obtained from the lookup tables are first converted into time and compared with the clock provided by the clock generator. The output of the comparator is applied to the XOR gates and gain blocks to generate the desired staircase wave as shown in figure 5.10.

The multiport switch selects either 1 or 0 at each raising edges of staircase wave. Thus, it generates a series of pulses required by the inverter.

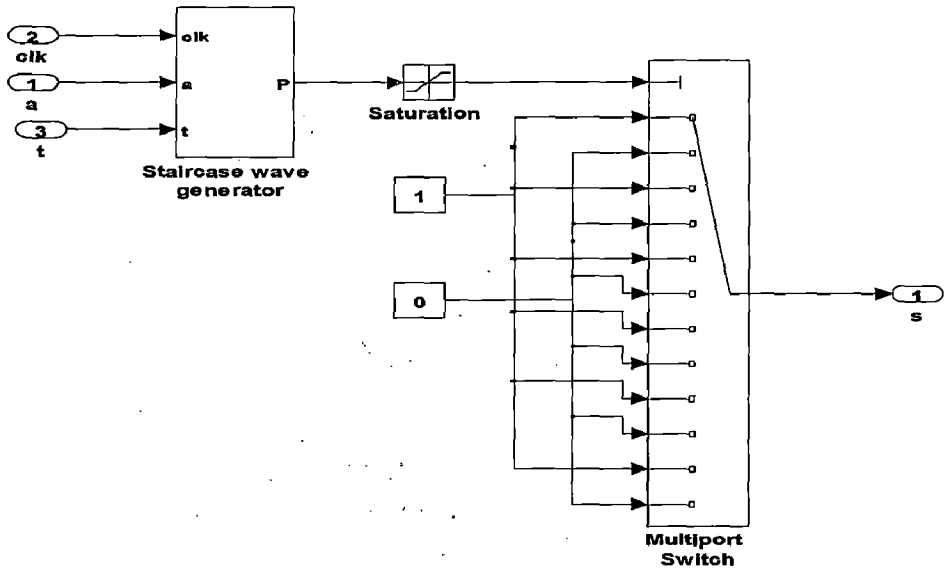


**Figure 5.9: Logic switching circuit**

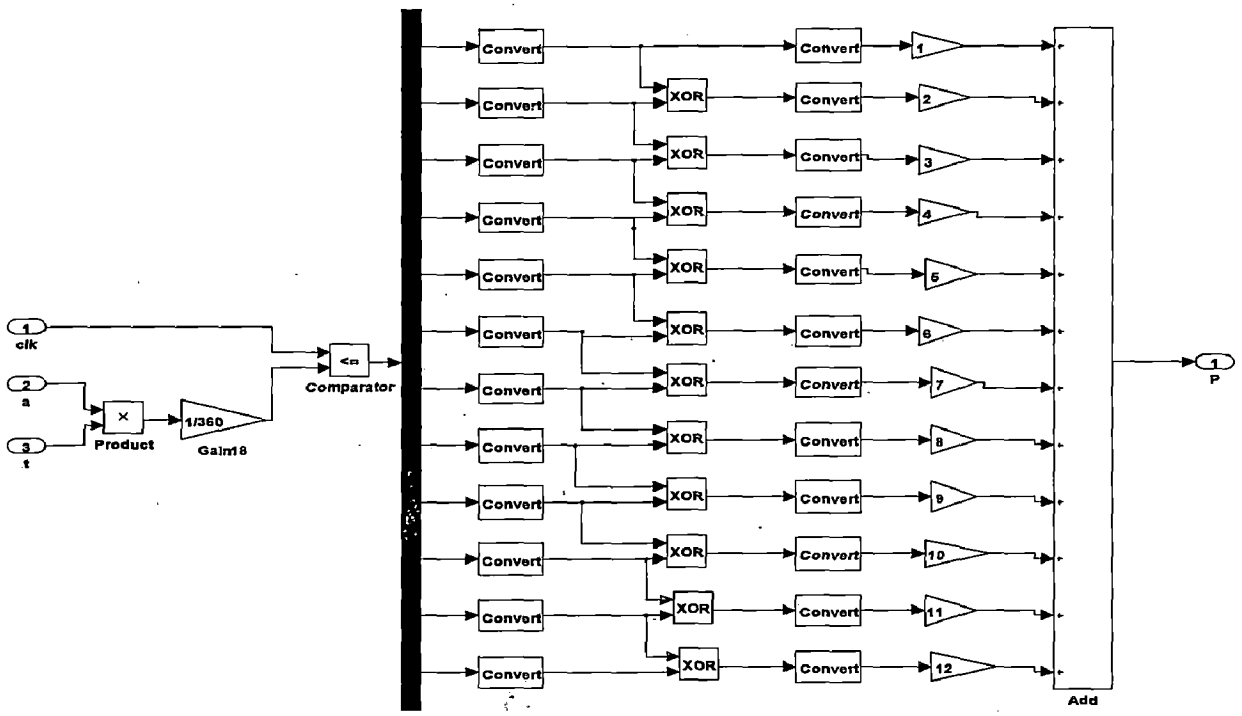


**Figure 5.10: Subsystem for generating staircase wave**

# Chapter 6
# Results and Discussions

This chapter presents the simulation results of line current and voltage waveforms along with the frequency spectrum of current at different operating points. Also, the variation of THD with the variation of modulation index and number of switching angles is presented.

## 6.1 Simulation Results

The simulation model developed in the previous chapter is simulated in MATLAB-SIMULINK environment. A 5hp, 4 pole, three phase induction motor is considered for the analysis (parameters given in Appendix – A). Simulation is carried out for various number of switching angles per quarter cycle at 0.8 modulation index. The current and voltage waveforms including the frequency spectrum of the current waveform are obtained for both harmonic elimination and harmonic minimization cases.

Figure 6.2 shows the phase to pole voltage waveform of the voltage source inverter employing harmonic control. This waveform is obtained at 0.8 modulation index when 11 number of switching angles per quarter cycle are considered. Figure 6.3 gives the output phase voltage ($V_{An}$) waveform at 0.8 modulation index with 11 switchings per quarter cycle.

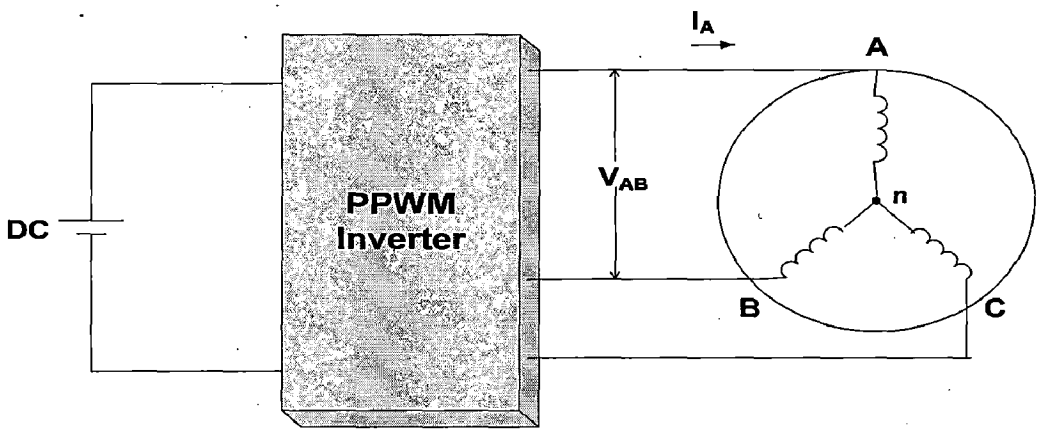


**Figure 6.1: Representation of line voltage and current**

Figures 6.4 to 6.13 show the line voltage ($V_{AB}$) and current ($I_A$) waveforms with line current harmonics spectra for $N$=3 to 11. It is to be noted that for harmonic elimination case, the highest harmonic eliminated is $(3N-1)$ for even values of $N$ or $(3N-2)$ for odd values of $N$. As mentioned in chapter 4, for harmonic minimization problem, the highest harmonic considered is 71.

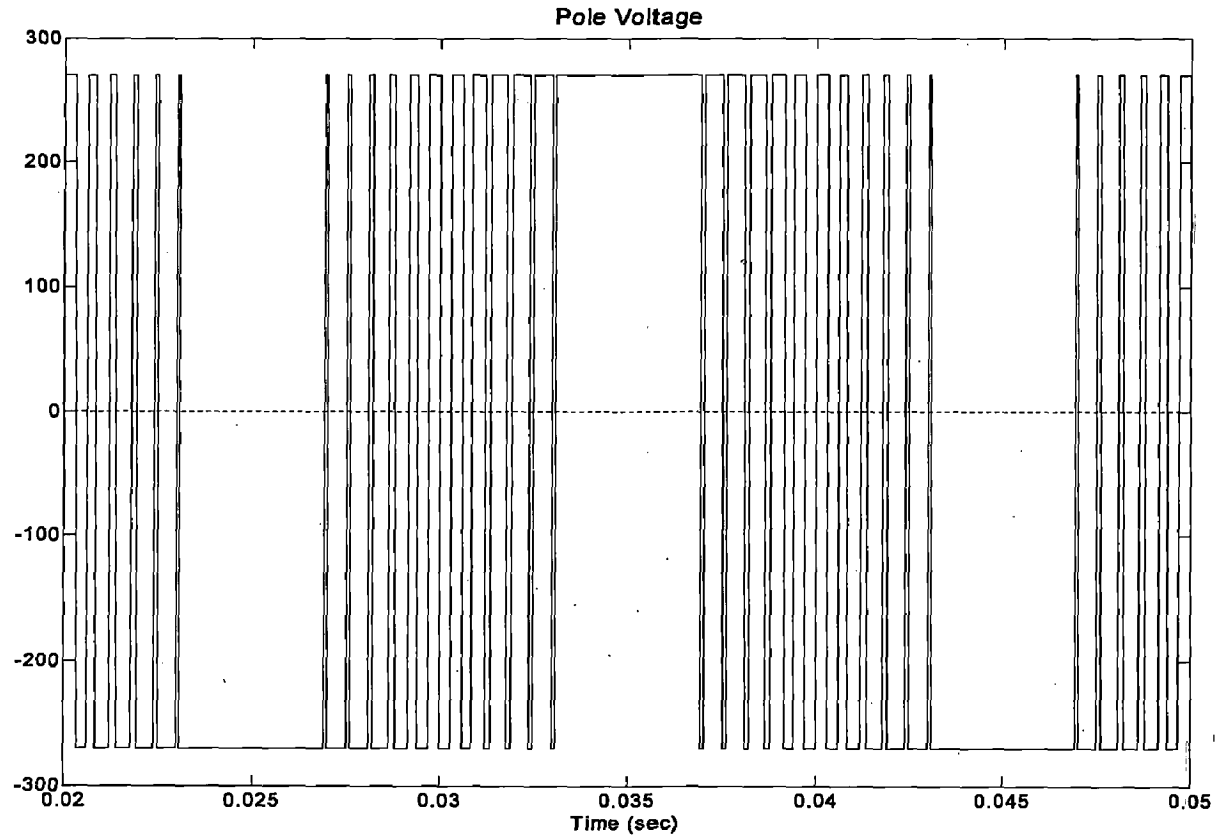


**Figure 6.2: Phase to Pole voltage (*N*=11)**

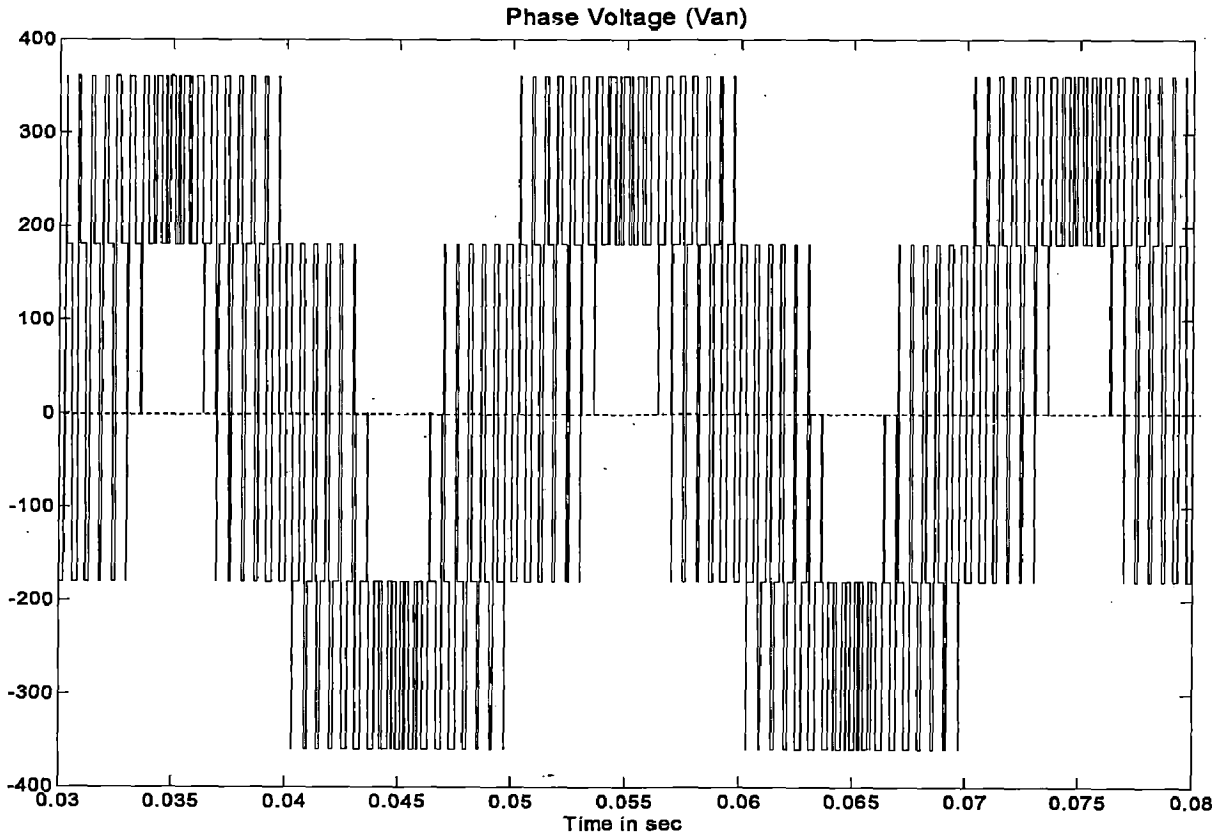


**Figure 6.3: Phase Voltage waveform $V_{An}$ (*N*=11)**

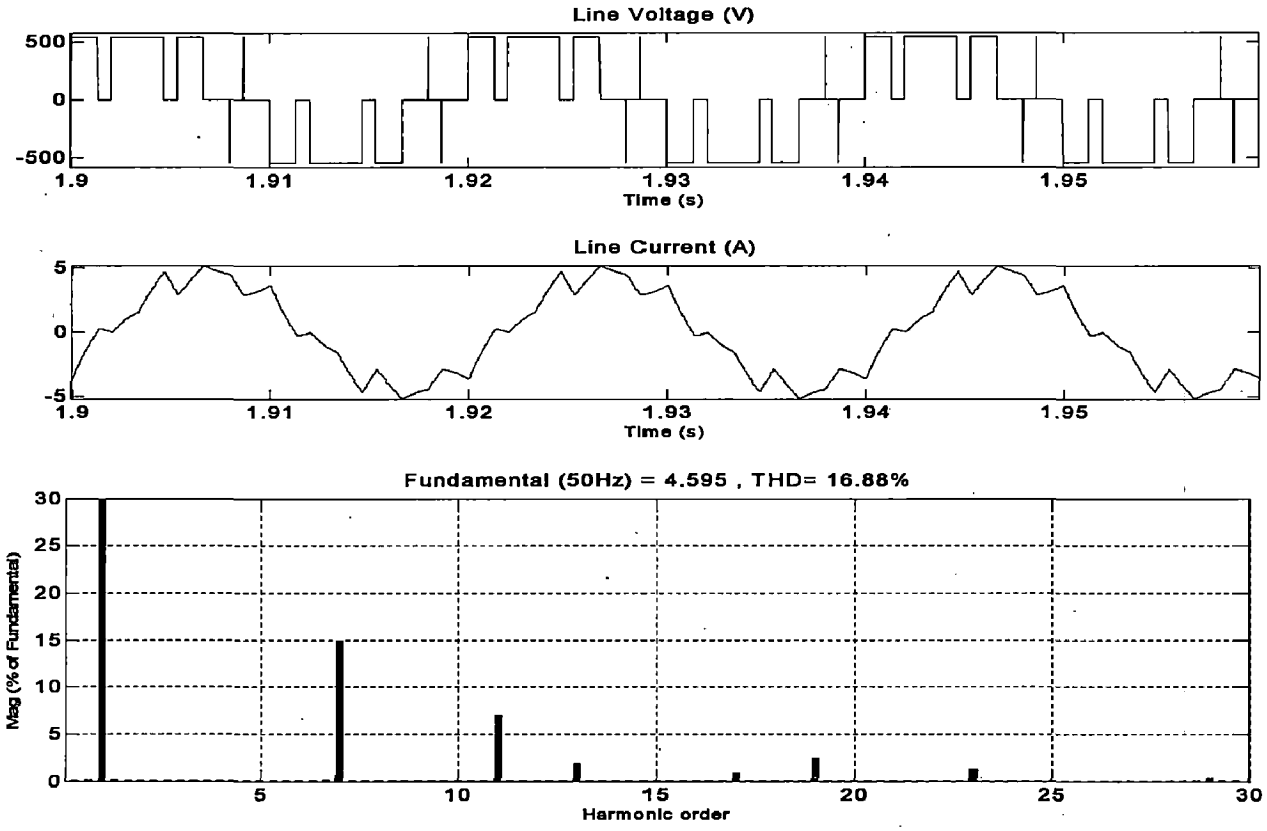


**(a) Harmonic Elimination**
**($5^{th}$ Harmonic is eliminated)**

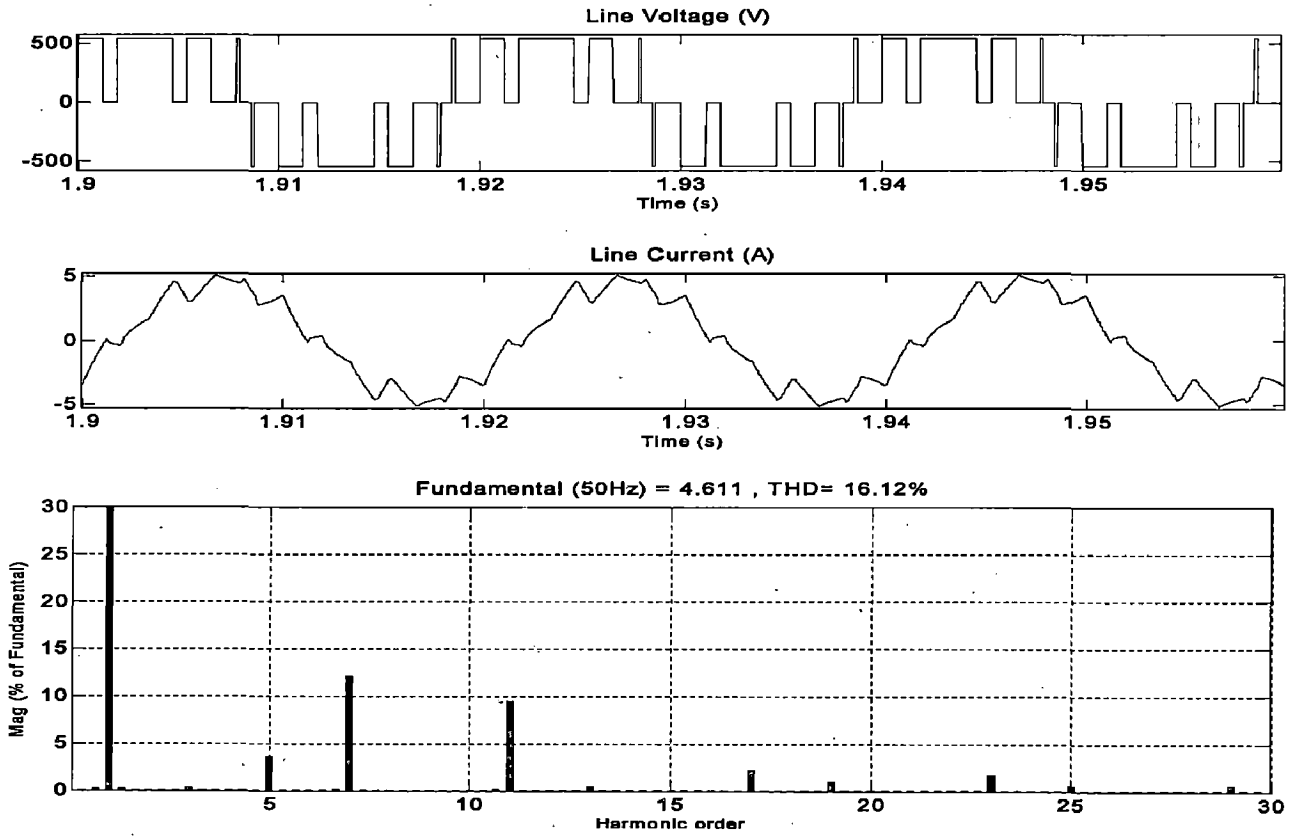


**(b) Harmonic Minimization**

**Figure 6.4: Line current and voltage for *N*=2 (M=0.8)**

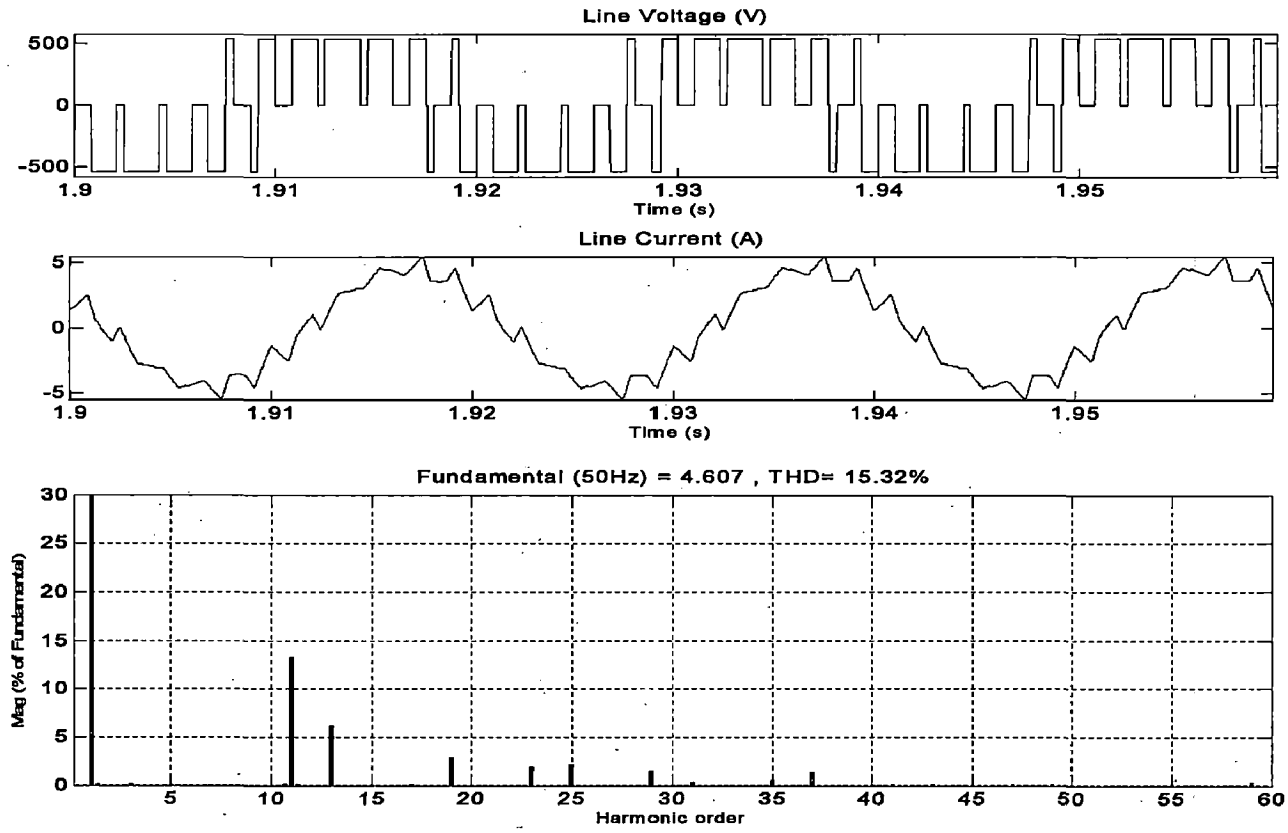


**(a) Harmonic Elimination**
**($5^{th}$ and $7^{th}$ Harmonics are eliminated)**

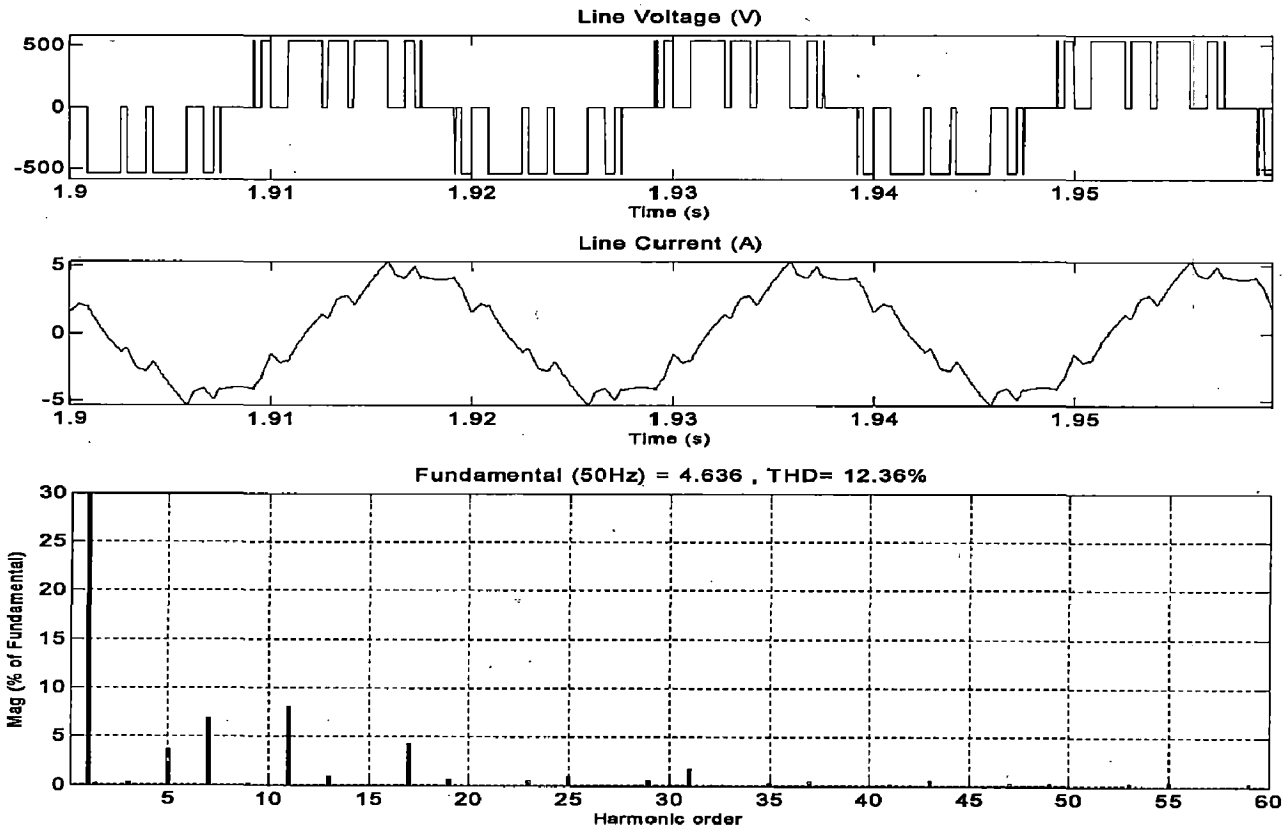


**(b) Harmonic Minimization**

**Figure 6.5: Line current and voltage for *N*=3 (M=0.8)**

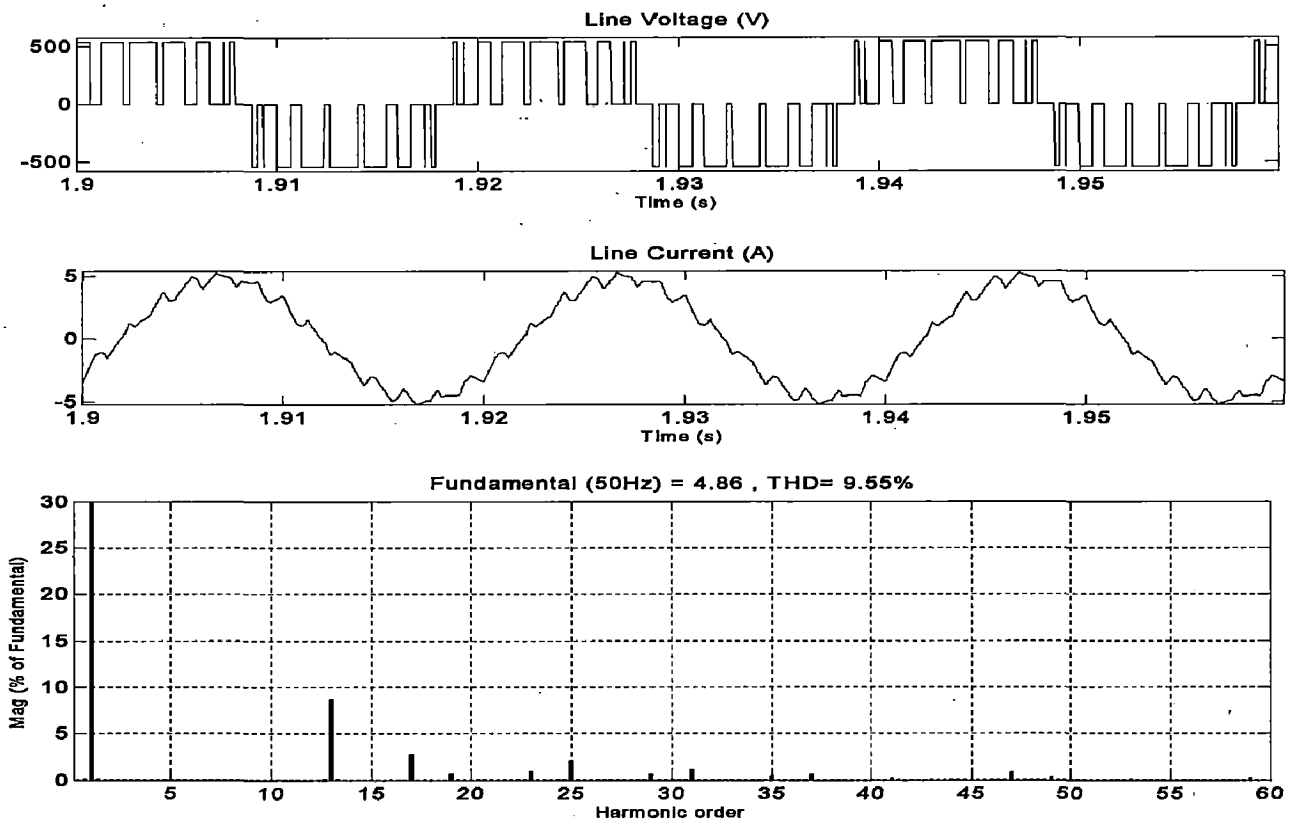


**(a) Harmonic Elimination**
**($5^{th}$ , $7^{th}$ and $11^{th}$ Harmonics are eliminated)**

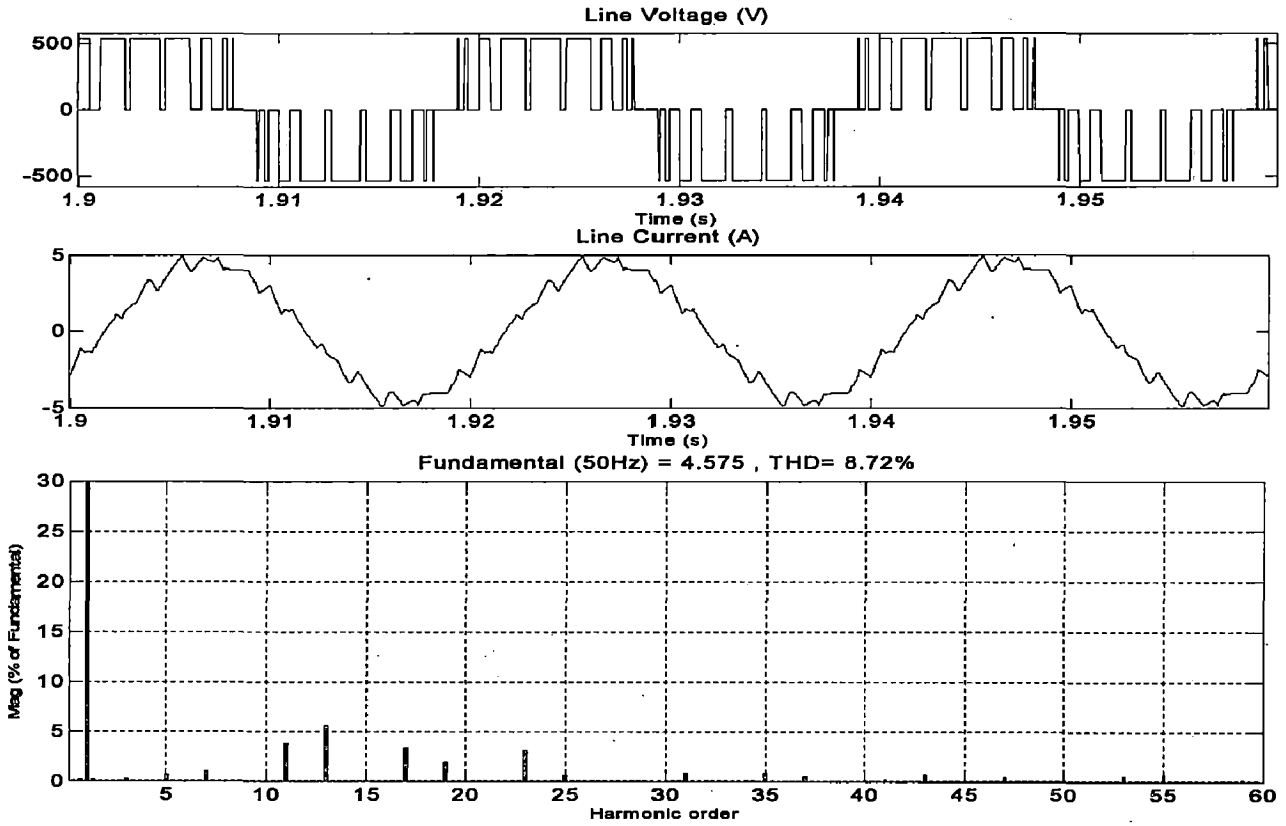


**(b) Harmonic Minimization**

**Figure 6.6: Line current and voltage for *N*=4 (M=0.8)**

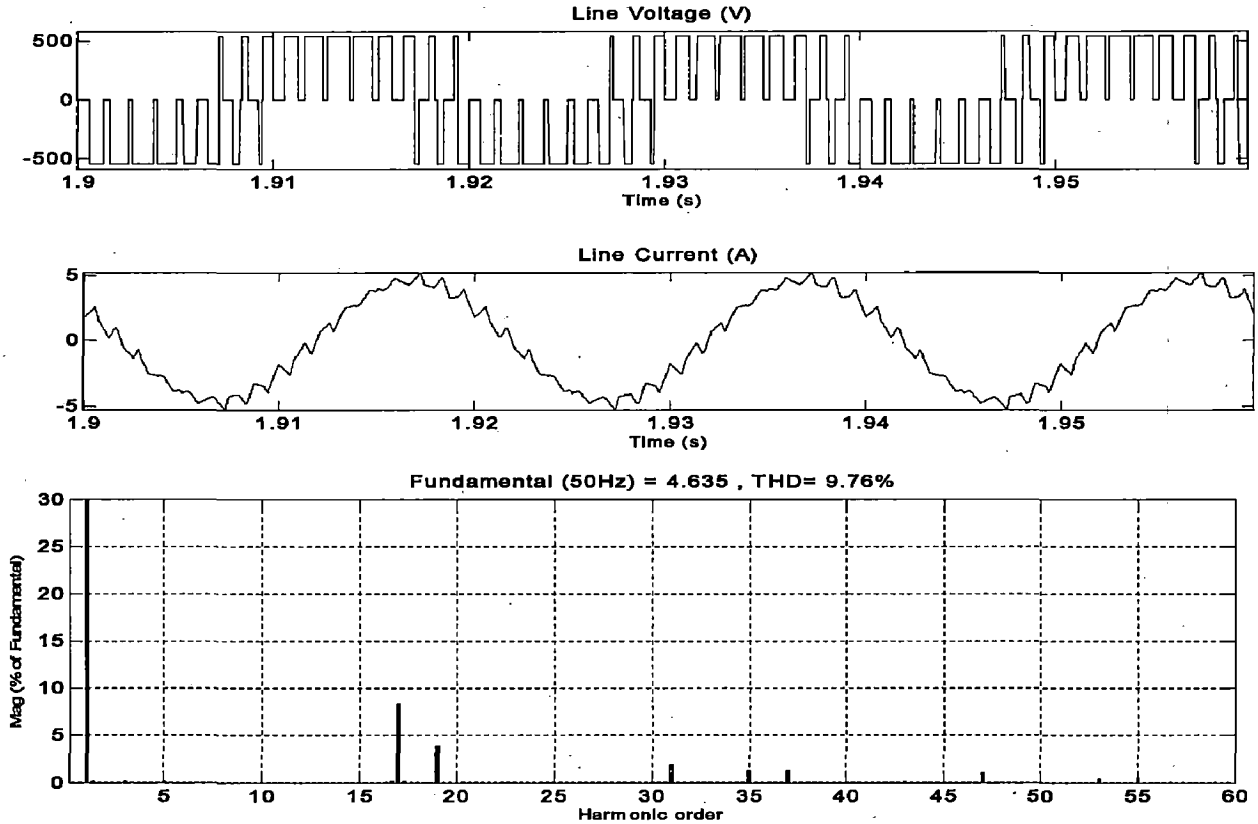


**(a) Harmonic Elimination**
**($5^{th}$ , $7^{th}$ , $11^{th}$ and $13^{th}$ Harmonics are eliminated)**

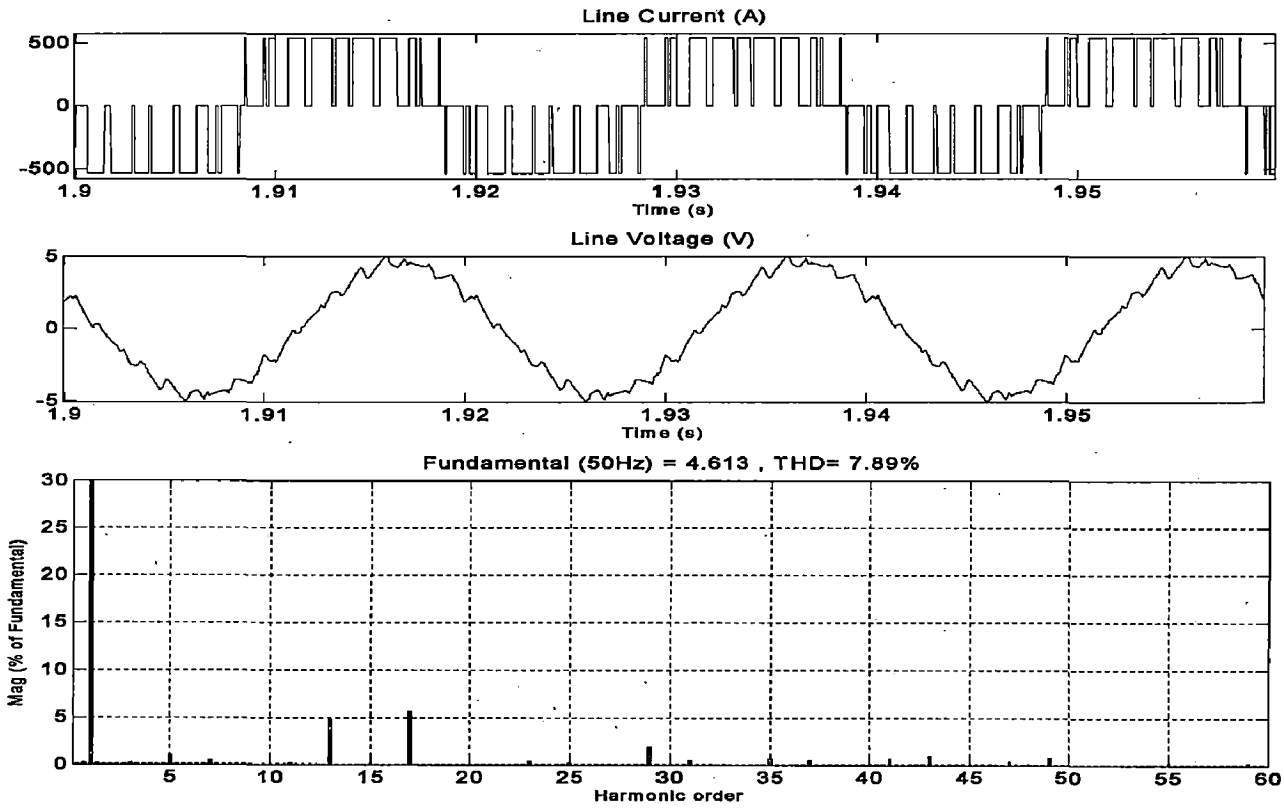


**(b) Harmonic Minimization**

**Figure 6.7: Line current and voltage for $N$=5 ($M$=0.8)**

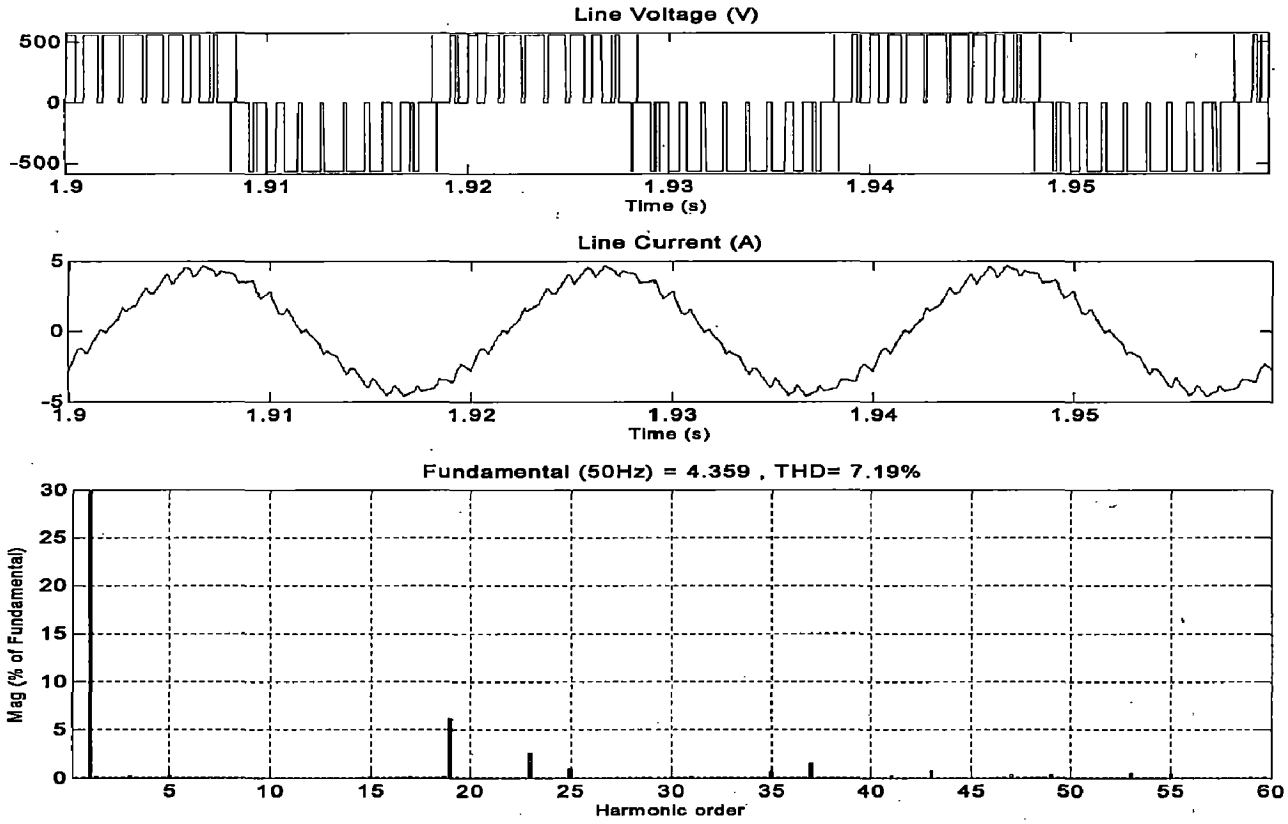


**(a) Harmonic Elimination**
**($5^{th}$ , $7^{th}$ , $11^{th}$ ,$13^{th}$ and $17^{th}$ Harmonics are eliminated)**

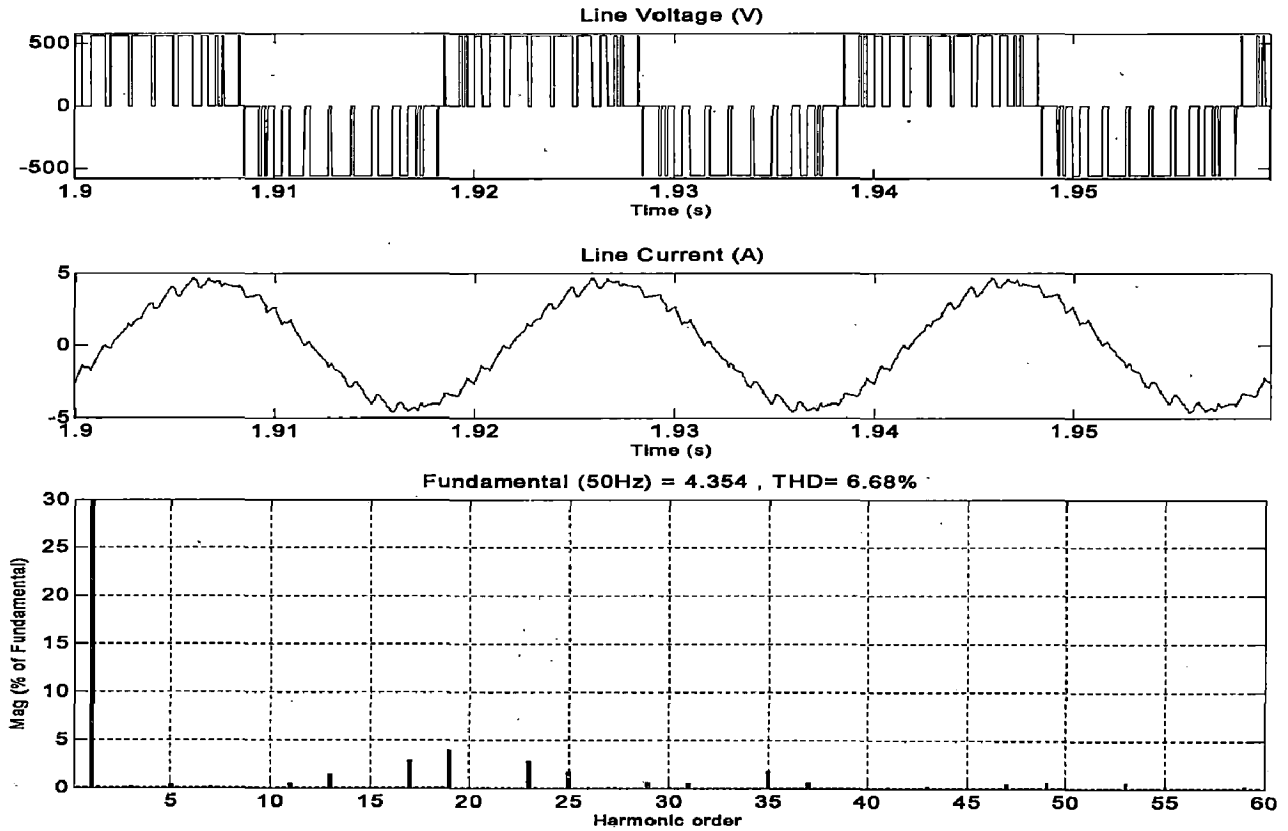


**(b) Harmonic Minimization**

**Figure 6.8: Line current and voltage for $N$=6 ($M$=0.8)**

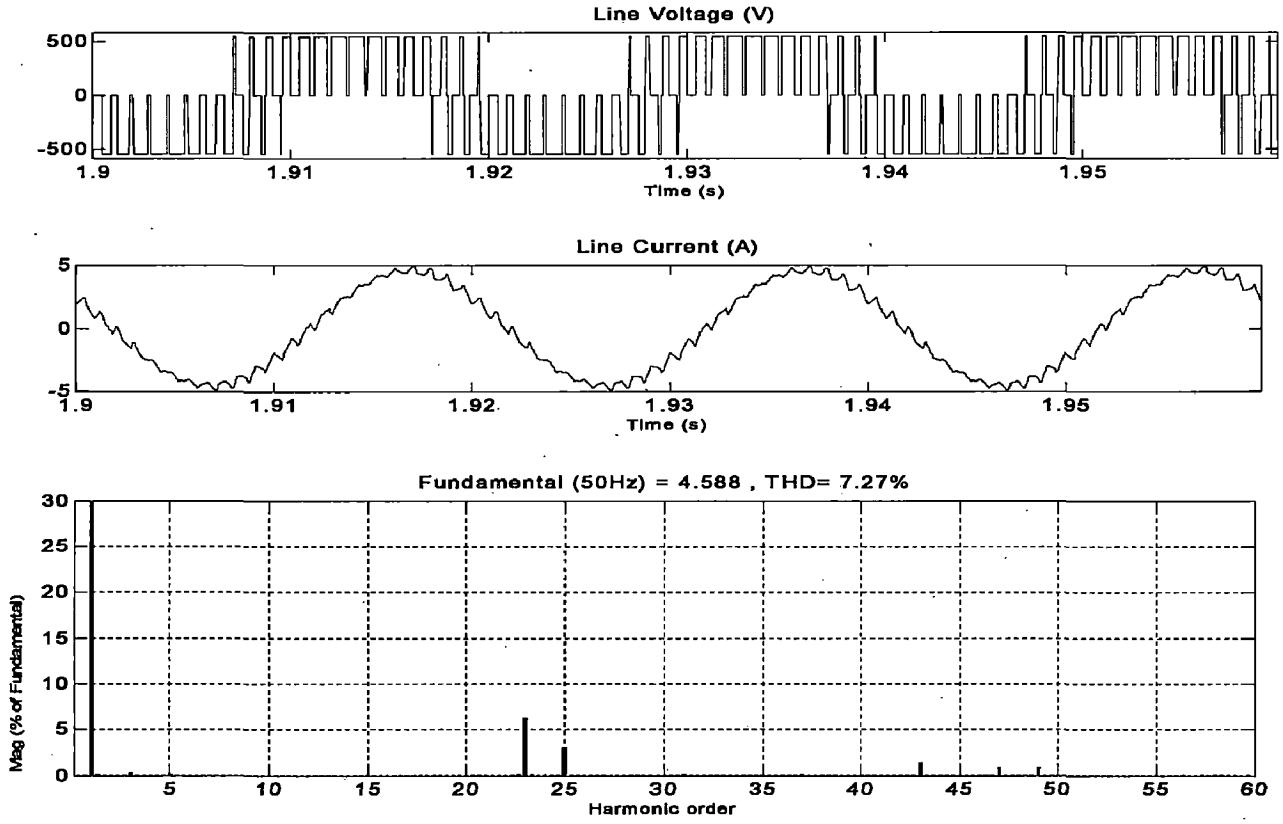


**(a) Harmonic Elimination**
**($5^{th}$ , $7^{th}$ , $11^{th}$ ,$13^{th}$ ,$17^{th}$ and $19^{th}$ Harmonics are eliminated)**

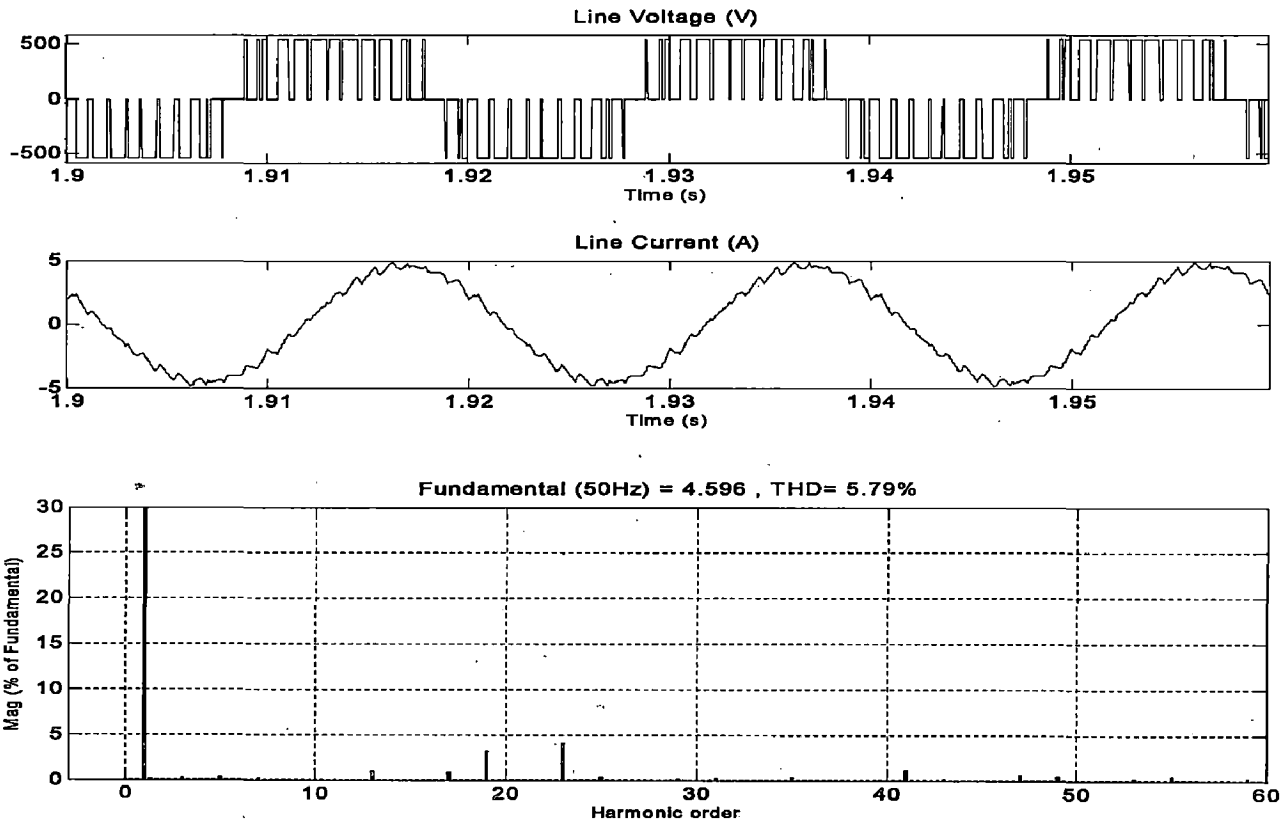


**(b) Harmonic Minimization**

**Figure 6.9: Line current and voltage for $N$=7 ($M$=0.8)**

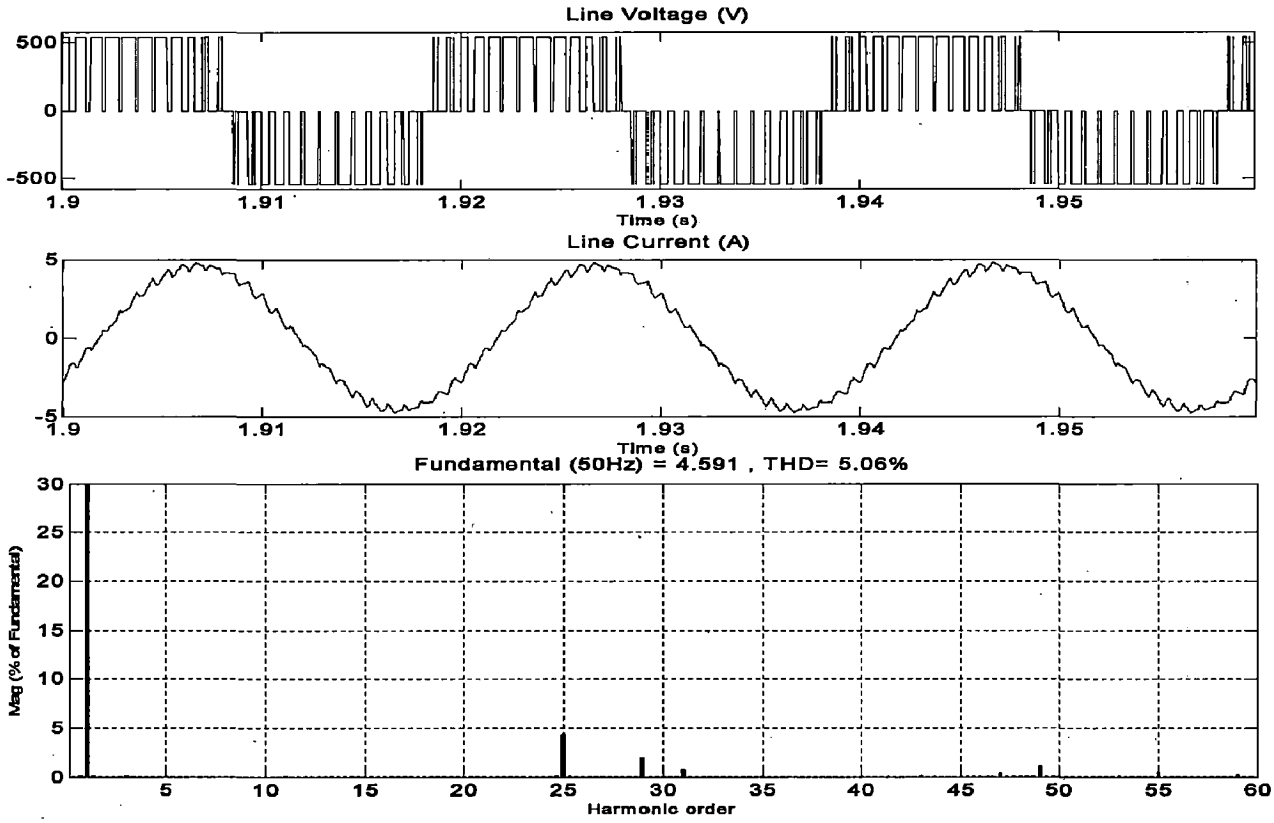


**(a) Harmonic Elimination**
**($5^{th}$ , $7^{th}$ , $11^{th}$ ,$13^{th}$ ,$17^{th}$ ,$19^{th}$ and $23^{rd}$ Harmonics are eliminated)**

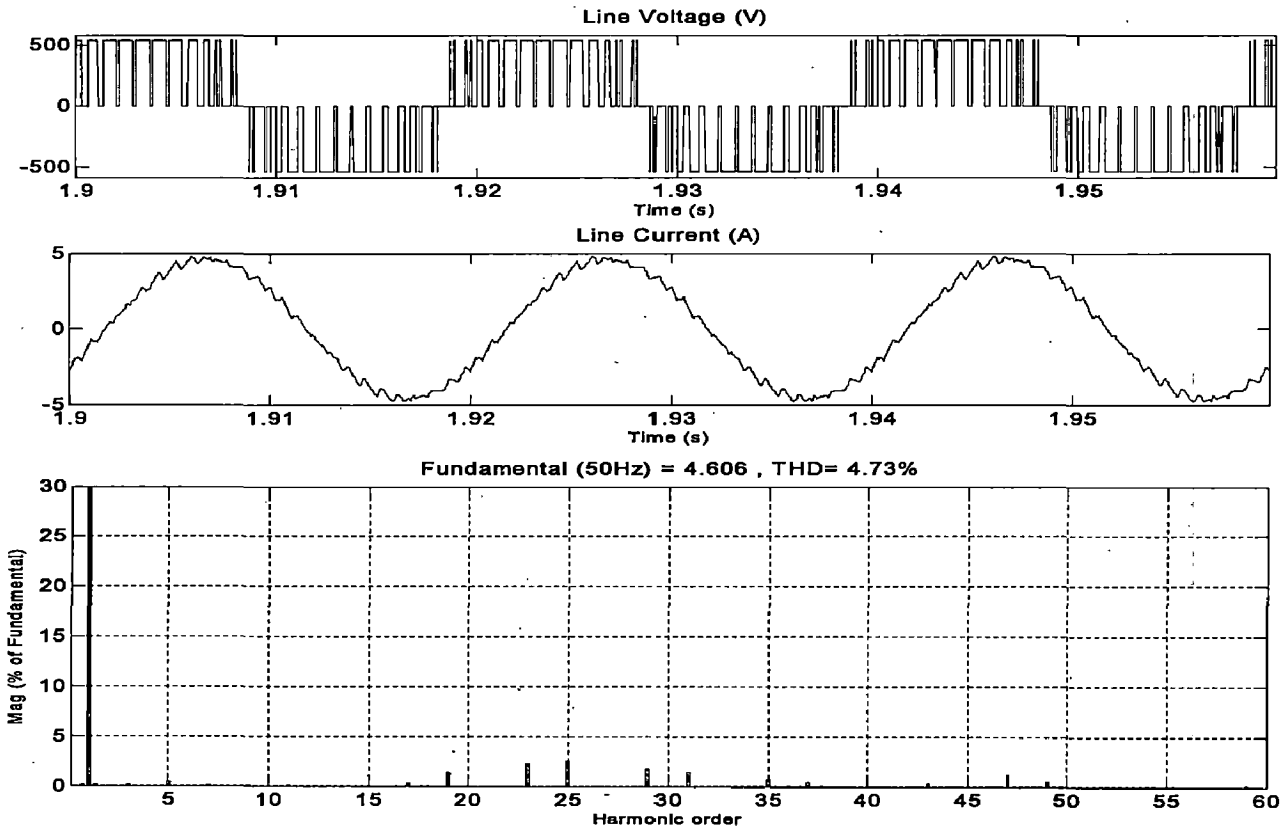


**(b) Harmonic Minimization**

**Figure 6.10: Line current and voltage for $N$=8 ($M$=0.8)**

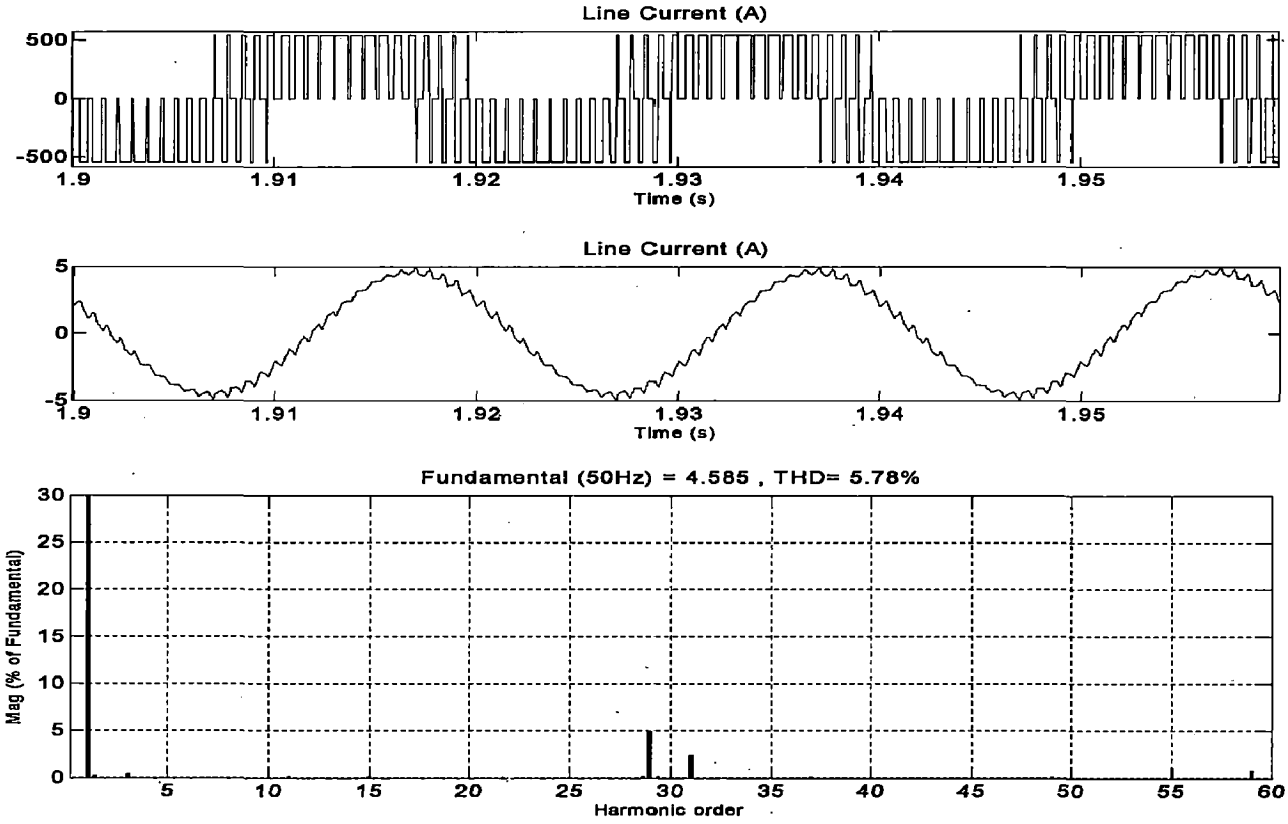


**(a) Harmonic Elimination**
**($5^{th}$ , $7^{th}$ , $11^{th}$ ,$13^{th}$ ,$17^{th}$ ,$19^{th}$ , $23^{rd}$ and $25^{th}$ Harmonics are eliminated)**

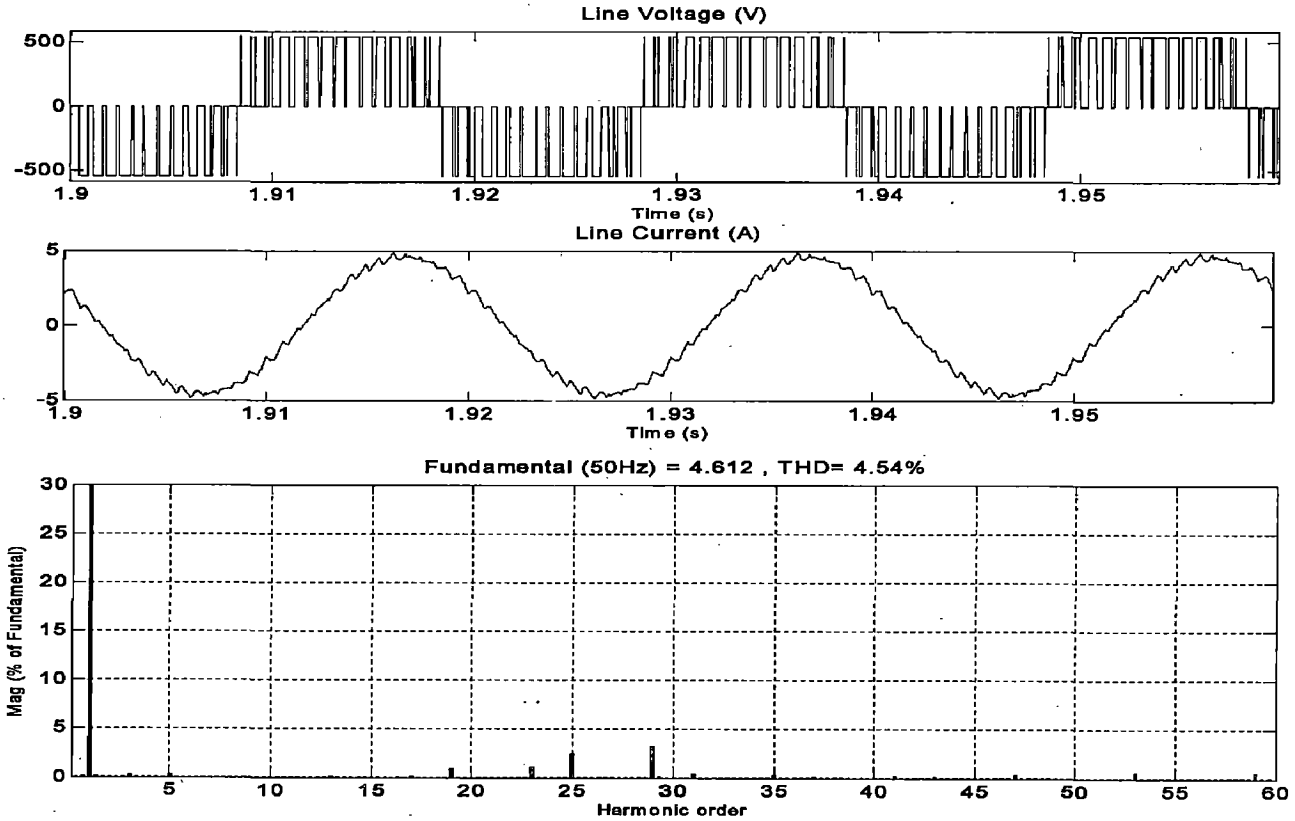


**(b) Harmonic Minimization**

**Figure 6.11: Line current and voltage for $N$=9 ($M$=0.8)**

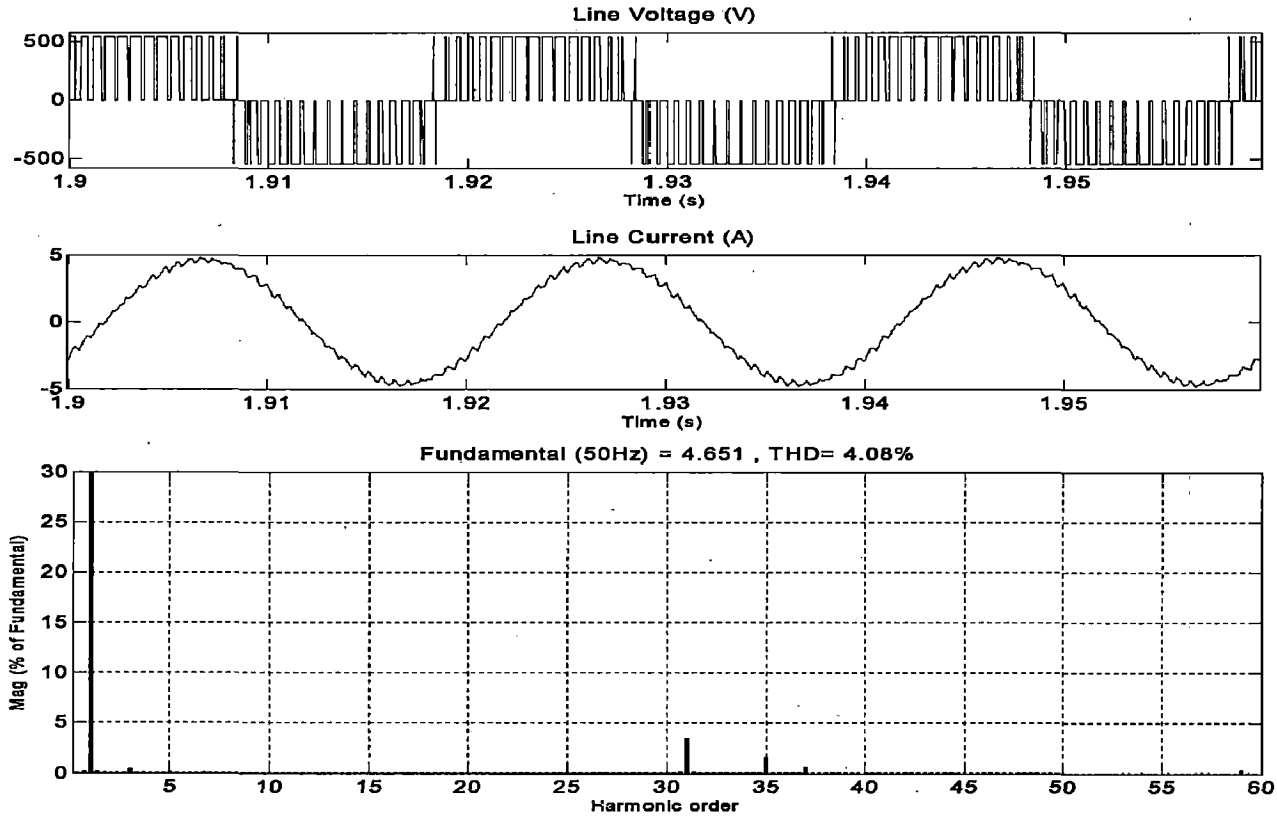


**(a) Harmonic Elimination**
**($5^{th}$ , $7^{th}$ , $11^{th}$ ,$13^{th}$ ,$17^{th}$ ,$19^{th}$ , $23^{rd}$ ,$25^{th}$ and $29^{th}$ Harmonics are eliminated)**

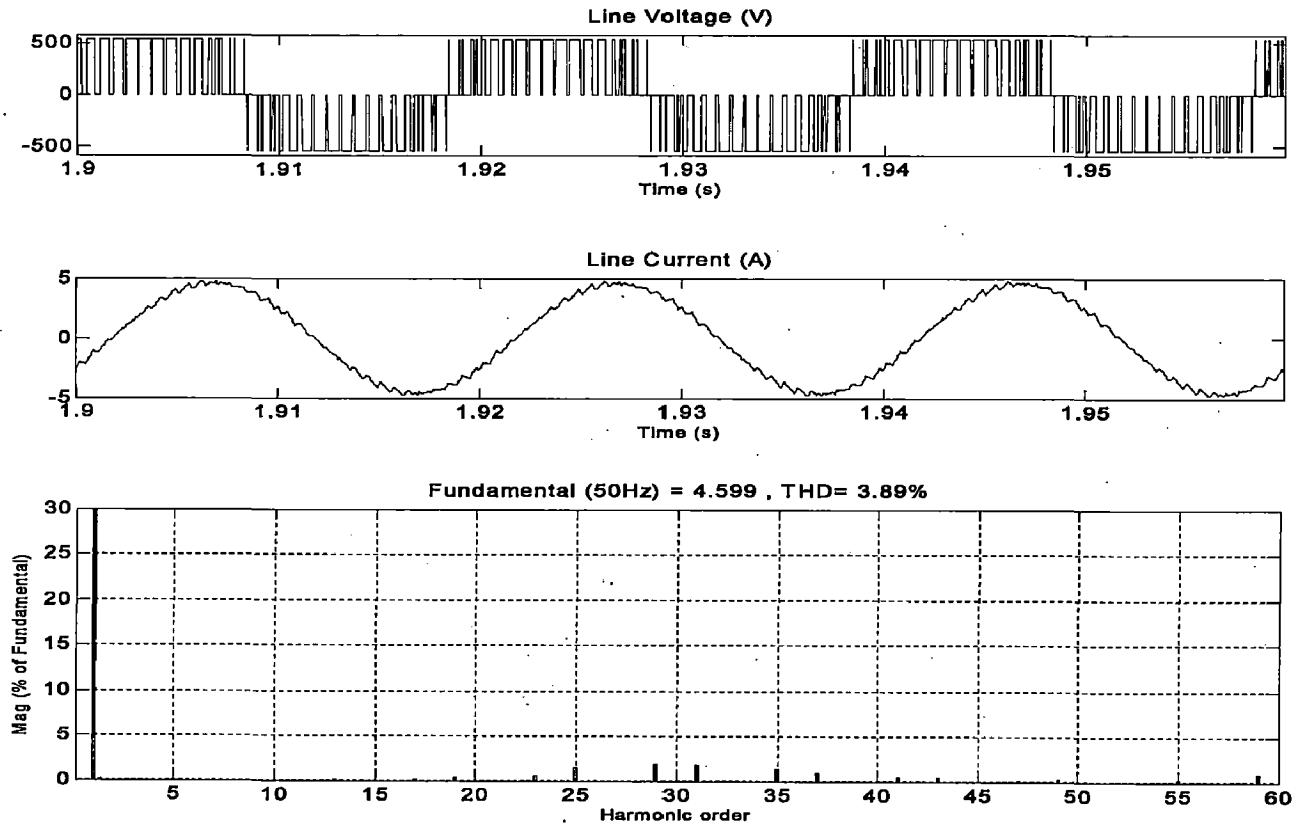


**(b) Harmonic Minimization**

**Figure 6.12: Line current and voltage for $N$=10 ($M$=0.8)**

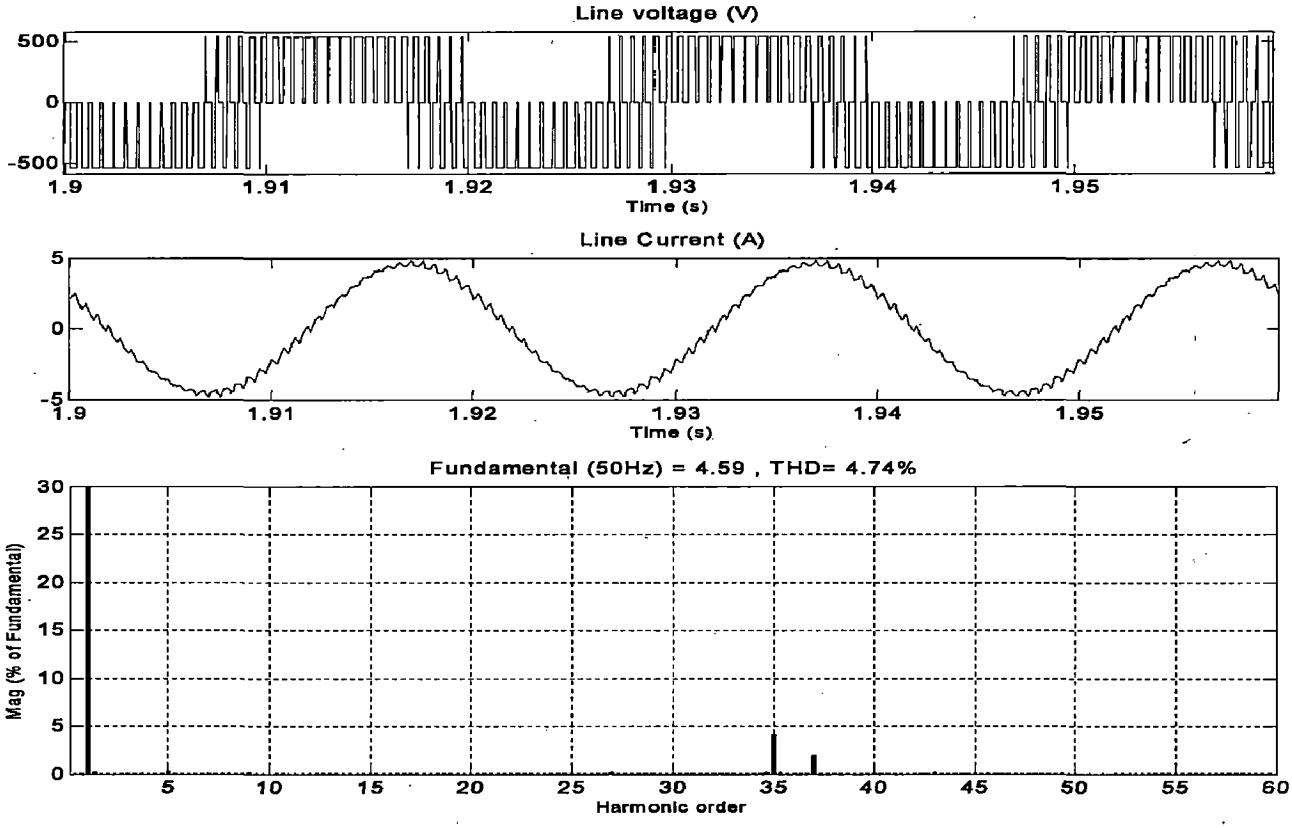


**(a) Harmonic Elimination**
**($5^{th}$ , $7^{th}$ , $11^{th}$ ,$13^{th}$ ,... , $31^{st}$ Harmonics are eliminated)**

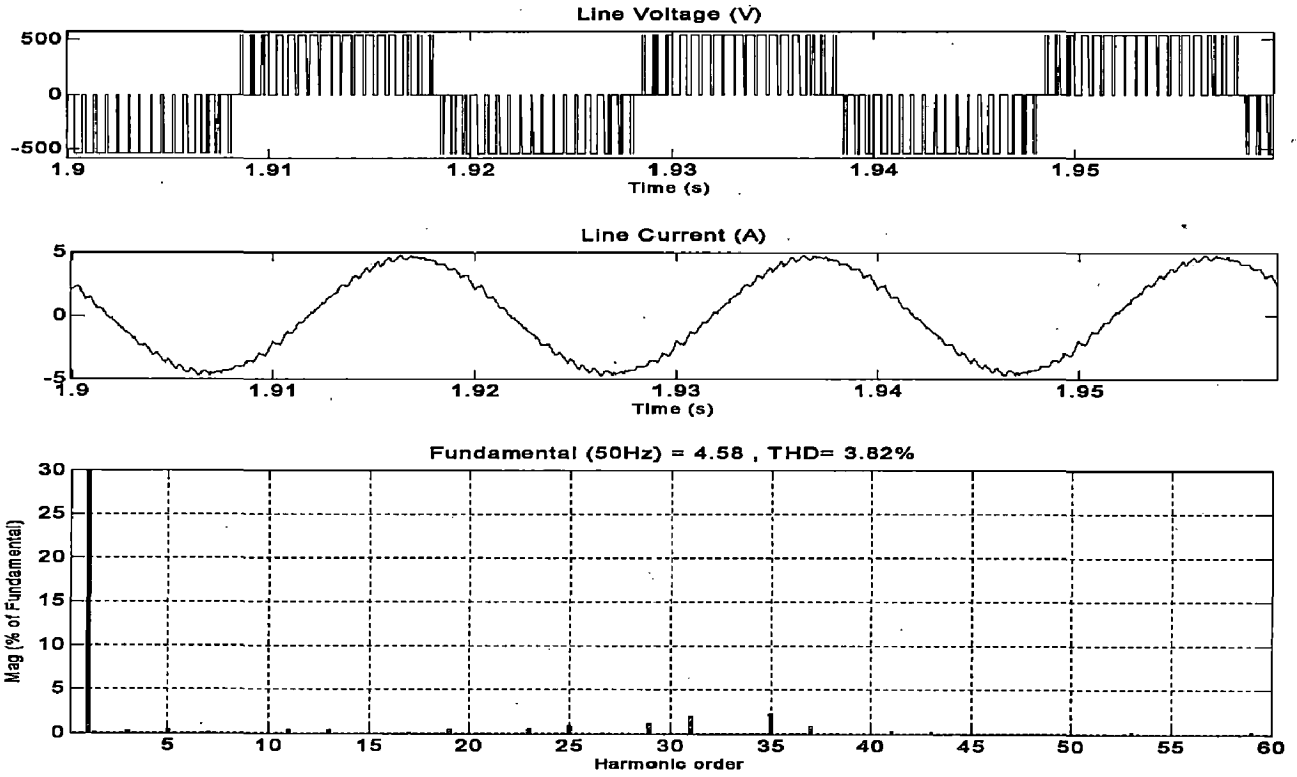


**(b) Harmonic Minimization**

**Figure 6.13: Line current and voltage for $N$=11 ($M$=0.8)**

Figure 6.14 shows the variation of THD with modulation index for various number of switching angles per quarter cycle where the dotted line gives the THD for harmonic minimization case and solid line gives the THD for harmonic elimination case. From figure, we can say that the total current harmonic distortion reduces with the increase in the number of harmonics eliminated.

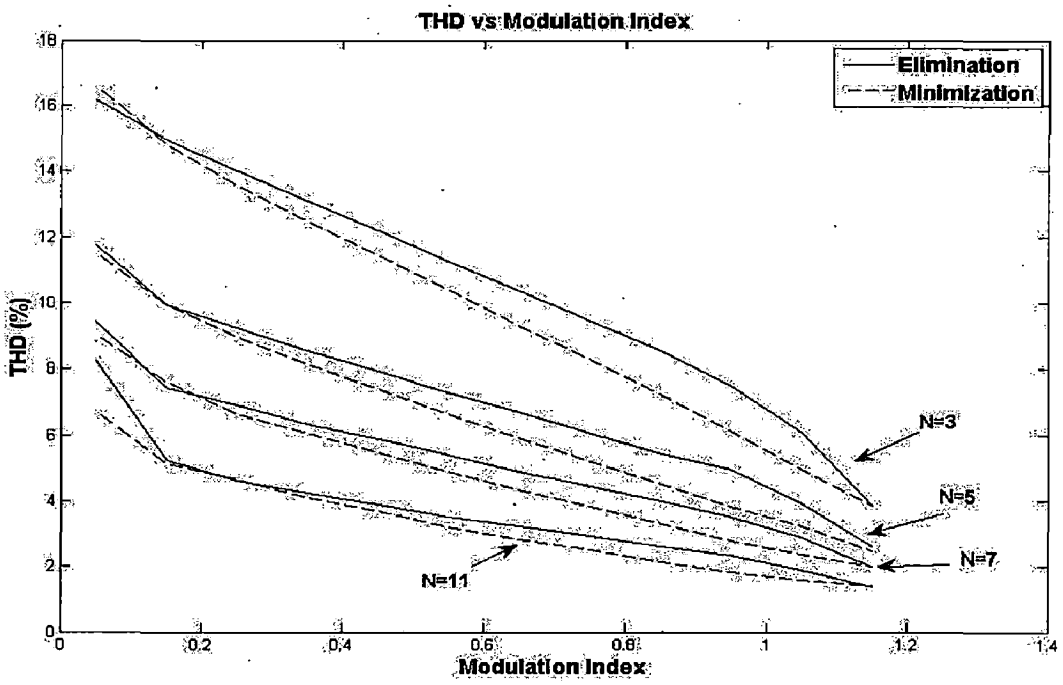


**Figure 6.14: Line current THD variation with Modulation Index**

Figure 6.15 shows the current THD variation with number of switchings per quarter cycle for various modulation indexes. It is seen from the figure that, the THD decreases as the number of switchings are increased.

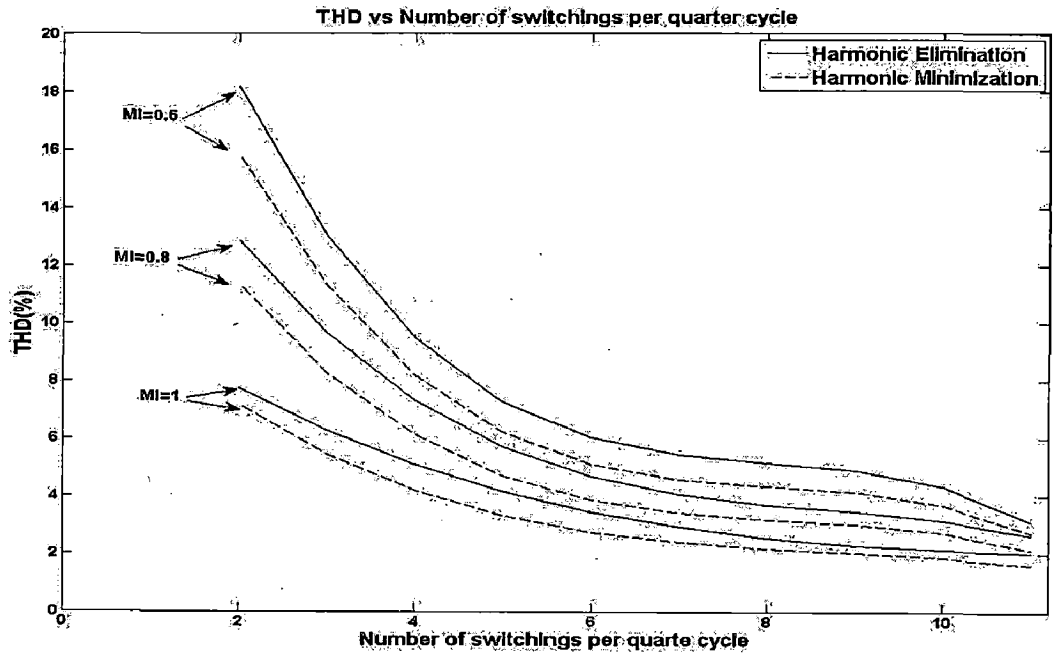


**Figure 6.15: Current THD variation with number of switchings (*N*)**

Figure 6.16 shows the induction motor response when fed form voltage source inverter employing selective harmonic elimination/minimization.

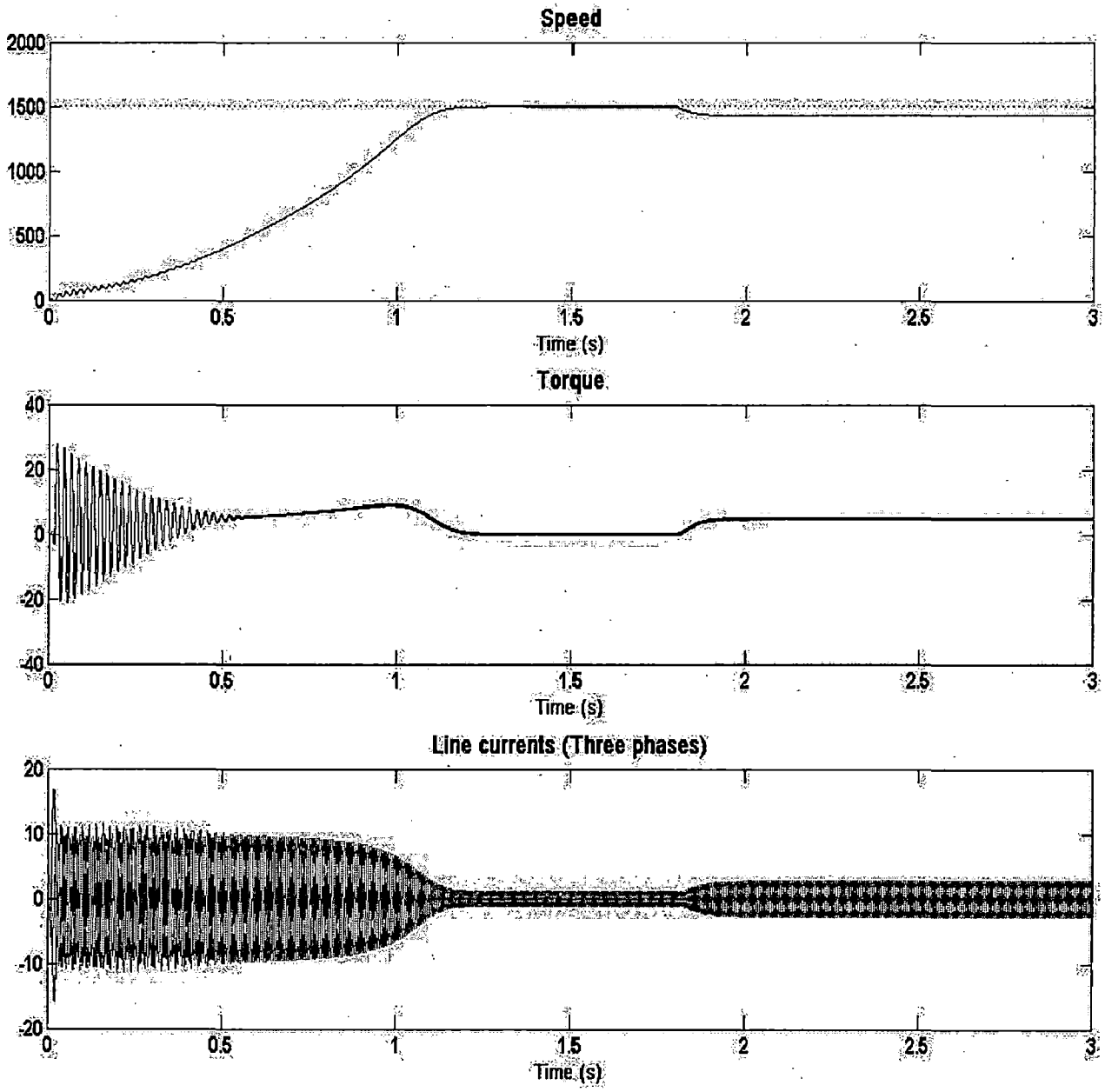


**Figure 6.16: Induction motor free acceleration characteristics when fed from harmonic controlled VSI**

## 6.2 Conclusions

The simulation results of the line voltage and current along with the frequency spectrum of the line current are presented for various values of number of switching angles per quarter cycle. It is found that, in harmonic elimination case the desired harmonics are completely eliminated. But, in harmonic minimization case the harmonics are not eliminated completely but they are attenuated so that the THD is low compared to other PWM techniques. It is also found that the THD is reduced with increase in the modulation index and number of switching angles per quarter cycle ($N$).

# Chapter 7
# Conclusions

The programmed pulse width modulation technique has been revisited which was originally proposed in 1973 by H.S.Patel and R.G. Hoft. A method to generate the optimal switching angles to eliminate a certain order of harmonics or to reduce the total harmonic distortion is introduced in this work. For this, two objective functions for eliminating and minimizing harmonics are formulated from the Fourier analysis of the inverter output voltage waveform. The design of the problem for optimizing these objective functions using nonlinear constrained optimization function is describe in detail. But, due to the transcendental nature of the objective functions, the main challenge associated is to obtain convergence which requires a proper initial guess to the solution.

A simple algorithm, namely solution at zero modulation index, is proposed to generate the initial guess to the problem for ensuring convergence. The algorithm was developed using MATLAB software and is run for a number of times independently to ensure the feasibility and quality of the solution. This method is found to be simple in implementation and fast in convergence. It is also proved an appropriate technique when over modulation operation is demanded, since it can find the solution for modulation indexes which are higher than unity. In order to prove the feasibility of and effectiveness of the proposed method, the algorithm is successfully applied to different operating points/cases including harmonic elimination & harmonic minimization problems and even & odd number of switching angles. Two sets of solution have been obtained for all the cases, one in $0^0$-$60^0$ range and other in $0^0$-$90^0$ range.

A simulation model of three phase inverted fed induction motor system was built and simulated for all the operating points in MATLAB-SIMULINK environment. A firing pulse generator with digital logic was designed for converting the optimal angles into firing pulses to the inverter. The waveforms and its frequency spectra are analyzed for all the operating points/cases.

Further work should focus on practical real time implementation of programmed PWM method which does not require online processing of the associated cumbersome calculations. The future work should also focus on extending this proposed method to optimization of various performance indexes in programmed PWM inverter fed induction motor drives, e.g., harmonic loss factor and magnetic noise etc.

# References


[1] Khaled El-Naggar and Tamer H. Abdelhamid, "Selective harmonic elimination of new family of multilevel inverters using genetic algorithms", Energy Conversion and Management, Volume 49, Issue 1, January 2008, pp: 89-95.

[2] Ajay Maheshwari and Khai D. T. Ngo, "Synthesis of Six-Step Pulse width-Modulated Waveforms with Selective Harmonic Elimination", IEEE Transactions on Power Electronics, VOL. 8, NO. 4 , October 1993, pp: 554-561.

[3] Wenyi Zhang, Shaoping Qu, Lemin Yang, Weiming Tong, Huiming Xu, "Research on Three-Phase Voltage-Source Selective Harmonic Elimination Inverter", IEEE/PES Transmission and Distribution Conference and Exhibition: Asia and Pacific, 2005, pp: 1-4.

[4] H. S. Patel and R. G. Hoft, "Generalized Techniques of Harmonic Elimination and Voltage Control in Thyristor Inverters: Part I- Harmonic Elimination," *IEEE Trans. Ind. Appl.*, vol. IA-9, no. 3, May/June 1973, pp. 310-317.

[5] H. S. Patel and R. G. Hoft, "Generalized harmonic elimination and voltage control in Thyristor inverters: Part II—Voltage control technique," *IEEE Trans. Ind. Applicat.*, vol. IE-10, Sept. /Oct. 1974, pp. 666–673.

[6] P. N. Enjeti and J. F. Lindsay, "Solving nonlinear equation of harmonic eliminations PWM in power control", Electronics letters, Vol 23, no. 12, pp: 656-657, 1987.

[7] Enjeti, P.N.; Ziogas, P.D.; Lindsay, J.F., "Programmed PWM techniques to eliminate harmonics: a critical evaluation", IEEE Transactions on Industry Applications, Mar/Apr 1990, Volume: 26, Issue: 2, pp: 302-316.

[8] Asumadu, J.A.; Hoft, R.G., "New algorithms for generation of notches in PWM waveforms using linear block codes", Annual IEEE Power Electronics Specialists Conference, 1992, pp: 465-472.

[9] Sidney R. Bowes, Paul R. Clark, "Regular-Sampled Harmonic-Elimination PWM Control of Inverter Drives", IEEE Transactions on Power Electronics. vol. 10, no. 5. September 1995, pp: 521-531.

[10] Jian Sun, Beineke, S. and Grotstollen, H. ," Optimal PWM based on real-time solution of harmonic elimination equations" , IEEE Transactions on Power Electronics, Jul 1996, Volume: 11, Issue: 4 pp: 612-621

[11] Toshiji Kato, "Sequential Homotopy-Based Computation of Multiple Solutions for Selected Harmonic Elimination in PWM Inverters", IEEE Transactions on Circuits and Systems—I: Fundamental Theory and Applications, vol. 46, no. 5, May 1999, pp:586-593.

[12] Dariusz Czarkowski, David V. Chudnovsky, Gregory V. Chudnovsky, Ivan W. Selesnick, "Solving the Optimal PWM Problem for Single-Phase Inverters", IEEE Transactions ON Circuits and Systems—I: Fundamental Theory and Applications, vol. 49, no. 4, April 2002, pp:465-475.

[13] Chiasson, J.N., Tolbert, L.M., McKenzie, K.J., Zhong Du, "A complete solution to the harmonic elimination problem", IEEE Transactions on Power Electronics, March 2004, Volume: 19, Issue: 2, pp: 491- 499.

[14] Wells, J.R.; Nee, B.M.; Chapman, P.L.; Krein, P.T., "Selective harmonic control: a general problem formulation and selected solutions", IEEE Transactions on Power Electronics, Nov. 2005, Volume: 20, Issue: 6, pp: 1337- 1345.

[15] Agelidis, V.G.; Balouktsis, A.; Balouktsis, I.; Cossar, C., "Multiple sets of solutions for harmonic elimination PWM bipolar waveforms: analysis and experimental verification", IEEE Transactions on Power Electronics, March 2006, Volume: 21, Issue: 2, pp: 415- 421.

[16] Blasko, V., "A Novel Method for Selective Harmonic Elimination in Power Electronic Equipment", IEEE Transactions on Power Electronics, Jan. 2007, Volume: 22, Issue: 1, pp: 223-228.

[17] Mohamed S.A. Dahidah, Vassilios G. Agelidis and Machavaram V. Rao, "Hybrid genetic algorithm approach for selective harmonic control", Energy Conversion and Management, Volume 49, Issue 2, February 2008, pp: 131-142.

[18] Tsorng-Juu Liang, O'Connell, R.M., Hoft, R.G., "Inverter harmonic reduction using Walsh function harmonic elimination method", IEEE Transactions on Power Electronics, Nov 1997, Volume: 12, Issue: 6, pp: 971-982

[19] MATLAB optimization toolbox user's guide, 2007. http://mathworks.com

[20] Ozpineci, B., Tolbert, L.M., "Simulink implementation of induction machine model - a modular approach", IEEE International Electric Machines and Drives Conference, 1-4 June 2003, Volume: 2, pp: 728- 734.

## Books:

[21] Bimal K. Bose, "Modern Power Electronics and AC Drives", Prentice Hall, 2002.

[22] P. C. Krause, "Analysis of Electric Machinery", MCGraw-Hill Book Company, 1986.

[23] M. Rashid, "Power Electronics: Circuits, Devices and Applications", 2nd edition, New York: Prentice-Hall, 1993.

[24] Power Semiconductor Controlled Drives - G K Dubey - Prentice-Hall International Edition 1989.

# Appendix – A

A 5hp, 400 volts, 3 phase, 50 Hz, 4-pole, delta connected squirrel cage induction motor is considered for the study.

Equivalent circuit constants of the Motor (referred to stator side):

Stator Resistance = 4.68 Ω

Rotor Resistance = 5.06 Ω

Stator Leakage Inductance = 0.0039 H

Rotor Leakage Inductance = 0.0039 H

Mutual Inductance = 0.93 H

and Moment of Inertia = 0.032 kg-$m^2$

# Appendix – B

**%% MAIN Program %%**

```
clc;
clear all;
global n;
global m;
global N;
ch=1;
while (ch ~= 4 )
    clc;
    display('*****************************************************************');
    display('************** CALCULATION OF SWITCHING ANGLES FOR HARMONIC
          CONTROL  **************');
    display('*****************************************************************');
    display('MENU - ');
    display('    1. Harmonic Elimination');
    display('    2. Harmonic Minimization');
    display('    3. Comparision of Harmonic elimination and minimization');
    display('    4. Exit');
    ch=input('Enter your choice:     ');
    switch(ch)
        case {1,2,3}          % Read Input
            n=input('\nEnter the Number of Switching Angles per Quarter cycle
                    \n');
            if ch ~= 1  % highest harmonic to be summed (harmonic minimization)
                N=input('\nEnter the Highest Harmonic to be Optimized\n');
            end
            amax=input('\nEnter the Maximum value of switching angles (60/90)')
            mmin=input('\nEnter the Minimum value of modulation index \n');
            deltam=input('\nEnter the stepsize for modulation index \n');
            mmax=input('\nEnter the Maximum value of modulation index \n');
        case 4
            break;
        otherwise
            clc;
            input('Invalid option (Press ENTER to continue) ');
            continue;
    end
    if mod(n,2)==0          % Inintial guess for odd number of switchings
        if amax == 60       % Inintial guess for 0 to 60 degree range
            theta=120/(n);
            i=1;
            x0(1)=0.1;
            for t=3:2:n-1
                x0(t)=theta*i;
                x0(t-1)=x0(t);
                i=i+1;
            end
            x0(n)=60;
        else                % Inintial guess for 0 to 90 degree range
            theta=120/(n+2);
            i=1;
            x0(1)=theta;
            for t=3:2:n-3
                x0(t)=theta*(i+1);
                x0(t-1)=x0(t)-0.01;
                i=i+1;
            end
```

```
        x0(n-2)=60-theta;
        x0(n-1)=60;
        x0(n)=60+theta;
    end
else                        % Inintial guess for even number of switchings
    if amax == 60           % Inintial guess for 0 to 60 degree range
        theta=120/(n+1);
        i=1;
        for t=2:2:n-1
            x0(t)=theta*i;
            x0(t-1)=x0(t);
            i=i+1;
        end
        x0(n)=60;

    else                    % Inintial guess for 0 to 90 degree range
        theta=120/(n+1);
        i=1;
        x0(1)=0.1;
        x0(2)=theta;
        for t=4:2:n-3
            x0(t)=theta*(i+1);
            x0(t-1)=x0(t)-0.01;
            i=i+1;
        end
        x0(n-2)=60-theta;
        x0(n-1)=60;
        x0(n)=60+theta;
    end
end
lb=zeros(1,n);              % Lower limit of the solution vector
ub=zeros(1,n);
for l=1:n
    ub(l)=amax;             % Upper limit of the solution vector
end
A=zeros(n-1,n);
for l=1:n-1                 % Linear inequality constraints: definition of A
    A(l,l)=1;
    A(l,l+1)=-1;
end
b=zeros(n-1,1);             % Linear inequality constraints: definition of b
for s=1:n-1
    b(s)=0;
end
Aeq=[];                     % Linear equality constraints
beq=[];
options = optimset('MaxFunEvals',10000,'MaxIter',10000,'GradObj','on');

switch (ch)
    case 1                  % switching angles for harmonic elimination problem
        i=1;
        for m=mmin:deltam:mmax
            [x_she]=fmincon(@obj_fun,x0,A,b,Aeq,beq,lb,ub,@mycon,options);
            for l=1:n
                a_she(l,i)=x_she(l);
            end
            mi(1,i)=m;
            i=i+1;
            x0=x_she;
        end
        figure(1);
```

```
    plot(mi,a_she,'LineWidth',1);
    xlabel('Modulation Index','fontsize',12,'fontweight','b');
    ylabel('Switching Angles','fontsize',12,'fontweight','b');
    title('Modulation Index vs Switching Angles (Harmonic
          Elimination)','fontsize',12,'fontweight','b');
    clc;
    disp('                                          Modulation Index ')
    disp(mi);
    disp('-------------------------------------------------------------');
    disp(a_she);
    input('Press Enter to continue');
case 2              % switching angles for harmonic elimination problem
    i=1;
    for m=mmin:deltam:mmax

      [x_shm]=fmincon(@obj_fun_thd,x0,A,b,Aeq,beq,lb,ub,@mycon,options);
        for l=1:n
            a_shm(l,i)=x_shm(l);
        end
        mi(1,i)=m;
        i=i+1;
        x0=x_shm;
    end
    figure(2);
    plot(mi,a_shm,'LineWidth',1);
    xlabel('Modulation Index','fontsize',12,'fontweight','b');
    ylabel('Switching Angles','fontsize',12,'fontweight','b');
    title('Modulation Index vs Switching Angles (Harmonic
          Minimization)','fontsize',12,'fontweight','b');
    clc;
    disp('                                          Modulation Index ')
    disp(mi);
    disp('-------------------------------------------------------------');
    disp(a_shm);
    input('Press Enter to continue');
case 3
    i=1;
    x0_shm=x0;
    for m=mmin:deltam:mmax
        [x_she]=fmincon(@obj_fun,x0,A,b,Aeq,beq,lb,ub,@mycon,options);
 [x_shm]=fmincon(@obj_fun_thd,x0_shm,A,b,Aeq,beq,lb,ub,@mycon,options);
        for l=1:n
            a_she(l,i)=x_she(l);
            a_shm(l,i)=x_shm(l);
        end
        mi(1,i)=m;
        i=i+1;
        x0=x_she;
        x0_shm=x_she;
    end
    figure(3)
    hSLines = plot(mi,a_she,'k','LineWidth',1);hold on
    hCLines = plot(mi,a_shm,'--b','LineWidth',1);
    hSGroup = hggroup;
    hCGroup = hggroup;
    set(hSLines,'Parent',hSGroup)
    set(hCLines,'Parent',hCGroup)
    set(get(get(hSGroup,'Annotation'),'LegendInformation'),...
        'IconDisplayStyle','on'); % Include this hggroup in the legend
    set(get(get(hCGroup,'Annotation'),'LegendInformation'),...
        'IconDisplayStyle','on'); % Include this hggroup in the legend
```

```
            legend('Harmonic Elimination','Harmonic minimization')
            axis([0 1.2 0 70])
            xlabel('Modulation Index','fontsize',14,'fontweight','b');
            ylabel('Switching Angles','fontsize',14,'fontweight','b');
            title('Modulation Index vs Switching
                  Angles','fontsize',14,'fontweight','b');
    end
end
```

**%% Objective function for harmonic elimination %%**

```
function [z,g]=obj_fun(x)

global n;
t=4/pi;
v=ones(3*n,1);

%%%%%%%%%%%%%%%% Objective function %%%%%%%%%%%%%%%%
if (n == 2)
    v(5)=1;
    v(5)=1-2*cosd(5*x(1))+2*cosd(5*x(2));
    z=v(5)*(t/5);
    z=z^2;
else if (mod(n,2) ~= 0)
        for k=1:(n-1)/2
            v(6*k-1)=1;
            v(6*k+1)=1;
            for l=1:n
                v(6*k-1)=v(6*k-1)+((-1)^l)*2*cosd((6*k-1)*x(l));
                v(6*k+1)=v(6*k+1)+((-1)^l)*2*cosd((6*k+1)*x(l));
            end
            v(6*k-1)=(t/(6*k-1))*v(6*k-1);
            v(6*k+1)=(t/(6*k+1))*v(6*k+1);
        end
        z=0;
        for l=1:(n-1)/2
            z=z+(v(6*l+1))^2+(v(6*l-1))^2;
        end
    else
        for k=1:(n/2)
            v(6*k-1)=1;
            v(6*k+1)=1;
            for l=1:n
                v(6*k-1)=v(6*k-1)+((-1)^l)*2*cosd((6*k-1)*x(l));
                v(6*k+1)=v(6*k+1)+((-1)^l)*2*cosd((6*k+1)*x(l));
            end
            v(6*k-1)=(t/(6*k-1))*v(6*k-1);
            v(6*k+1)=(t/(6*k+1))*v(6*k+1);
        end
        sum=0;
        for l=1:(n/2)-1
            sum=sum+(v(6*l+1))^2+(v(6*l-1))^2;
        end
        l=l+1;
        z=sum+(v(6*l-1))^2;
    end
end
```

```
%%%%%%%%%%%%%% Gradient %%%%%%%%%%%%%%%%%
if nargout > 1
    g=zeros(1,n);
    if (n==2)
        for h=1:n
            g(1,1)=t*4*sind(5*x(1))*v(5);
            g(1,2)=-t*4*sind(5*x(2))*v(5);
        end
    else if (mod(n,2) ~= 0)
            for h=1:n
                sum1=0;
                for k=1:(n-1)/2
                    sum1=sum1+v(6*k-1)*sind((6*k-
                        1)*x(h))+v(6*k+1)*sind((6*k+1)*x(h));
                end
                g(1,h)=sum1*(4*((-1)^(h+1))*t);
            end
        else
            for h=1:n
                sum1=0;
                for k=1:(n/2)-1
                    sum1=sum1+v(6*k-1)*sind((6*k-
                         1)*x(h))+v(6*k+1)*sind((6*k+1)*x(h));
                end
                k=k+1;
                sum1=sum1+v(6*k-1)*sind((6*k-1)*x(h));
                g(1,h)=sum1*(4*((-1)^(h+1))*t);
            end
        end
    end
end
```

**%% Objective function for harmonic minimization %%**

```
function [z,g]=obj_fun_thd(x)

global n;
global N;
t=4/pi;

%%%%%%%%%%%%%%%% Objective function %%%%%%%%%%%%%%%%
if ( mod((N-1),6) == 0 )

    for k=1:((N-1)/6)
        v(6*k-1)=1;
        v(6*k+1)=1;
        for l=1:n
            v(6*k-1)=v(6*k-1)+((-1)^l)*2*cosd((6*k-1)*x(l));
            v(6*k+1)=v(6*k+1)+((-1)^l)*2*cosd((6*k+1)*x(l));
        end
        v(6*k-1)=(t/(6*k-1))*v(6*k-1);
        v(6*k+1)=(t/(6*k+1))*v(6*k+1);
    end
    sum=0;
    for l=1:((N-1)/6)
        sum=sum+((v(6*l+1))/(6*l+1))^2+((v(6*l-1))/(6*l-1))^2;
    end

else
    for k=1:((N+1)/6)
```

```
        v(6*k-1)=1;
        v(6*k+1)=1;
        for l=1:n
            v(6*k-1)=v(6*k-1)+((-1)^l)*2*cosd((6*k-1)*x(l));
            v(6*k+1)=v(6*k+1)+((-1)^l)*2*cosd((6*k+1)*x(l));
        end
        v(6*k-1)=(t/(6*k-1))*v(6*k-1);
        v(6*k+1)=(t/(6*k+1))*v(6*k+1);
    end
    sum=0;
    for l=1:(((N+1)/6))-1
        sum=sum+((v(6*l+1))/(6*l+1))^2+((v(6*l-1))/(6*l-1))^2;
    end
    l=l+1;
    sum=sum+((v(6*l-1))/(6*l-1))^2;
end
z=sum;


%%%%%%%%%%%%%% Gradient %%%%%%%%%%%%%%%%%
if nargout > 1
    if ( mod((N-1),6) == 0 )
        for h=1:n
        g(1,h)=0;
        for k=1:(N-1)/6
            g(1,h)=g(1,h)+(v(6*k-1)*sind((6*k-1)*x(h)))/(((6*k-
                  1)^2)+v(6*k+1)*sind((6*k+1)*x(h)))/((6*k+1)^2);
        end
        g(1,h)=g(1,h)*(4*((-1)^(h+1))*t);
        end
    else
        for h=1:n
        g(1,h)=0;
        for k=1:((N+1)/6)-1
            g(1,h)=g(1,h)+(v(6*k-1)*sind((6*k-1)*x(h)))/((6*k-
                   1)^2)+(v(6*k+1)*sind((6*k+1)*x(h)))/((6*k+1)^2);
        end
        k=k+1;
        g(1,h)=g(1,h)+(v(6*k-1)*sind((6*k-1)*x(h)))/((6*k-1)^2);
        g(1,h)=g(1,h)*(4*((-1)^(h+1))*t);
        end
    end
end
```

**%% Constraint function %%**

```
function [c,ceq] = mycon(x)

global n;
global m;
t=4/pi;

v(1)=1;
for l=1:n
    v(1)=v(1)+(-1)^l*2*cosd(x(l));
end
v(1)=t*v(1);
ceq(1)=abs(v(1))-m;
c=[];
```